DEVELOPMENT OF A COMPUTER CODE TO ANALYSE FLUID TRANSIENTS IN PRESSURIZED PIPE SYSTEMS

A THESIS SUBMITTED TO
THE GRADUATE SCHOOL OF NATURAL AND APPLIED SCIENCES
OF
MIDDLE EAST TECHNICAL UNIVERSITY

BY

HASAN DALGIÇ

IN PARTIAL FULFILLMENT OF THE REQUIREMENTS
FOR
THE DEGREE OF MASTER OF SCIENCE
IN
CIVIL ENGINEERING

JUNE 2017

ABSTRACT

DEVELOPMENT OF A COMPUTER CODE TO ANALYSE FLUID TRANSIENTS IN PRESSURIZED PIPE SYSTEMS

Dalgıç, Hasan
M.S., Department of Civil Engineering
Supervisor : Prof. Dr. Zafer Bozkuş

June 2017, 133 pages

Sudden change of flow conditions in a pipeline may cause the flow to become time dependent and would start an undesirable physical phenomenon called water hammer. These sudden changes can be caused by variety of scenarios and some of them include valve operations (opening or closing), sudden power loss at pump stations and load rejections or load acceptance at the turbines, etc. Because of its very costly to solve, and sometimes deadly results, it is quite important that transient scenarios be considered for pipe systems at design stage to ensure safety and longevity of them.

The present study is an attempt to develop a comprehensive computer software that is capable of simulating, analysing and solving most commonly encountered fluid transient events. The ultimate goal of the study is to have a local computer program to be used in our country, instead of buying expensive software from abroad in this field.

Thus, the code developed in the present study will be enhanced further in the future with the contributions of others. However, in its current form, the code is already capable of using many boundary conditions to tackle a large variety of problems

involving fluid transients. Within the code, the Method of Characteristics are used to solve the basic unsteady pipe flow equations.

The code developed is titled as H-Hammer and it utilizes AutoCAD, Visual Basic 6.0 and MS Excel all together for the purpose of analyses. The accuracy of the software was tested by solving some existing problems offered in the important textbooks written in the field by those who contributed significantly in the fluid transient area. Comparisons of the results show that the results of the developed software is in good agreement with the solutions given in those books.

Keywords: Waterhammer, Transient Scenarios, Pressurized Pipe Flows, Method of Characteristics, Waterhammer Computer Code

ÖZ

BASINÇLI BORU SİSTEMLERİNDE ZAMANLA DEĞİŞEN AKIMLARIN ANALİZİNİ YAPMAK İÇİN BİR BİLGİSAYAR KODU GELİŞTİRİLMESİ

Dalgıç, Hasan
Yüksek Lisans, İnşaat Mühendisliği Bölümü
Tez Yöneticisi : Prof. Dr. Zafer Bozkuş

Haziran 2017, 133 sayfa

Bir boru hattında akım koşullarının aniden değişerek zamana bağlı hale gelmesi su darbesi diye adlandırılan ve hiç de arzu edilmeyen fiziksel bir olayı başlatır. Bu ani değişiklikler çok çeşitli senaryolardan kaynaklanabilir ki, bunların bir kısmı vana operasyonları (açma veya kapama), pompa istasyonlarında güç kayıbı ya da turbinlerin yük atması veya yük kabul etmesi vb. şeyler olabilir. Çözümü çok pahalı ve bazen ölümcül olan sonuçları yüzünden, zamanla değişen akım senaryolarının boru hatlarının güvenliğini ve uzun ömürlü olmalarını sağlamak için tasarım aşamasında dikkate alınmaları oldukça önemlidir.

Bu çalışma, en yaygın olarak karşılaşılan su darbesi senaryolarını taklit edecek, analiz edecek ve çözecek kapsamlı bir bilgisayar kodu geliştirme çabasıdır. Çalışmanın nihai hedefi bu alandaki pahalı olan ticari programların yurtdışından satın alınmasından ziyade, yerel bir bilgisayar programına sahip olmaktır.

Dolayısı ile bu çalışmada üretilen kod gelecekte başkalarının katkıları ile geliştirilerek daha kapsamlı bir hale getirilecektir. Ancak, program şu anki hali ile bile çok sayıda su darbesi problemleri ile uğraşacak birçok sınır koşulunu

kullanabilecek yetenektedir. Kod içinde, zamanla değişen boru akımlarının temel denklemleri, Karakteristikler Metodu ile çözülmüştür.

Geliştirilen kod H-Hammer olarak adlandırılmış olup, analizleri gerçekleştirmek amacı ile AutoCAD, Visual Basic 6.0 ve MS Excel programlarından birlikte yararlanmaktadır. Programın doğruluğu su darbesi alanında önemli katkılar vermiş kişilerce yazılmış kitaplar içerisinde yer alan mevcut problemleri çözerek test edilmiştir. Sonuçların kıyaslanması geliştirilen kodun verdiği sonuçların kitaplarda verilen çözümlerin sonuçlarına çok yakın olduğunu göstermiştir.

Keywords: Su Darbesi, Zamana Bağlı Akım Senaryoları, Basınçlı Boru Akımı, Karakteristikler Metodu, Su Darbesi Bilgisayar Kodu.

ACKNOWLEDGEMENTS

It was a difficult task to complete this thesis and it would not have beeen possible to complete it without the support of people who were there to guide me during this process. I have my greatest gratitude to Prof. Dr. Zafer BOZKUŞ who made it possible for me to complete this thesis and for taking his time to review this work. Thanks to his guidance and constant encouragement I was able to maintain my motivation and enthusiasm throughout my study.

Also I would like to thank my family for supporting me throughout my journey of Masters Degree Studies. I finally would like to acknowledge all of my instructors from the Hydromechanics Laboratory of Civil Eng. Department who shared their invaluable knowledge with me over the years.

TABLE OF CONTENTS

LIST OF TABLES

LIST OF FIGURES

LIST OF SYMBOLS

A	Pipe cross sectional area
a	Acoustic speed (Pressure wave speed)
A_G	Valve opening area
B	Allievi constant or pipeline constant
C^+, C^-	Names of the characteristic equations
C_P, C_M	Known constants in characteristic equations
C_{orf}	Orifice head loss coefficient
C_D	Valve loss coefficient
D	Diameter of pipe
E	Young's modulus of elasticitiy
E_m	Valve time constant
e	Wall thickness of pipe
f	Friction factor of pipe
g	Gravitational acceleration
H	Head value
H_R	Rated pumping head
h	Dimensionless head ratio
K	Bulk modulus of elasticity
L	Length of pipe
L_1	Continuity equation
L_2	Momentum equation
L_{SP}	Length of the stand pipe that connects surge tank to system
m	Polytropic gas equation exponent
N_R	Rated rotational speed of pump
P	Pressure
Q	Discharge value

Q_R	Rated discharge of pump
Q_{SP}	Discharge flowing into our out from stand pipe which connects surge tank
r	Radius of pipe
t	Time
Δt	Time increment
T_R	Rated torque of pump
tdh	Total dynamic head
V	Velocity of fluid
V_0	Initial velocity of fluid
$\forall$	Control volume
$\forall_{air}$	Volume of the entrapped air inside air chamber
WH, WB	Dimensionless turbo pump characteristics
WR^2	Moment of inertia of rotating parts of turbo pump
W_{ext}	External loads
z	Elevation of pipe above datum
α	Dimensionless speed ratio
β	Dimensionless torque ratio
υ	Dimensionless discharge ratio
σ_1	Unit axial stress
σ_2	Unit lateral stress
ξ_1	Unit longitudinal strain or axial unit strain
ξ_2	Unit lateral strain
ξ_t	Total lateral or circumferential unit strain
μ	Poisson's ratio
ω	Radial speed of pump
γ	Specific weight of fluid
ρ	Mass density
τ	Dimensionless number that describes discharge coefficient multiplied by valve opening area.

λ	Method of characteristics multiplier
η_R	Rated efficiency of pump

CHAPTER 1

INTRODUCTION

1.1 General

Devices such as valves, pumps or any other mechanical equipment that can disturb the steady state flow conditions can trigger a transient event. Without precautions these transient events can lead to catastrophic events. For example a hydroelectric power plant in Russia which is named as Sayano-Shushenskaya (2009) was completely destroyed due to sudden stoppage of one of its turbines. At the end of this event, 76 people lost their lives and approximately $310 million worth of damage was inflicted.

The main objective of the transient analysis is to carry out simulations of such situations and enable engineers to take necessary precautions in order to prevent destructive nature of pressure variations during transient events. Properly performed analyses will lead to a safer design without the need of over-designing which will guarantee better system control and engineers can judge the situation more in depth with the known pressure and discharge information obtained from such simulations.

1.2 Literature Review

There are a great number of previous studies that implement arithmetic, graphical, characteristics, algebraic, implicit, linear analysis and other methods to solve transient events.

Allievi (1902, 1913) and Bergeron (1935, 1936) developed a solution for the basic unsteady flow equations using graphical methods. Downside of the graphical analysis was that it was limited to single pipelines for practicality and assumes that pipe flow is without friction.

Streeter and Wylie (1967) developed an explicit approach called the Method of Characteristics (MOC) to solve transient equations which is the method used in this thesis as well as the most widespread method available for simulation of transients.

Kepkep (1976) used first order finite difference technique to solve partial differential equations and developed a computer code to analyse fluid transients in closed conduits.

Wiggert and Sundquist (1977) used fixed grids to project characteristics from outside the fundamental grid size for solving pipeline transients. The purpose of their analysis is to show effects of spacing, interpolation and grid size on numerical attenuation and dispersion.

Wiggert and Sundquist (1979) used method of characteristics to investigate gaseous cavitation problems. They developed an analytical model based on method of characteristics which solves the transient equations for pressure, velocity and void fraction due to cavitation and gas release. They solved the amount of gas release dependent on the amount of difference between saturation and instantaneous line pressures.

Özer (1980) used explicit solution technique to solve boundary equations and created a computer code to analyse fluid transients in pipe networks.

Shimada and Okushima (1984) used series solution method and a Newton-Raphson method to solve transient equations. They calculated only maximum water hammer pressure with a constant friction factor.

Karney (1984) developed a computer code to analyse fluid transients in large pipe networks.

MacCormak scheme were used by Chaudhry and Hussaini (1985) to numerically solve transient equations. MacCormak method is suitable for analyzing flows having shocks and bores since it is second-order accurate both in space and time. They used

forward finite difference in the corrector and backward finite difference in the predictor parts.

Pezzinga (1999) used a quasi-two-dimensional model to solve transient equations in pipes and pipe networks. This model was based on mixing length hypothesis in the turbulent zone and on Newton's law in the viscous sublayer.

Saral (2000) developed a computer code to analyse transients in closed conduits. Code was written in Fortran programming language. The method of characteristics were used to solve partial differential equations. In his study modular approach is used to model topology with an iterational computational grid.

Ramezani (2001) developed a computer model named "Water Hammer Analysis in Small Hydropower Schemes (WHASH)". She used rectangular grid method of characteristics to solve transient problems found at penstocks.

Ghidaoui and Mansour (2002) used two-layer and five-layer eddy viscosity models to solve turbulence water hammer models as well as accuracy of quasi-steady and axisymmetric assumptsions are evaluated in their research. They add a dimensionless parameter to assess the accuracy of the quasi-steady turbulence models in water hammer problems. It was found that results of both models concured with each other therefore turbulence modelling of water hammer flows were insensitive to the magnitude and distribution of the eddy viscosity within the pipe core.

Ghidaoui and Zhao (2003) solved water hammer flow using a quasi-two dimensional turbulent model. Moreover, Ghidaoui and Zhao (2004) developed first and second-order explicit finite volume Godunov-type schemes for transient problems. The finite volume approach ensures conservation of mass and momentum is preserved along the solution. Application of boundaries are similar to method of characteristics and very similar results are obtained compared to method of characteristics analysis. Moreover, it was found that second-order Godunov-type scheme requires much less memory storage compared to method of characteristics and first-order Godunov-type scheme.

Cannizzaro and Pezzinga (2005) studied whether non - friction energy dissipation in transient cavitating flows can be attributed to thermic exchange between gas bubbles and the surrounding liquid or to gas release and solution process. A proposed model contains a two-dimensional numerical model for liquid flow with a small amount of free gas. It is found that a two-dimensional model can give accurate results if suitable calibration of the model parameters are chosen.

Greyvenstein (2006) developed a model based on implicit Finite Difference method. Their approach is based on simultaneous pressure correction which is valid for both liquid and gas flows as well as for isothermal and non-isothermal flows. The results have shown that the proposed method's advantages are its speed over a range of problems, accuracy, stability and flexibility.

Koç (2007) developed a computer code to analyse fluid transients. Method of characteristics were used to solve partial differential equations and computer code is written in C# programming language.

Bozkuş (2008) analysed water hammer problems in Çamlıdere – İvedik Water Treatment Plant Pipeline. He simulated a valve closure scenario for this pipeline using a computer code written in Fortran programming language. As a result of his research optimum valve closure times were found for the safe operation of this pipeline.

Afshar and Rohani (2008) proposed an implicit method of characteristics method to solve transient equations. They derived all the equations in a pipeline system in an element-wise manner and solved the final system of equations for the unknown nodal heads and flows.

Bozkuş and Dursun (2014) investigated a method of protection for water hammer problems in Yesilvadi Hydropower Plant. They simulated the instant load rejection of this power plant with and without a pressure relief valve and compared the results. From comparison it is seen that pressure relief valves are effective in decreasing

turbine runaway speed. However, it is observe dthat incorrect operation of these valves causes higher transient pressure waves.

Bozkuş, Çalamak and Rezaei (2016) investigated performance of a pumped discharge line with joint use of protective devices against water hammer. From their research it was found that without protective devices pipe system experiences very low pressures and in some cases it is below vapor pressure of the liquid. Moreover, further investigations are conducted adding protective devices to the system such as flywheel, air chamber and in-line check valves. As a result they found out that single use of these protective devices are economically inefficient whereas joint use of in-line check valves and air chambers results in more economical and safer design.

Bozkuş and Dinçer (2016) investigated water hammer problems in a Wind-Hydro Hybrid power plant. They used a commercially available software to solve water hammer events caused by sudden load rejection of the turbine at the plant, with and without surge tank and compared the results.

Apart from academical studies there are also commercial softwares in this field such as Bentley Hammer and Wanda. These softwares are capable of simulating transients for pipe networks and pipelines including large variety of boundary conditions.

1.3 Objective of the Thesis

In this thesis a computer software is developed for the purpose of establishing different scenarios and conducting transient simulations. The chosen solution approach for this software is the method of characteristics which solves non-linear continuity and conservation of momentum partial differential equations in space and time. Variety of boundary conditions are introduced to the software enabling user to obtain solutions to the transient scenarios.

Moreover, this software utilizes AutoCAD's powerful graphical and drawing capacity to create scenarios which is very practical as well as it uses Microsoft Excel as its database to store results of the analysis which would be very practical for design engineers. The list given below explains briefly what H-Hammer software is capable of;

- It can create a topography of the pipe route from AutoCAD drawing model.
- It has the advantage of using AutoCAD utilities allowing user to create their scenarios in an infinite model space which eases users' experience for creating schematics.
- Its schematic views of the scenarios are user friendly and easy to assemble.
- It can calculate pressure wave speed for given parameters, time interval, distance intervals for the given parameters.
- It can calculate friction factor by Colebrook-White equation.
- It can calculate pump moment of inertia and other required pump parameters by empirical formulas which are useful in case user is not able to receive experimental data from manufacturer.
- It will combine real pipe profile elevations and pressure values obtained from transient analysis to make cavitation analysis and stress analysis.
- As a result of cavitation and stress analysis it will calculate necessary pipe thicknesses and signal the cavitation locations and durations.

- It has powerful graphing options which enable user to plot graphs of pressure vs. time, pressure vs. distance, discharge vs. time and discharge vs distance.
- It can animate the motion of pressure waves upon completion of analysis and compare this motion in combination with the pipe profile drawn by the user on AutoCAD.

CHAPTER 2

FORMULATION OF THE MODEL

The model implements the use of explicit method of characteristics (MOC) which were explained in detail by Wylie and Streeter (1993). Basis of explicit method of characteristics are continuity and conservation of momentum equations written in partial differential form. The following sections will give brief description of Wylie and Streeter' s (1993) work and show the derivation of transient equations.

2.1 Arithmetic Derivation of Pressure Wave Speed

In integral form, conservation of momentum in the x-direction is given below:

$$\sum F_x = \frac{d}{dt}\int_{CV} V\rho dV + \int_{CS} V\rho(\vec{V} \cdot \vec{n})dA \qquad \textbf{(2.1)}$$

In the present study, we are dealing with the one-dimensional solution of conservation of momentum and continuity equations therefore equations are written for the x-direction.

Eq. (2.1) is applied to the control volume given in Figure 2-1, which is shown in Figure 2-2.

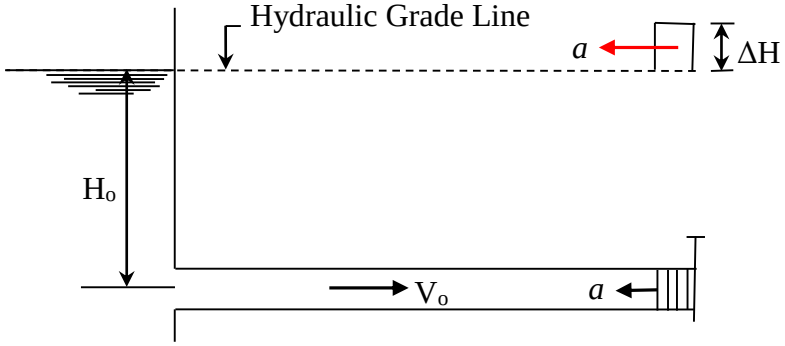

Figure 2-1: Upstream reservoir and downstream valve, Wylie and Streeter (1993)

Figure 2-1 illustrates the instant when the downstream valve is closed a pressure wave propagates towards upstream at a speed "*a*" which is the speed of sound in the liquid, also called acoustic speed. In order to apply the momentum equation for this case control volume shown on Figure 2-2 is used.

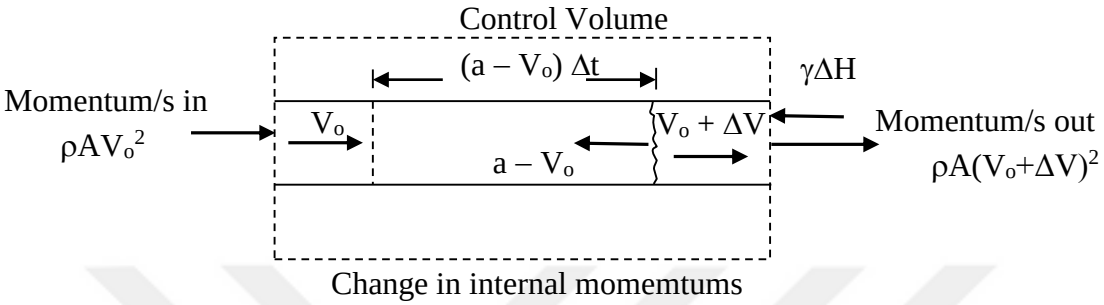

Figure 2-2: Transient state control volume, Wylie and Streeter (1993)

Unsteady Part:

$$\frac{d}{dt}\int_{CV} V\rho d\forall = \rho\frac{A(a-V_0)}{\Delta t}\Delta t(V_0+\Delta V-V_0) = \rho A(a-V_0)\Delta V \qquad \textbf{(2.2)}$$

Fluxes:

$$\int_{CS} V\rho(\vec{V}\,.\,\vec{n})dA = \rho A(V_0+\Delta V)^2 - \rho A V_0^2 \qquad \textbf{(2.3)}$$

Combined Form becomes:

$$\rho A(a-V_0)\Delta V + \rho A(V_0+\Delta V)^2 - \rho A V_0^2 = -\gamma\Delta HA \qquad \textbf{(2.4)}$$

Where the sum of the forces acting on the control volume in Eq. (2.1) is expressed by $\sum F_x = -\gamma\Delta HA$

By neglecting the small quantity of ΔV^2 and simplifying the equation by noting that we obtain the pressure head increase.

$$\Delta H = -\frac{a\Delta V}{g}\left(1+\frac{V_0}{a}\right) \approx -\frac{a\Delta V}{g} \qquad \textbf{(2.5)}$$

Also it should be kept in mind that Eq. (2.5) and Eq. (2.6) are valid as long as the valve closure is completed in less than $2L/a$ seconds, that is, the pressure wave

generated at the downstream valve travels upstream where it is reflected by the reservoir and comes back to the elbow within $2L/a$ seconds, and meets the closed valve.

In brief if the flow is suddenly stopped at the downstream then $\Delta V=-V_0$ which results in pressure head increase $\Delta H=aV_0/g$. This result will illustrate us that in case of high velocities and sudden flow stoppages we might face very high positive pressure fluctuation at the downstream end of our pipe and for the upstream operations opposite sign of this equation can be used. In summation form our equation becomes:

$$\sum \Delta H = \mp \frac{a}{g} \sum \Delta V \qquad \textbf{(2.6)}$$

This equation shows the relationship between the flow change and magnitude of pressure changes. The minus sign must be used for waves travelling towards upstream and plus sign must be used for waves travelling towards downstream end of pipe.

It must be noted that in all of these equations a pressure wave speed denoted as "a". Below here the pressure wave speed will be derived by considering length and cross sectional area changes of pipes as well as compressibility of liquid due to high pressures. In brief pressure wave speed must depend on:

- Bulk modulus of elasticity of liquid (to satisfy compressibility of liquid during transient event)
- Young's modulus of elasticity of pipe material (to satisfy elongation or cross sectional expansions/contractions during transient event)
- Support type of pipe
- Pipe dimensions such as pipe diameter, wall thickness.

During a transient event depending on the support type due to suddenly closed valve as shown in Figure 2-3 may cause pipe to stretch in length by Δs. With the assumption that this stretching motion occurs during L/a seconds after the valve closure we can deduce that mass entering the pipe during this time is $\rho A V_0 L/a$. Since

we assumed that the motion occurs in L/*a* seconds then its velocity becomes *a*Δs/L therefore velocity of the fluid at the gate is changed by ΔV=Δs*a*/L-V_0. This extra mass is contained within the pipe by increasing its cross-sectional area, by filling the extra volume cause by stretch of Δs as well as compressing the liquid that were already inside due to its higher pressure. In equation form this situation can be expressed by using continuity principle as following:

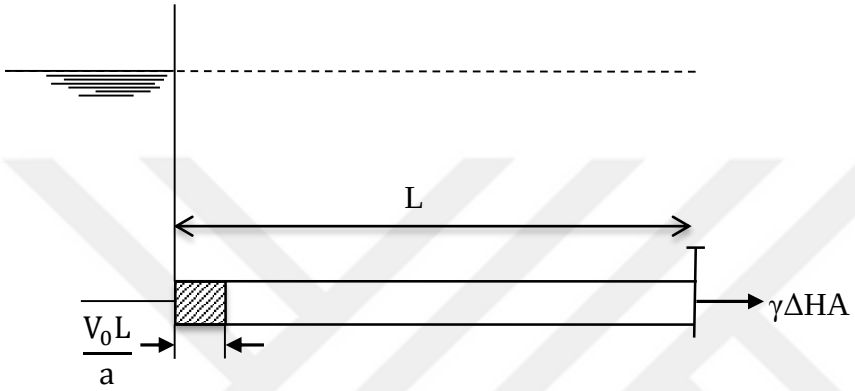

Figure 2-3: Continuity relations in pipe, Wylie and Streeter (1993)

$$\rho A V_0 \frac{L}{a} = \rho L \Delta A + \rho A \Delta s + L A \Delta \rho \qquad \textbf{(2.7)}$$

After solving Eq. (2.7) together with ΔV=Δsa/L-V_0 the below equation is obtained:

$$-\frac{\Delta V}{a} = \frac{\Delta A}{A} + \frac{\Delta \rho}{\rho} \qquad \textbf{(2.8)}$$

In order to eliminate ΔV from Eq. (2.8) a new equation is derived by combination of Eq. (2.6) and Eq. (2.8) which simplifies wave speed as:

$$a^2 = \frac{g \Delta H}{\Delta A/A + \Delta \rho/\rho} \qquad \textbf{(2.9)}$$

It is known that bulk modulus of elasticity of liquids are defined as;

$$K = \frac{\Delta P}{\Delta \rho/\rho} = -\frac{\Delta P}{\Delta \forall/\forall} \qquad \textbf{(2.10)}$$

After rearranging Eq. (2.9) by considering Eq. (2.10) a new expression for the wave speed is obtained:

$$a^2 = \frac{K/\rho}{1 + (K/A)(\Delta A/\Delta P)} \quad \textbf{(2.11)}$$

Eq. (2.11) can be modified in order to implement support type and youngs modulus of elasticity effect on the wave speed. There are three support cases:

a) Pipe anchored at its upstream end only

b) Pipe anchored throughout against axial movement

c) Pipe anchored with expansion joints throughout

The term $\Delta A/(A\,\Delta P)$ from Eq. (2.11) must be evaluated for these three cases. In order to do that we need to define Poisson's ratio, μ, which is defined by

$$\mu = -\frac{lateral\ unit\ strain}{axial\ unit\ strain} = -\frac{\xi}{\xi_1} \quad \textbf{(2.12)}$$

Also it is known that change in area is the result of a total lateral or circumferential strain, ξ_t

$$\xi_t = \xi_2 - \mu\xi_1 \quad \textbf{(2.13)}$$

Relationship between stress and strain can be shown as below:

$$\xi_2 = \frac{\sigma_2}{E} \qquad \xi_1 = \frac{\sigma_1}{E} \quad \textbf{(2.14)}$$

Where;

σ_1= axial unit stress

σ_2= lateral unit stress

The equations of these stresses are given below:

Derivation of lateral (hoop) unit stress:

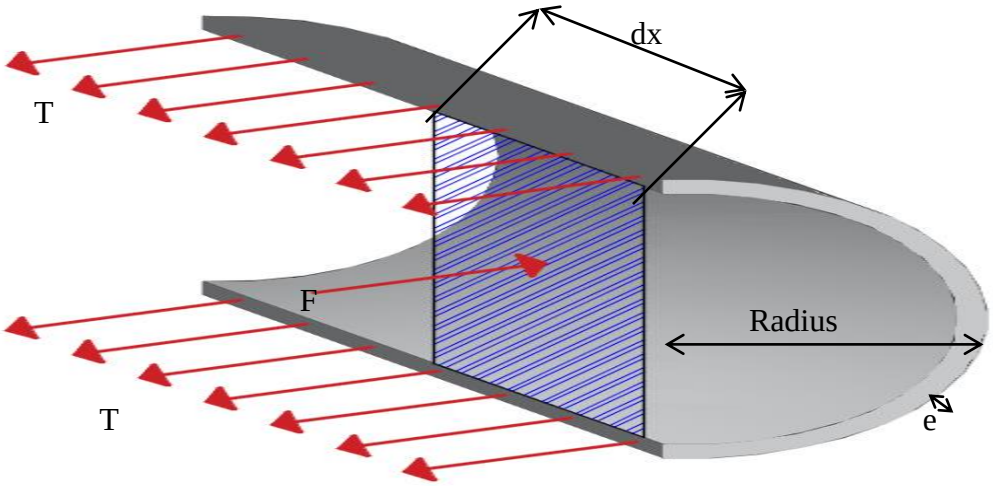

Figure 2-4: 3-D view for circumferential pipe stress

Considering the pipe shown in Figure 2-4 it can be assumed that it has internal pressure value 'P' and unit length of 'dx' therefore;

$$F = P(2r)dx \quad \textbf{(2.15)}$$

$$T = \sigma_2 A_{wall} = \sigma_2 e(dx) = Tensile\ forces \quad \textbf{(2.16)}$$

$$F = 2T \quad \textbf{(2.17)}$$

$$\sigma_2 = \frac{P(2r)}{2e} = Lateral\ unit\ stress \quad \textbf{(2.18)}$$

Derivation of axial unit stress:

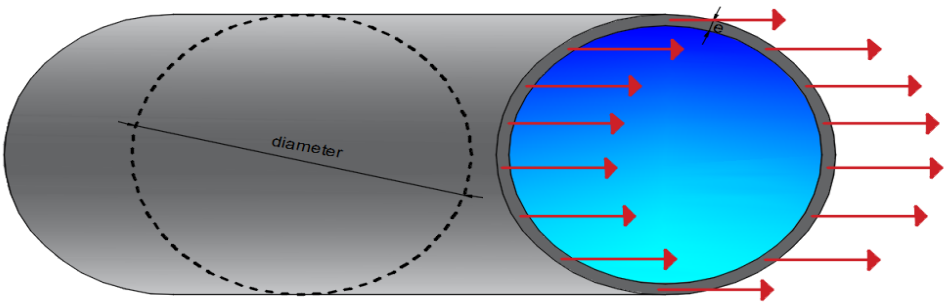

Figure 2-5: Cross section view for axial pipe stress

Considering the pipe shown in Figure 2-5;

$$F = P\pi r^2 \tag{2.19}$$

$$A = 2\pi re \tag{2.20}$$

$$\sigma_1 = \frac{F}{A} = \frac{P\pi r^2}{2\pi rt} = \frac{DP}{4e} \tag{2.21}$$

Finally the stress equations are expressed as shown below;

$$\sigma_2 = \frac{T_f}{e} = \frac{\gamma HD}{2e} \qquad \sigma_1 = \frac{\gamma HA}{\pi De} = \frac{DP}{4e}$$

Case a: Pipe anchored at its upstream end only

$$\frac{\Delta A}{A\Delta P} = \frac{2\Delta\xi_T}{\Delta P} = \frac{2}{\Delta P}(\Delta\xi_2 - \mu\Delta\xi_1) = \frac{2}{\Delta PE}(\Delta\sigma_2 - \mu\Delta\sigma_1) = \frac{D}{Ee}\left(1 - \frac{\mu}{2}\right) \tag{2.22}$$

Case b: Pipe anchored throughout therefore $\boldsymbol{\xi_1 = 0}$, and $\boldsymbol{\sigma_1 = \mu\sigma_2}$, so

$$\frac{\Delta A}{A\Delta P} = \frac{2}{\Delta PE}(\Delta\sigma_2 - \mu^2\Delta\sigma_2) = \frac{D}{Ee}(1 - \mu^2) \tag{2.23}$$

Case c: Pipe anchored with expansion joints throughout $\boldsymbol{\sigma_1 = 0}$, $\mu = 0$ so

$$\frac{\Delta A}{A\Delta P} = \frac{2\Delta\sigma_2}{\Delta PE} = \frac{D}{Ee} \tag{2.24}$$

Now that $\Delta A/(A\,\Delta P)$ term is obtained in terms of different anchorage scenarios therefore wave speed equation can be written as;

$$a = \frac{\sqrt{K/\rho}}{\sqrt{1 + [(K/E)(D/e)]c_1}} \tag{2.25}$$

Value of c_1 will take the values as shown below depending on the cases described above;

a) $c_1 = 1 - \frac{\mu}{2}$

b) $c_1 = 1 - \mu^2$

c) $c_1 = 1$

Eq. (2.25) is the final form of the pressure wave speed and is used on transient events for calculation of pressure and discharge fluctuations.

Figure 2-6 shows sequence of events triggered by a sudden valve closure located at the downstream end of a pipe attached to a constant-head reservoir. No friction is considered in this simple system. T_r is equal to $2L/a$. It is the time duration for the wave to travel upstream and get reflected by the reservoir and come back to the valve.

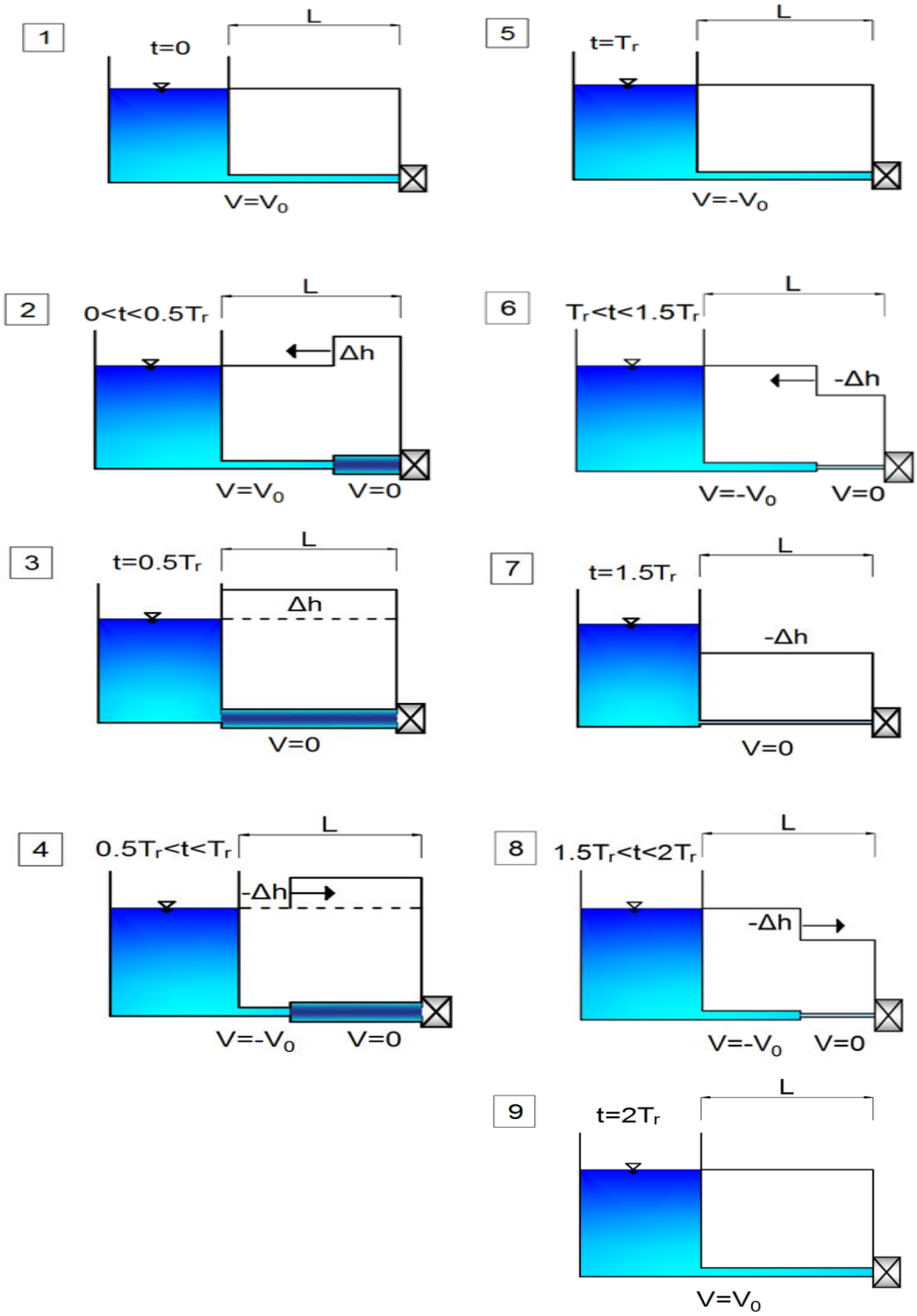

Figure 2-6: Sequence of events for one period (T=4L/a) after sudden valve closure

2.2 Derivation of Partial Differential Equations for Transient Flow

In this section equation of motion and continuity equation will be applied to a control volume in a pipe in order to derive partial differential transient equations. In the next sections details of the derivations will be presented.

2.2.1 Conservation of Mass

To apply the continuity equation to an inclined pipe segment of Figure 2-7 the following assumptions are made;

- Flow and wave motions are one dimensional, i.e. planar
- Conduit is elastic and constant cross-section
- Fluid is single-phase liquid and is "slightly" compressible
- Control volume is nontranslating (fixed)

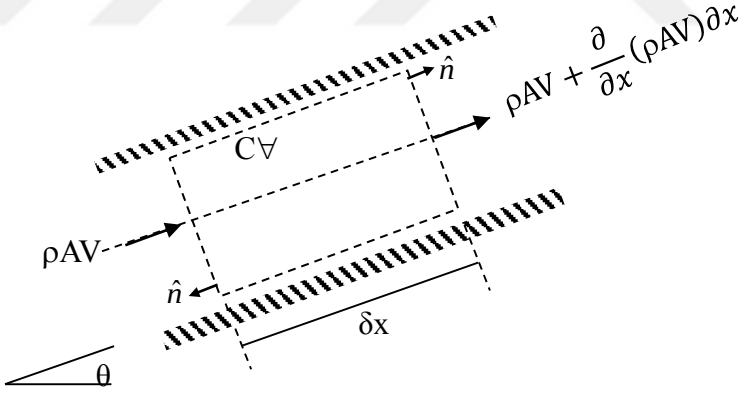

Figure 2-7: Continuity equation control volume

In Figure 2-7 the mass fluxes of fluid entering and exiting the control volume can be seen. Conservation of mass law, given in Eq. (2.26) is applied to the above control volume.

$$\frac{\partial}{\partial t}\int_{C\forall}\rho d\forall + \sum_{CS}\rho\vec{V}(\vec{A}.\vec{n}) = 0 \qquad \textbf{(2.26)}$$

This law indicates that the rate of mass inflow into the control volume is just equal to the time rate of increase of mass within the control volume.

Further simplifications yields below equation steps (assuming density is constant in the control volume);

$$\frac{\partial}{\partial t}\int_{C\forall}\rho d\forall = \frac{\partial}{\partial t}\rho\int_{C\forall} d\forall = \frac{\partial}{\partial t}(\rho A\delta x) = \frac{\partial}{\partial t}(\rho A)\delta x \qquad \textbf{(2.27)}$$

$$\sum_{CS}\rho\vec{V}(A.\vec{n}) = \sum_{CS}\rho VA = \left[\rho VA + \frac{\partial}{\partial x}(\rho VA)\delta x\right] - \rho VA = \frac{\partial}{\partial x}(\rho VA)\delta x \qquad \textbf{(2.28)}$$

By substituting Eqs. (2.27 – 2.28) into the Eq. (2.26) below equation is obtained;

$$\frac{\partial}{\partial t}(\rho A\delta x) + \frac{\partial}{\partial x}(\rho VA)\delta x = 0 \qquad \textbf{(2.29)}$$

By dividing Eq. (2.29) by δx and taking partial derivatives below equation is obtained;

$$\rho\frac{\partial A}{\partial t} + \mathrm{A}\frac{\partial \rho}{\partial t} + \rho\mathrm{A}\frac{\partial V}{\partial x} + \mathrm{VA}\frac{\partial \rho}{\partial x} + \rho\mathrm{V}\frac{\partial A}{\partial x} = 0 \qquad \textbf{(2.30)}$$

We know that $\frac{\delta\rho}{\rho} = \frac{\delta P}{K}$ and $\frac{\delta \mathrm{A}}{A} = \frac{\mathrm{D}\delta \mathrm{P}}{\mathrm{Ee}}$ or $\frac{\delta \mathrm{A}}{\mathrm{A}} = \frac{Dc_1}{Ee}\delta P$ (c_1 is close to 1).

Therefore, further simplifications can be done to reduce equation to a simpler form;

$$\frac{1}{K}\left(\frac{\partial P}{\partial t} + V\frac{\partial P}{\partial x}\right) + \frac{D}{Ee}\left(\frac{\partial P}{\partial t} + V\frac{\partial P}{\partial x}\right) + \frac{\partial V}{\partial x} = 0 \qquad \textbf{(2.31)}$$

$$\left(\frac{1}{K} + \frac{D}{Ee}\right)\left(\frac{\partial P}{\partial t} + V\frac{\partial P}{\partial x}\right) + \frac{\partial V}{\partial x} = 0 \qquad \textbf{(2.32)}$$

$$\left(\frac{\partial P}{\partial t} + V\frac{\partial P}{\partial x}\right) + \frac{1}{\left(\frac{1}{K} + \frac{D}{Ee}\right)}\frac{\partial V}{\partial x} = 0 \qquad \textbf{(2.33)}$$

$$\frac{1}{\left(\frac{1}{K} + \frac{D}{Ee}\right)}\frac{(K/\rho)\rho}{K} = \rho\frac{K/\rho}{\left(1 + \frac{KD}{Ee}\right)} = \rho a^2 \qquad \textbf{(2.34)}$$

$$\left(\frac{\partial P}{\partial t} + V\frac{\partial P}{\partial x}\right) + \rho a^2 \frac{\partial V}{\partial x} = 0 \qquad \textbf{(2.35)}$$

Lastly, the partial differential form of continuity equation is obtained as shown in Eq. (2.36);

$$L_1 = \frac{1}{\rho}\left(\frac{\partial P}{\partial t} + V\frac{\partial P}{\partial x}\right) + a^2 \frac{\partial V}{\partial x} = 0 \qquad \textbf{(2.36)}$$

In which Eq. (2.36) is labeled as L_1.

2.2.2 Conservation of Momentum

Conservation of momentum in integral form is shown in Eq. (2.37);

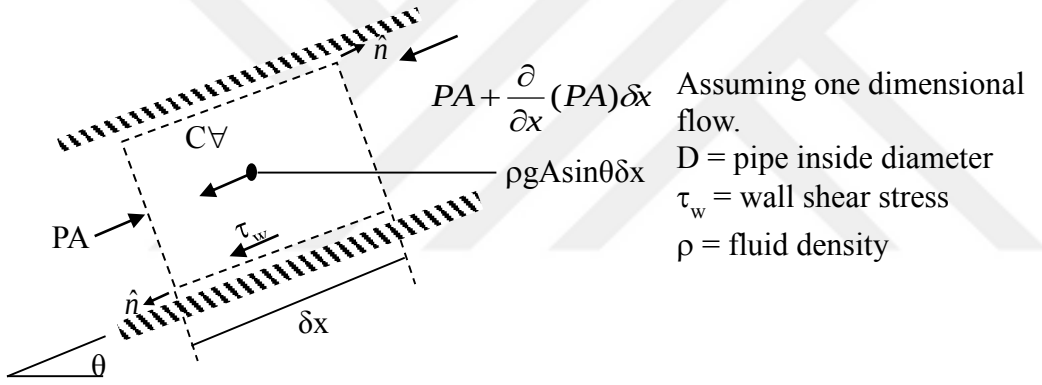

Figure 2-8: Conservation of momentum control volume

$$\sum F_x = \frac{\partial}{\partial t}\int_{C\forall} \rho V d\forall + \sum_{CS} \rho V_x (\vec{V}\hat{n}) A \qquad \textbf{(2.37)}$$

The above equation indicates that mass times acceleration is equal to sum of all forces acting on the control volume. Summation of forces acting on the control volume is;

$$\sum F_x = PA - \left[PA + \frac{\partial}{\partial x}(PA)\delta x\right] - \tau_w \pi D \delta x - \rho g A \sin\theta\, \delta x \qquad \textbf{(2.38)}$$

By neglecting second order effect of changes in pipe area due to pressure changes it reduces to;

$$\sum F_x \cong -\left(A\frac{\partial P}{\partial x} + \tau_w \pi D + \rho g A \sin\theta\right) \tag{2.39}$$

Now net rate of momentum change inside the control volume and the flux terms can be written as shown below;

$$\frac{\partial}{\partial t}\int_{C\forall} \rho V d\forall = \frac{\partial}{\partial t}\left(\rho V \int_{C\forall} d\forall\right) = \frac{\partial}{\partial t}(\rho V A \delta x) = \frac{\partial}{\partial t}(\rho V A)\delta x \tag{2.40}$$

$$\begin{aligned}\sum_{CS} \rho V_x (\vec{V}\hat{n}) A &= \sum_{CS} \rho V^2 A = \left[\rho V^2 A + \frac{\partial}{\partial x}(\rho V^2 A)\delta x - \rho V^2 A\right] \\ &= \frac{\partial}{\partial x}(\rho V^2 A)\delta x\end{aligned} \tag{2.41}$$

By using Eqs. (2.40 – 2.41) momentum equation can be written as shown below;

$$-\left(A\frac{\partial P}{\partial x} + \tau_w \pi D + \rho g A \sin\theta\right)\delta x = \frac{\partial}{\partial t}(\rho V A)\delta x + \frac{\partial}{\partial x}(\rho V^2 A)\delta x \tag{2.42}$$

By expanding the right hand side of Eq. (2.42);

$$\frac{\partial}{\partial t}(\rho V A) + \frac{\partial}{\partial x}(\rho V^2 A) = V\left[\frac{\partial}{\partial t}(\rho A) + \frac{\partial}{\partial x}(\rho V A)\right] + \rho A\left(\frac{\partial V}{\partial t} + V\frac{\partial V}{\partial x}\right) \tag{2.43}$$

It should be noted that on the right hand side of Eq. (2.43) the first expression within the brackets represents the continuity equation, that is Eq. (2.29) which is equal to zero.

$$\left[\frac{\partial}{\partial t}(\rho A) + \frac{\partial}{\partial x}(\rho V A)\right] = 0$$

Therefore by further simplification of Eq. (2.42) below equations are derived;

$$-\left(A\frac{\partial P}{\partial x} + \tau_w \pi D + \rho g A \sin\theta\right)\delta x = +\rho A\left(\frac{\partial V}{\partial t} + V\frac{\partial V}{\partial x}\right) \tag{2.44}$$

Dividing Eq. (2.44) by ρA and substituting $A = \pi D^2/4$;

$$-\left(\frac{1}{\rho}\frac{\partial P}{\partial x} + \frac{4\tau_w}{\rho D} + g\sin\theta\right) = \frac{\partial V}{\partial t} + V\frac{\partial V}{\partial x} \tag{2.45}$$

Final form of momentum equation is given by Eq. (2.46) with the expression F below;

$$\frac{4\tau_w}{\rho D} + g\sin\theta = F$$

$$L_2 = \frac{1}{\rho}\frac{\partial P}{\partial x} + \frac{\partial V}{\partial t} + V\frac{\partial V}{\partial x} + F = 0 \qquad \textbf{(2.46)}$$

In which Eq. (2.46) is labeled as L_2.

2.3 Solution by Method of Characteristics

The partial differential form of continuity and momentum equations were derived previously and the final form of these equations were given as Eq. (2.36) and Eq. (2.46). By using an unknown multiplier λ these two equations are combined linearly as;

$$L = L_1 + \lambda L_2 = \frac{\partial P}{\partial t} + V\frac{\partial P}{\partial x} + \rho a^2\frac{\partial V}{\partial x} + \lambda\left(\frac{\partial V}{\partial t} + V\frac{\partial V}{\partial x} + \frac{1}{\rho}\frac{\partial P}{\partial x} + F\right) = 0 \qquad \textbf{(2.47)}$$

By arranging the terms in the following way, we obtain Eq. (2.48);

$$\left[\frac{\partial P}{\partial t} + \left(V + \frac{\lambda}{\rho}\right)\frac{\partial P}{\partial x}\right] + \lambda\left[\frac{\partial V}{\partial t} + \left(V + \frac{\rho a^2}{\lambda}\right)\frac{\partial V}{\partial x}\right] + \lambda F = 0 \qquad \textbf{(2.48)}$$

Since P= P(x , t) and V= V(x , t) using the chain rule from calculus, these terms can be written as;

$$\frac{dV}{dt} = \frac{\partial V}{\partial t} + \frac{\partial V}{\partial x}\frac{dx}{dt} \qquad \textbf{(2.49)}$$

$$\frac{dP}{dt} = \frac{\partial P}{\partial t} + \frac{\partial P}{\partial x}\frac{dx}{dt} \qquad \textbf{(2.50)}$$

For Eqs. (2.49) and (2.50) to be valid, Eq. (2.51) should be satisfied;

$$\left(V + \frac{\lambda}{\rho}\right) = \frac{dx}{dt} = \left(V + \frac{\rho a^2}{\lambda}\right) \qquad \textbf{(2.51)}$$

$$\lambda = \pm\rho A \qquad \textbf{(2.52)}$$

$$\frac{dx}{dt} = V \pm a \qquad \textbf{(2.53)}$$

By substituting Eq. (2.49 – 2.50) and value of λ into Eq. (2.48) a new equation is obtained as;

$$\left.\begin{aligned} \frac{dx}{dt} &= V + a \\ \frac{1}{\rho}\frac{dP}{dt} + a\frac{dV}{dt} + aF &= 0 \end{aligned}\right\} : C^{+} \qquad \textbf{(2.54)}$$

$$\left.\begin{aligned} \frac{dx}{dt} &= V - a \\ \frac{1}{\rho}\frac{dP}{dt} - a\frac{dV}{dt} - aF &= 0 \end{aligned}\right\} : C^{-} \qquad \textbf{(2.55)}$$

Since magnitude of acoustic speed is much larger than flow velocity V we can simplify Eq. (2.53) as;

$$\frac{dx}{dt} \approx \pm a$$

In summary;

$$\pm\frac{1}{\rho}\frac{dP}{dt} - a\frac{dV}{dt} - aF = 0 \qquad \text{compatibility equations}$$

and

$$\frac{dx}{dt} \approx \pm a \qquad \text{characteristic equations}$$

(+) compatibility equation is valid on the (+) characteristic line and (-) compatibility equation is valid on the (-) characteristic line.

$\frac{dx}{dt} = +a$ and $\frac{dx}{dt} = -a$ terms represent two straight lines having slopes of $+\frac{1}{a}$ and $-\frac{1}{a}$ respectively. Figure 2-9 shows the space – time domain intervals with those C^{+} and C^{-} lines.

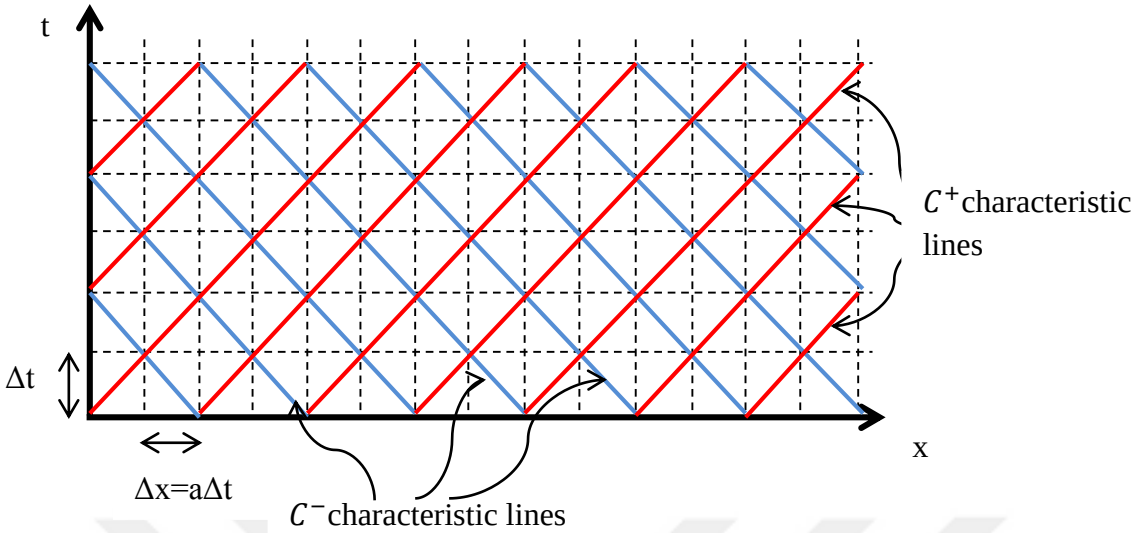

Figure 2-9: Compatibility equations grid system

Solution of compatibility equations will begin from a known steady state flow at t=0 and start to build the solution by solving two compatibility equations together in space and time. Physically these lines represent the path in which a disturbance travels.

As it can be seen from Figure 2-9 there is a condition that must be satisfied in order to obtain accurate results from the solutions of these equations, this condition is called 'Courant Condition'.

Courant condition states that;

$$\frac{\Delta x}{\Delta t} \leq a \qquad \textbf{(2.56)}$$

By rearranging Eqs. (2.54 – 2.55) in terms of discharges and head values;

$$\left.\begin{aligned} \frac{dx}{dt} &= +a \\ \frac{g}{a}\frac{dH}{dt} + \left(\frac{1}{A}\frac{dQ}{dt}\right) + \frac{fQ|Q|}{2DA^2} &= 0 \end{aligned}\right\} : C^+ \qquad \textbf{(2.57)}$$

$$\left.\begin{aligned} \frac{dx}{dt} &= -a \\ -\frac{g}{a}\frac{dH}{dt} + \left(\frac{1}{A}\frac{dQ}{dt}\right) + \frac{fQ|Q|}{2DA^2} &= 0 \end{aligned}\right\} : C^- \qquad \textbf{(2.58)}$$

Therefore, two ordinary differential equations with two unknown variables, which are Q and H, are obtained in which H is the piezometric head and equal to $z + \frac{P}{\gamma}$. Since the time interval used for the transient analysis purposes are usually small, a first-order finite difference scheme is suggested for solving these two equations simultaneously by Wylie and Streeter (1978). However, when there are large friction losses then a second order approximation may yield more accurate results therefore second order approximation should be used in such cases in order to avoid instability of finite-difference scheme.

2.3.1 Time Discretization of Compatibility Equations

As mentioned previously first order approximation yields sufficiently accurate results except for high friction schemes, in other words, when the friction term dominates the equation. In this section compatibility equations will be discretized in time using both first-order and second-order approximations. Illustration of the system of finite difference approximation scheme can be seen on Figure 2-10.

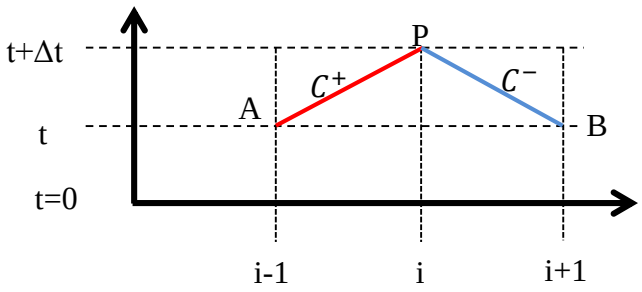

Figure 2-10: Characteristics lines for point solution in x-t plane

2.3.1.1 First Order Approximation

By multiplying Eqs. (2.57 – 2.58) by $\frac{adt}{g} = \frac{dx}{g}$ (from courant condition $a\Delta t = dx$) equations are converted into integration form along characteristics line. In integration form Eq. (2.57 – 2.58) can be written as;

$$\int_{H_A}^{H_P} dH + \frac{a}{gA}\int_{Q_A}^{Q_P} dQ + \frac{f}{2gDA^2}\int_{X_A}^{X_P} Q|Q|dx = 0 \qquad \textbf{(2.59)}$$

By applying the first order approximation to the above integration form the below equations are obtained;

$$H_P - H_A + \frac{a}{gA}(Q_P - Q_A) + \frac{f\Delta x}{2gDA^2}Q_A|Q_A| = 0 \qquad \textbf{(2.60)}$$

A similar integration between points B-P yields;

$$H_P - H_B - \frac{a}{gA}(Q_P - Q_B) - \frac{f\Delta x}{2gDA^2}Q_B|Q_B| = 0 \qquad \textbf{(2.61)}$$

The above Eqs. (2.60 – 2.61) show the basic algebraic relations that describe the propagation of head and discharge in a pipeline during a transient event. Solving the above equations for the unknown H_P the two equations can be written as;

$$C^+: H_P = H_A - \frac{a}{gA}(Q_P - Q_A) - \frac{f\Delta x}{2gDA^2}Q_A|Q_A| \qquad \textbf{(2.62)}$$

$$C^-: H_P = H_B + \frac{a}{gA}(Q_P - Q_B) + \frac{f\Delta x}{2gDA^2}Q_B|Q_B| \qquad \textbf{(2.63)}$$

By denoting;

$\frac{a}{gA} = B$ and $R = \frac{f\Delta x}{2gDA^2}$ the equation simplifies as

$$C^+: H_P = H_A - B(Q_P - Q_A) - RQ_A|Q_A| \quad \textbf{(2.64)}$$

$$C^-: H_P = H_B + B(Q_P - Q_B) + RQ_B|Q_B| \quad \textbf{(2.65)}$$

Further simplification can be made by adding two more constants into Eqs. (2.64 – 2.65) called as C_P and C_M;

$$C_P = H_{i-1} + BQ_{i-1} - RQ_{i-1}|Q_{i-1}| \quad \textbf{(2.66)}$$

$$C_M = H_{i+1} - BQ_{i+1} + RQ_{i+1}|Q_{i+1}| \quad \textbf{(2.67)}$$

The final and most simplified form of the compatibility equations reduce to (in nodal form);

$$C^+: H_{P_i} = C_P - BQ_{P_i} \quad \textbf{(2.68)}$$

$$C^-: H_{P_i} = C_M + BQ_{P_i} \quad \textbf{(2.69)}$$

In brief, solution starts from the known values of Q_{A_t}, H_{A_t}, Q_{B_t}, H_{B_t} at $t = t_0$ and proceeds to find the unknown $Q_{P_{t+\Delta t}}$, $H_{P_{t+\Delta t}}$ values at point P (Note that the time interval increases as solution proceeds further by $t_j = t_{j-1} + \Delta t$).

Moreover, for every node along the pipeline the same calculations are done over time and space but there might be boundaries on some nodes and these boundaries must also be implemented through the solution matrix which will later be discussed at 'Chapter 3'

CHAPTER 3

BOUNDARY EQUATIONS

In ‘Chapter 2’ derivation of compatibility equations and the solution structure of these equations were illustrated. Briefly, these compatibility equations are computed in time and space through nodal points along the pipe in order to simulate transient variation of pressure and discharge. Now some basic boundary conditions must be introduced in order to complete simulations of complex scenarios. The boundaries that were used in the development of H-Hammer is listed below:

1. Pipe Section
2. Series Junction
3. Branching Junction
4. Upstream Reservoir with Constant Head
5. Upstream Reservoir with Variable Head
6. Centrifugal Pumps (Single-Series-Parallel Connected)
7. Air Chamber with Orifice
8. Interior Valve
9. Downstream Valve
10. Surge Tank with Standpipe
11. Air Valve
12. Downstream Reservoir with Constant Head
13. Downstream Dead End
14. Air Chamber with Standpipe
15. Surge Tank with Throttled Orifice

Equations for these boundaries will be presented in this chapter and by using these boundaries transient events can be simulated.

3.1 Interior Pipe Section

Eqs. (2.68 – 2.69) are solved simultaneously in order to obtain head and discharge value located in the interior part of the solution domain.

If there are no series junctions ,which means diameters of the series pipes are same, and if pipe material is the same then the pressure wave speed value of these nodes will have the equal magnitude.

Therefore, having equal pressure wave speed magnitude and cross sectional area the compatibility equations can be further simplified by solving Eqs. (2.68 – 2.69) can be solved simultaneously.

Further simplified equations of transient pressure head, discharge and Figure 3-1 that shows identical series pipes are given below;

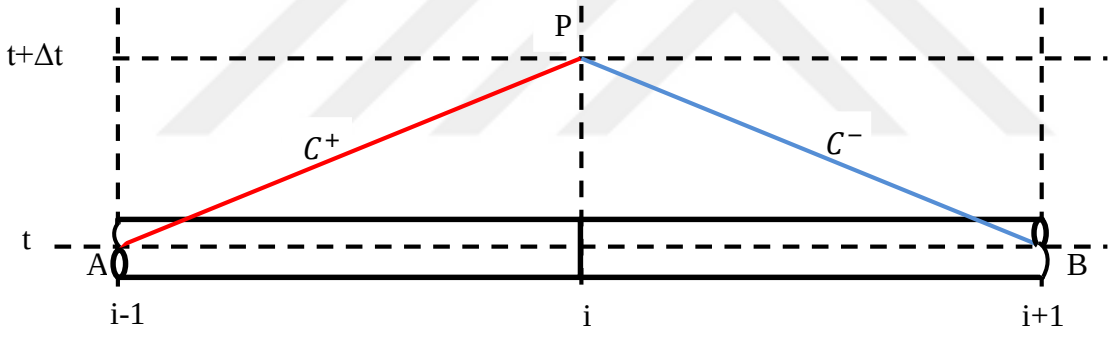

Figure 3-1: Solution of identical pipes connected in series

$$H_{P_i} = \frac{1}{2}(C_P + C_M) \quad \textbf{(3.1)}$$

$$Q_{P_i} = \frac{(C_P - H_{P_i})}{B} \quad \textbf{(3.2)}$$

C_P, C_M were introduced in Eqs. (2.66 – 2.67) and as previously shown $B = \frac{a}{gA}$

3.2 Series Junction

Although very similar to 'Pipe Section' formulation there are minor differences when there is series junctions on the pipeline system in terms of transient solution. Series junction can occur due to change in diameter or pressure wave speed between consecutive pipe sections.

On identical pipes connected in series, simultaneous solution of the compatibility equations yields Eq. (3.1) and Eq. (3.2). However, this is no longer true for pipes that are not identical since B values are not the same in each pipe anymore.

$$B_1 = \frac{a_1}{gA_1}, \qquad B_2 = \frac{a_2}{gA_2}$$

Typically, either the diameter or the wave speed of consecutive pipes have different values. In order to solve series junction Eq. (2.68 – 2.69) should be solved simultaneously only on this case BQ_{P_i} terms will not cancel each other and thus general solution will be different compared to Eq. (3.1 – 3.2).

To solve compatibility equation for series junction two assumptions are made;

- Continuity is preserved along the junction point (Q_1=Q_2 on below Figure 3-2)

$$Q_{P_{1,NS}} = Q_{P_{2,1}} \tag{3.3}$$

- There is a common pressure head on left and right side of the junction

$$H_{P_{1,NS}} = H_{P_{2,1}} \tag{3.4}$$

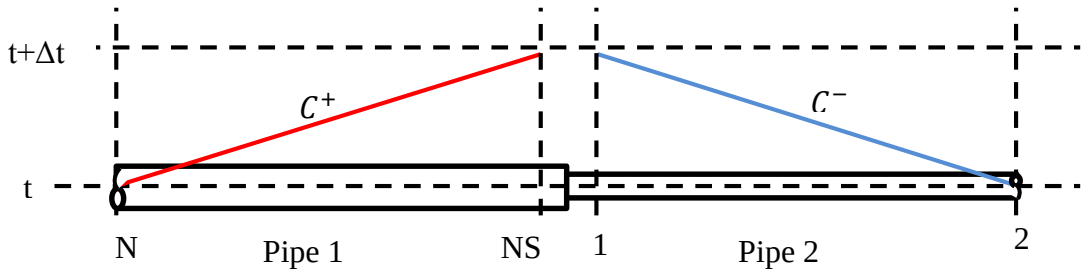

Figure 3-2: Solution of series junction pipes

Double subscript on above equations illustrates pipe number and node number respectively.

Therefore, the simultaneous solution of Eqs (2.68 – 2.69 – 3.3 – 3.4) yields;

$$Q_{P_{2,1}} = \frac{\left(C_{P_1} - C_{M_2}\right)}{B_1 + B_2} \qquad \textbf{(3.5)}$$

The other unknowns can be determined by directly inputting discharge value into either Eq. (2.68) or Eq. (2-69).

3.3 Branching Junction

Branching junctions are solved very similar to series junction by using continuity and assuming a common head at the junction location by neglecting minor losses. However, on this case although heads are equal at the junction, discharges maybe different in each pipe. Figure 3-3 illustrates the compatibility equations that are used in branching junctions.

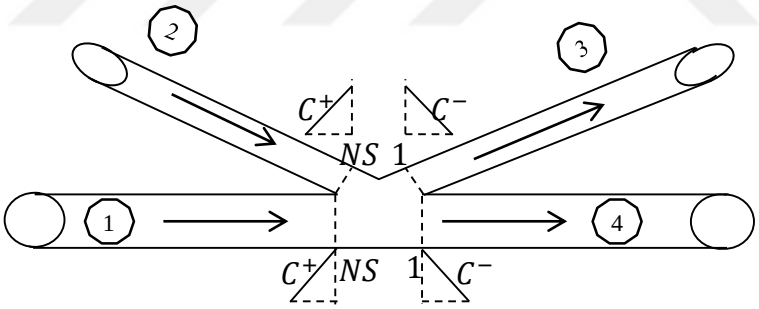

Figure 3-3: Solution of branching junction pipes

From Figure 3-3 the continuity equation can be written as;

$$Q_{P_{1,NS}} + Q_{P_{2,NS}} - Q_{P_{3,1}} - Q_{P_{4,1}} = 0 \qquad \textbf{(3.6)}$$

Moreover, by neglecting the minor losses a common head can be used for all pipes as;

$$H_P = H_{P_{1,NS}} = H_{P_{2,NS}} = H_{P_{3,1}} = H_{P_{4,1}} \qquad \textbf{(3.7)}$$

By using above assumptions and Eqs. (2.68 – 2.69), discharge at each node can be formulated as shown below;

$$Q_{P_{1,NS}} = -\frac{H_P}{B_1} + \frac{C_{P_1}}{B_1}$$

$$Q_{P_{2,NS}} = -\frac{H_P}{B_2} + \frac{C_{P_2}}{B_2}$$

$$-Q_{P_{3,1}} = -\frac{H_P}{B_3} + \frac{C_{M_3}}{B_3}$$

$$-Q_{P_{4,1}} = -\frac{H_P}{B_4} + \frac{C_{M_4}}{B_4}$$

By substituding all the discharge formulations in Eq. (3.6);

$$\sum Q_P = 0 = -H_P \sum^{i} \frac{1}{B_i} + \frac{C_{P_1}}{B_1} + \frac{C_{P_2}}{B_2} + \frac{C_{M_3}}{B_3} + \frac{C_{M_4}}{B_4} \quad \textbf{(3.8)}$$

By rearranging Eq. (3.8);

$$H_P = \frac{\frac{C_{P_1}}{B_1} + \frac{C_{P_2}}{B_2} + \frac{C_{M_3}}{B_3} + \frac{C_{M_4}}{B_4}}{\sum\left(\frac{1}{B_i}\right)} \quad \textbf{(3.9)}$$

Therefore, common pressure head in branching junction location can be calculated by using Eq. (3.9) and discharge in each pipe at the junction can be calculated by inputting this pressure head into the relevant compatibility.

3.4 Upstream Reservoir with Constant Head

During the short duration of transient events the water surface elevation of large upstream reservoirs can be assumed as constant. Mathematically and physically this boundary can be described as;

$H_{P_i} = H_R$ Where $H_R = \text{Constant Reservoir Head above the datum}$

Figure 3-4 illustrates compatibility equation and solution grid for upstream constant head boundary;

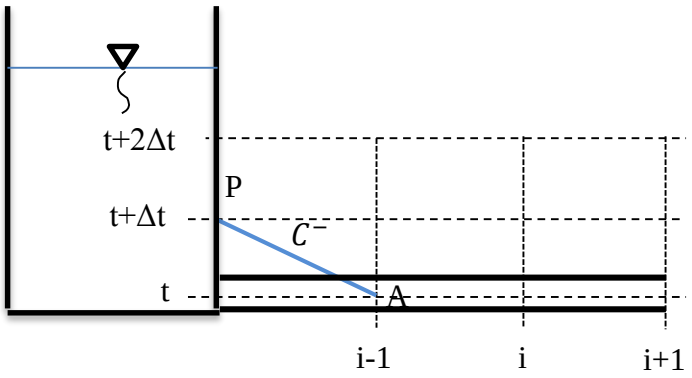

Figure 3-4: Solution of upstream reservoir with a constant head

Figure 3-4 shows that in order to find discharge from the upstream reservoir a single C^- compatibility equation is used along with the upstream boundary condition. By starting from the known steady solution values one can obtain transient discharge values from the upstream reservoir boundary with the assumption that reservoir head is constant throughout the solution. The relating discharge equation is given below for transient solution of upstream reservoir;

$$Q_{P_R} = (H_{P_R} - C_M)/B \qquad \textbf{(3.10)}$$

3.5 Upstream Reservoir with Variable Head

Transient solution of upstream reservoir with variable head is almost similar to the upstream reservoir with constant head with only a minor difference in the assumption of constant head. Solution of upstream reservoir with variable head boundary requires a definition of head change in a known manner, i.e. a sine wave. In H-Hammer software sinusoidal waves are defined for this boundary therefore reservoir head will vary in time as a sinusoidal waves. The mathematical illustration of this boundary is given below as;

$$H_{P_R} = H_R + \Delta H \sin(\omega t) \qquad \textbf{(3.11)}$$

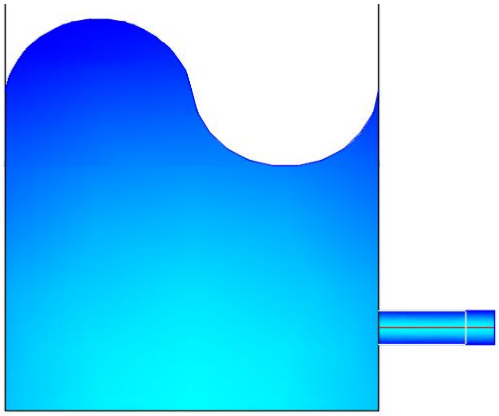

Figure 3-5: Physical illustration of upstream reservoir with variable head

in which ω is the circular frequency and ΔH is the amplitude of wave. Finally, Eq. (3.10) can be used to find unknown discharge value at each time step.

3.6 Centrifugal Pumps

Method of characteristics may be used to analyze transient events during pumping operations. In order to analyze centrifugal pumps two parameters must be incorporated into pressure head and discharge equations, which are change in pump head and pump torque. Pump head and torque changes during the transient event therefore a special boundary for the pump end of a pipeline have to be developed. In this chapter, first events following a complete power failure is explained and then dimensionless-homologous turbopump characteristics and their usages are overviewed. Lastly, the boundary conditions for single, series, parallel and complex ordered pump stations are developed. Equations are taken from Wylie and Streeter (1978).

3.6.1 Events Following a Complete Power Failure

Energy used to rotate the impeller is created by the torque exerted on the rotating shaft by the pump motor. This rotational motion of impeller causes flow through the pump and develops total dynamic head on the discharge flange of pump. In other

words, total head increase on the discharge side of the pump is provided by this motion and mathematical equation can be shown as (Wylie and Streeter's (1993));

$$tdh = \frac{V_d^2}{2g} + \frac{P_d}{\gamma} + z_d - \left(\frac{V_s^2}{2g} + \frac{P_s}{\gamma} + z_s\right) \quad \textbf{(3.12)}$$

After a power failure first, impeller' s motion is retarded due to failure of energy source. This retardation of impeller motion results in reduced total dynamic head and discharge which in return causes negative pressure waves to propagate downstream from discharge line and positive pressure waves to propagate towards the upstream of the suction line.

Next, flow in discharge line is reduced rapidly to zero and eventually reverse flow conditions occur while the impeller still rotates in the normal direction. When impeller rotates in normal direction and reverse flow through the pump occurs simultaneously, the pump is said to be operating in the zone of energy dissipation.

The rotation of impeller continues due to moment of inertia but it slows down rapidly and stops momentarily, upon this momentary stop impeller starts to rotate in reverse direction. This type of operation is called zone of turbine. When the pump operates in the zone of turbine the rotation speed of impeller increases in the reverse direction until it reaches a run away speed. With the increase in reverse speed, reverse flow through the pump is reduced due to effect of choking, this pump operation is called as reversed speed dissipation zone. As a result of this, positive and negative pressure waves are produced in the discharge and suction flanges of pumps.

Pipeline profile and time differentiation of hydraulic grade line should be superposed to each other because hydraulic grade line might fall below pipeline profile at some location. This causes vacuum due to negative pressures and water column separation might occur. When these separated water columns later rejoin an excessive amount of positive pressure is produced therefore it is highly undesirable case to have water column separation. Counter measures against pump transients should be allocated in

consideration of such cases and these precautions includes but not limited to air chambers, surge tanks and air valves.

3.6.2 Dimensionless-Homologous Turbopump Characteristics

Flow conditions can be described for a turbine as it can be for a pump. However a set of characteristics data is needed for each wicket gate settings. There are four quantities that are used to characterize turbine motion during pump operations which are the total dynamic head H, the discharge Q, the shaft torque T and the rotational speed of impeller N.

In most cases Q and N are preliminary determined and may be considered independent. From the known values of Q and N the values of H and T are determined in consideration of two assumptions which are;

1. The steady state characteristics hold for unsteady-state situations. Values of H and T are determined for each time step from the changing values of Q and N
2. Homologous relationships are valid.

Homologous relations mean that geometrically similar series of turbomachines may have similar turbine characteristics. These similarities are represented by;

$$\frac{H_1}{(N_1 D_1)^2} = \frac{H_2}{(N_2 D_2)^2} \quad \textbf{(3.13)}$$

$$\frac{Q_1}{\left(N_1 {D_1}^3\right)} = \frac{Q_2}{\left(N_2 {D_2}^3\right)} \quad \textbf{(3.14)}$$

Subscripts on above equations refer to two different sized units of centrifugal pumps. On above equations since D values are constants they can be taken out of the homologous relationships equations hence reducing it to;

$$\frac{H_1}{{N_1}^2} = \frac{H_2}{{N_2}^2} \quad \textbf{(3.15)}$$

$$\frac{Q_1}{N_1} = \frac{Q_2}{N_2} \quad \textbf{(3.16)}$$

Moreover, homologous relationships theory assumes that efficiency does not change with the size of the unit therefore;

$$\frac{T_1 N_1}{Q_1 H_1} = \frac{T_2 N_2}{Q_2 H_2} \tag{3.17}$$

By performing combinations of Eqs (3.15 - 3.16 – 3.17) final form of three homologous relationships are obtained as;

$$\frac{T_1}{{N_1}^2} = \frac{T_2}{{N_2}^2} \qquad \frac{H_1}{{Q_1}^2} = \frac{H_2}{{Q_2}^2} \qquad \frac{T_1}{{Q_1}^2} = \frac{T_2}{{Q_2}^2} \tag{3.18}$$

The above equations can be nondimensionalized by referring to rated condition values of centrifugal pump;

$$h = \frac{H}{H_R} \quad \beta = \frac{T}{T_R} \quad \upsilon = \frac{Q}{Q_R} \quad \alpha = \frac{N}{N_R} \tag{3.19}$$

Subscript R indicates the rated values of these quantities which means magnitudes at best efficiency.

Dimensionless-homologous relationships may now be expressed as shown below;

$$\frac{h}{\alpha^2}\ vs\ \frac{\upsilon}{\alpha} \qquad \frac{\beta}{\alpha^2}\ vs\ \frac{\upsilon}{\alpha} \qquad \frac{h}{\upsilon^2}\ vs\ \frac{\alpha}{\upsilon} \qquad \frac{\beta}{\upsilon^2}\ vs\ \frac{\alpha}{\upsilon} \tag{3.20}$$

Plot of $\frac{h}{\alpha^2}$ as ordinate and $\frac{\upsilon}{\alpha}$ as abscissa yields head-discharge relationship for any speed α for that unit. Moreover, similarly to the previous plot $\frac{\beta}{\alpha^2}$ as ordinate and $\frac{\upsilon}{\alpha}$ as abscissa illustrates torque-discharge relationship.

Mathematically it is difficult to handle these relationships without further simplification. The main reason why it is difficult is due to α value becoming zero at one point during analysis this causes some parameters to go to infinity therefore results in overflow error. To avoid this problem Marchal, Flesch and Suter devised a new curvature system which are;

$$\frac{h}{\alpha^2 + \upsilon^2}\ vs\ \tan^{-1}\frac{\upsilon}{\alpha} \quad and \quad \frac{\beta}{\alpha^2 + \upsilon^2}\ vs\ \tan^{-1}\frac{\upsilon}{\alpha} \tag{3.21}$$

By using Eq. (3.21) one can plot all four quadrants of a pump operation on a polardiagram of $\theta = \tan^{-1}\frac{v}{\alpha}\ vs\ r = \frac{h}{\alpha^2+v^2}$ and $\theta = \tan^{-1}\frac{v}{\alpha}\ vs\ r = \frac{\beta}{\alpha^2+v^2}$ which represents two closed curves that gives relationship between head and torque of the pump unit. Values of these curves at a certain angle can be found by below equations;

$$WH(x) = \frac{h}{\alpha^2 + v^2} \qquad WB(x) = \frac{\beta}{\alpha^2 + v^2} \qquad x = \pi + \tan^{-1}\frac{v}{\alpha} \qquad \textbf{(3.22)}$$

Furthermore, in most cases manufacturers of pumps can not provide data for full sutter curve and designers may obtain pump curves for only normal operating zone. In such cases the curves must be extended by performing a similitude analysis for the centrifugal pumps that have similar specific speeds and shapes. Currently in the literature there are complete sutter curve data for three different specific speeds which are N_s= 35, N_s= 147 and N_s= 261 in SI units. By making use of these known data sets a similitude analysis should be performed to complete unknown parts of sutter curve.

Zone of Turbine	Zone of Energy Dissipation	Normal Zone	Reversed Speed Dissipation Zone
$\nu \leq 0$	$\nu < 0$	$\nu \geq 0$	$\nu > 0$
$\alpha < 0$	$\alpha \geq 0$	$\alpha \geq 0$	$\alpha < 0$

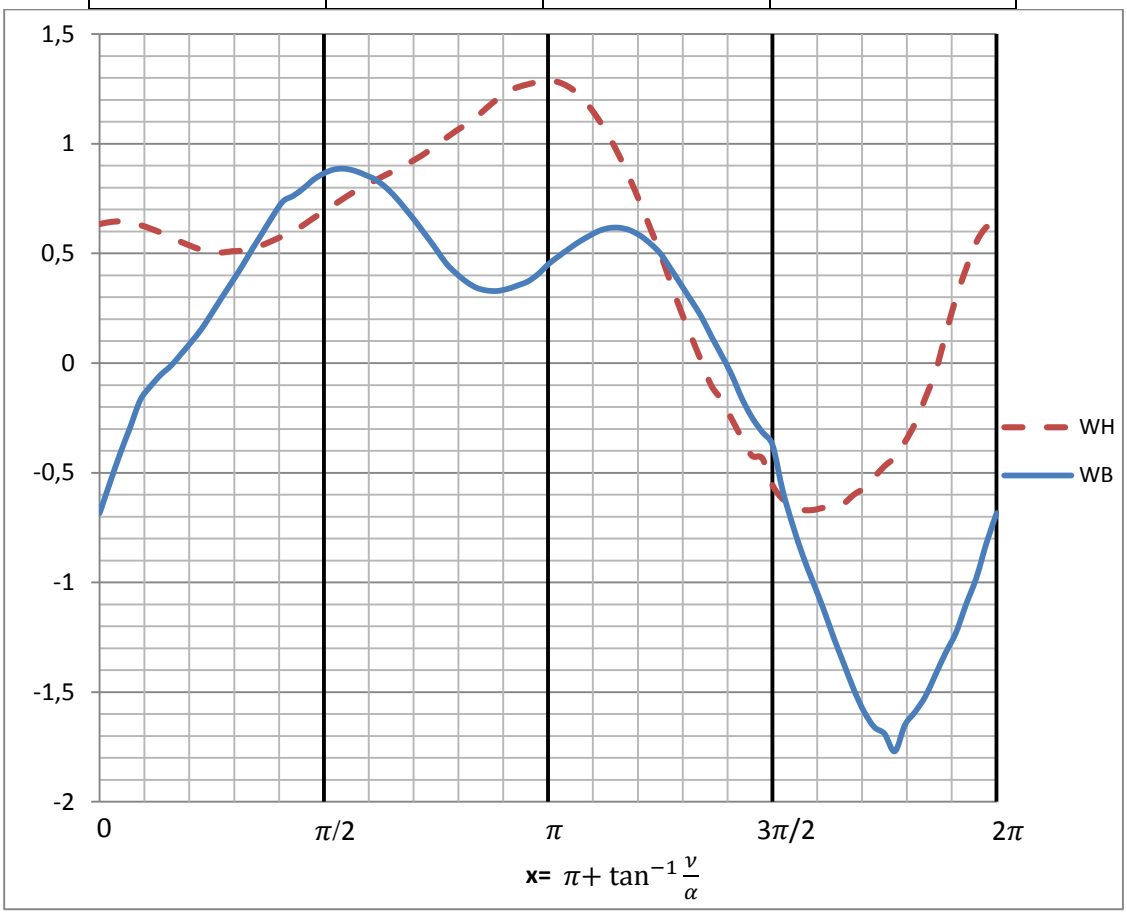

Figure 3-6: Complete Suter curve and pump operation zones

3.6.3 Transient Equations for Pump Failure

Two equations are developed in order to solve transient behaviour of pump operations which are;

- Head – Balance equation across the pump or if there is a valve across the pump and its discharge valve

- Torque – Angular Deceleration equation for rotating impeller and other masses

3.6.3.1 Head Balance Equation

There are three elements contributing to the head balance equation of pump boundary and these elements are head value at suction line, total dynamic head, valve head loss and pumping head. Below Eq. (3.23) describes relationship between these elements;

$$H_S + tdh - (H_{valve-loss}) = H_P \quad \textbf{(3.23)}$$

Moreover, below Figure 3-7 illustrates the grid relationships used on method of characteristics;

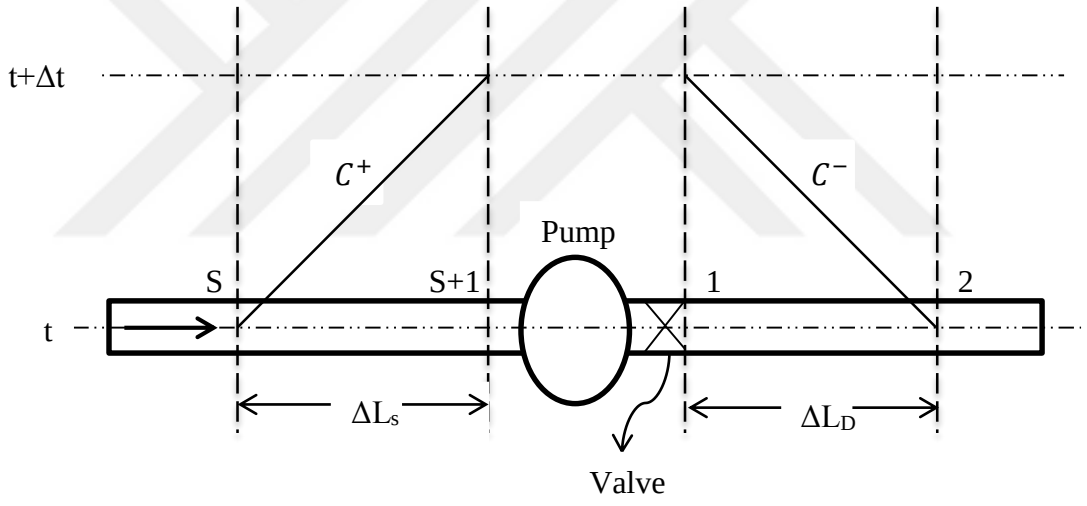

Figure 3-7: Grids for pump boundary equations

H_s on Eq. (3.23) is piezometric head at the suction flange of pump. Assuming there are S number of reaches on the suction side of the pump (S reaches = S + 1 sections) below C^+ equation can be written;

$$HS(S+1)_{t+\Delta t} = HS(S)_t - BS[QS(S+1)_{t+\Delta t} - QS(S)_t] - RS.QS(S)_t|QS(S)_t| \quad \textbf{(3.24)}$$

In more simplified form;

$$HS(S+1)_{t+\Delta t} = HCP - BS[QS(S+1)_{t+\Delta t}] \quad \textbf{(3.25)}$$

For the discharge flange assuming P is the first and B is the second section of the grid; C^- equation can be written as;

$$HP(1)_{t+\Delta t} = H(2)_t + B[QP(1)_{t+\Delta t} - Q(2)_t] + R.Q(2)_t|Q(2)_t| \quad \textbf{(3.26)}$$

In more simplified form;

$$HP(1)_{t+\Delta t} = HCM + B[QP(1)_{t+\Delta t}] \quad \textbf{(3.27)}$$

Assuming conservation of mass law holds for the discharge throughout suction to discharge flanges below equations can be written;

$$QSP(S+1) = QP(1) \quad \textbf{(3.28)}$$

By using the dimensionless homologous relationships an equation for total dynamic head is derived as shown below;

$$tdh = H_R.h = H_R(\alpha^2 + \nu^2)WH(\pi + \tan^{-1}\frac{\nu}{\alpha}) \quad \textbf{(3.29)}$$

In order to find WH value in the vicinity of operational value parabolic sutter curves must be linearized. This linearization can be done by storing values of WH with small intervals and replacing curves by straight lines by using these stored data. However, intervals should be small enough to represent curve with high accuracy. Figure 3-8 represents linearization of a WH segment;

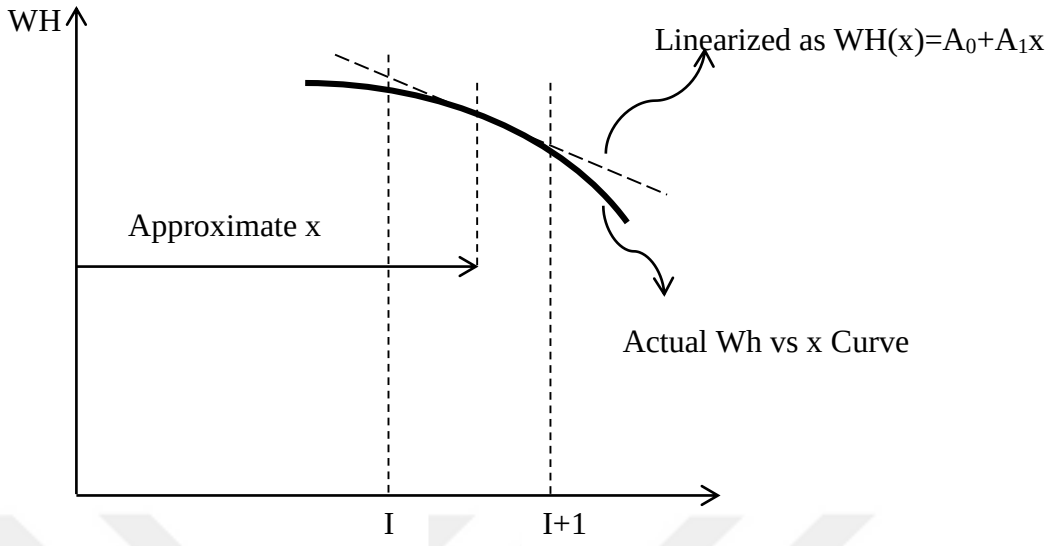

Figure 3-8: Linearization of WH segments

On above Figure 3-8, I=x/Δx+1

Equation of line after the linearization of this curve is a simple line equation as given below;

$$WH = A_0 + A_1 x \quad \textbf{(3.30)}$$

Values of A_0 and A_1 can be found from simple line geometry and is shown below;

$$A_1 = [WH(I+1) - WH(I)]/\Delta x \quad \textbf{(3.31)}$$

$$A_0 = WH(I+1) - I.A_1\Delta x \quad \textbf{(3.32)}$$

By substituding Eq. (3.30) into Eq. (3.29) the final form of tdh is obtained as;

$$tdh = H_R(\alpha^2 + \nu^2)\left[A_0 + A_1(\pi + \tan^{-1}\frac{\nu}{\alpha})\right] \quad \textbf{(3.33)}$$

Equation of valve head loss can be written as;

$$H_{valve-loss} = \frac{\Delta H \nu|\nu|}{\tau^2} \quad \textbf{(3.34)}$$

Where ΔH is the head loss across the valve for flow Q_R at τ =1. Values of τ can be found from the valve closure equation in a tabular form depending on time. By substituting Eqs. (3.34 – 3.33 – 3.27 – 3.25) into Eq. (3.23);

$$HCP - BS[QS(S+1)_{t+\Delta t}] + H_R(\alpha^2+\nu^2)\left[A_0 + A_1(\pi + \tan^{-1}\frac{\nu}{\alpha})\right] - \frac{\Delta H\nu|\nu|}{\tau^2} = HCM + B[QP(1)_{t+\Delta t}] \quad \textbf{(3.35)}$$

To further simplify above equation;

$$HPM = HCP - HCM \qquad QP(1) = \nu Q_R \qquad BSQ = (BS+B)Q_R$$

and Eq. (3.35) further reduces to;

$$F1 = HPM - BSQ.\nu + H_R(\alpha^2+\nu^2)\left[A_0 + A_1(\pi + \tan^{-1}\frac{\nu}{\alpha})\right] - \frac{\Delta H\nu|\nu|}{\tau^2} = 0 \quad \textbf{(3.36)}$$

Eq. (3.36) is the final form of head balance equation in which only two unknown remains which are ν and α. Later on this equation will be solved together with the speed change equation that will be derived next.

3.6.3.2 Torque – Angular Decelaration Equation

As explained previously during the transient event speed of pump impeller decelerates up to the instant point of halt and then starts to accelerate in reverse direction until run away speed is reached. The main reason behind this speed change is the unbalanced torque applied by rotating parts of the centrifugal pumps. This unbalanced torque can be shown as;

$$T = -\frac{WR_g^2}{g}\frac{d\omega}{dt} \quad \textbf{(3.37)}$$

where;

W= Weight of the rotating parts and entrained liquid (mass x gravitational acceleration)

R_g= Radius of gyration of the rotating mass

ω= Angular velocity in radians/s

$\frac{d\omega}{dt}$= Change in angular velocity over time which is angular acceleration

The above unbalanced torque value can be equated to the average of the T_0 at the beginning of time step Δt and T_p which is the unknown torque value at the end of Δt. Below equations illustrate these relationships;

$$\omega = N_R \frac{2\pi}{60}\alpha \qquad \beta_0 = \frac{T_0}{T_R} \qquad \beta = \frac{T_P}{T_R} \tag{3.38}$$

By using above equations;

$$\beta = \frac{WR_g^2}{g}\frac{N_R}{T_R}\frac{\pi}{15}\frac{(\alpha_0 - \alpha)}{\Delta t} - \beta_0 \tag{3.39}$$

Above equation can be simplified by defining a new variable;

$$C_{31} = \frac{WR_g^2}{g}\frac{N_R}{T_R}\frac{\pi}{15\Delta t} \tag{3.40}$$

Eq. (3.39) becomes;

$$\beta + \beta_0 - C_{31}(\alpha_0 - \alpha) = 0 \tag{3.41}$$

By using the same linearization technique, which was shown on Figure 3-8, below equation is derived;

$$\frac{\beta}{\alpha^2 + \nu^2} = WB(x) = B_0 + B_1(\pi + \tan^{-1}\frac{\nu}{\alpha}) \tag{3.42}$$

By combining Eq. (3.41) and Eq. (3.42) a new equation is derived which is called speed change equation;

$$F2 = (\alpha^2 + \nu^2)\left[B_0 + B_1\left(\pi + \tan^{-1}\frac{\nu}{\alpha}\right)\right] + \beta_0 - C_{31}(\alpha_0 - \alpha) = 0 \tag{3.43}$$

3.6.4 Single Pump Boundary

In principle for all pump boundaries F1 and F2 equations should be solved together by using an iterative technique similar to Newton-Raphson, Runge Kutta or

Bisection method etc. As shown below these equations are solved by using Newton-Raphson on this section.

$$F1 + \frac{\partial F1}{\partial \nu}\Delta\nu + \frac{\partial F1}{\partial \alpha}\Delta\alpha = 0 \quad \textbf{(3.44)}$$

$$F2 + \frac{\partial F2}{\partial \nu}\Delta\nu + \frac{\partial F2}{\partial \alpha}\Delta\alpha = 0 \quad \textbf{(3.45)}$$

At the beginning of an iteration initial ν and α values can be found by;

$$\nu = 2\nu_0 - \nu_{00} \quad \textbf{(3.46)}$$

$$\alpha = 2\alpha_0 - \alpha_{00} \quad \textbf{(3.47)}$$

Where ν_{00} and α_{00} denotes one time step before calculation step.

Results of partial derivatives are as shown below;

$$\frac{\partial F1}{\partial \nu} = -BSQ + H_R\left\{2\nu\left[A_0 + A_1\left(\pi + \tan^{-1}\frac{\nu}{\alpha}\right)\right] + A_1\alpha\right\} - \frac{2\Delta H|\nu|}{\tau^2} \quad \textbf{(3.48)}$$

$$\frac{\partial F1}{\partial \alpha} = H_R\left\{2\alpha\left[A_0 + A_1\left(\pi + \tan^{-1}\frac{\nu}{\alpha}\right)\right] - \nu A_1\right\} \quad \textbf{(3.49)}$$

$$\frac{\partial F2}{\partial \nu} = 2\nu\left[B_0 + B_1\left(\pi + \tan^{-1}\frac{\nu}{\alpha}\right)\right] - \alpha B_1 \quad \textbf{(3.50)}$$

$$\frac{\partial F2}{\partial \alpha} = 2\alpha\left[B_0 + B_1\left(\pi + \tan^{-1}\frac{\nu}{\alpha}\right)\right] - \nu B_1 + C_{31} \quad \textbf{(3.51)}$$

In order to find converged solution $\Delta\alpha$ and $\Delta\nu$ values at each time step should be calculated. These values are calculated by;

$$\Delta\alpha = \frac{\left(\frac{F2}{\frac{\partial F2}{\partial \nu}} - \frac{F1}{\frac{\partial F1}{\partial \nu}}\right)}{\left(\frac{\frac{\partial F1}{\partial \alpha}}{\frac{\partial F1}{\partial \nu}} - \frac{\frac{\partial F2}{\partial \alpha}}{\frac{\partial F2}{\partial \nu}}\right)} \qquad \Delta\nu = \frac{-F1}{\frac{\partial F1}{\partial \nu}} - \Delta\alpha\left(\frac{\frac{\partial F1}{\partial \alpha}}{\frac{\partial F1}{\partial \nu}}\right) \quad \textbf{(3.52)}$$

After each iteration results of Eq. (3.52) is added to the last values of α and ν until a certain level of tolerance is reached;

$$\alpha = \alpha + \Delta\alpha \quad \textbf{(3.53)}$$

$$\nu = \nu + \Delta\nu \quad \textbf{(3.54)}$$

In terms of accuracy, below tolerance level is seen to yield in sufficiently correct results;

$$|\Delta\alpha| + |\Delta\nu| < TOL \; in \; which \; TOL = 0.0002 \quad \textbf{(3.55)}$$

Iteration can be finalized upon reaching the desired tolerance level. However, after finalizing the iteration A_0, A_1, B_0 and B_1 values must be checked by using the new ν and α values. It was previously found that;

$$I = \frac{x}{\Delta x} + 1 \qquad x = (\pi + \tan^{-1}\frac{\nu}{\alpha})$$

Therefore, the new II value is written as;

$$II = (\pi + \tan^{-1}\frac{\nu_{after\ iteration}}{\alpha_{after\ iteration}}) \quad \textbf{(3.56)}$$

If I=II then solution is represented by proper vicinity of line segments. However, if I≠II then the procedure should be repeated from the beginning by replacing I with II. This loop should continue for 3 or 4 times and if solution is not found then loop should be stopped since solution can not be obtained.

Moreover, if there is a valve in front of the pump and τ value of this valve becomes smaller than 0.0001 then pump equations can be bypassed since valve is nearly close and no flow reaches to the pump.

If a check valve is used in front of our pump unit an equation for this case should be derived aswell. Functionality of check valves prevent reverse flow going into the pump therefore whenever reverse flow reaches at pump node check valves closes the path and after this pump boundary can be bypassed since no flow acts on pump. Below equation is derived to simulate check valve motion;

$$F3 = HCP - HCM + H_R.\alpha^2.WH\left(\frac{\pi}{\Delta x} + 1\right) \quad \textbf{(3.57)}$$

If F3<0 then there is reverse flow hence check valve closes preventing reverse flow reaching pump.

3.6.5 Pump Boundary with Pumps Connected in Series

If two pump has less distance than aΔt between them then they must be treated as series connected pumps. Discharge relationship for a simple series connected pump boundary as shown in Figure 3-9 are derived below;

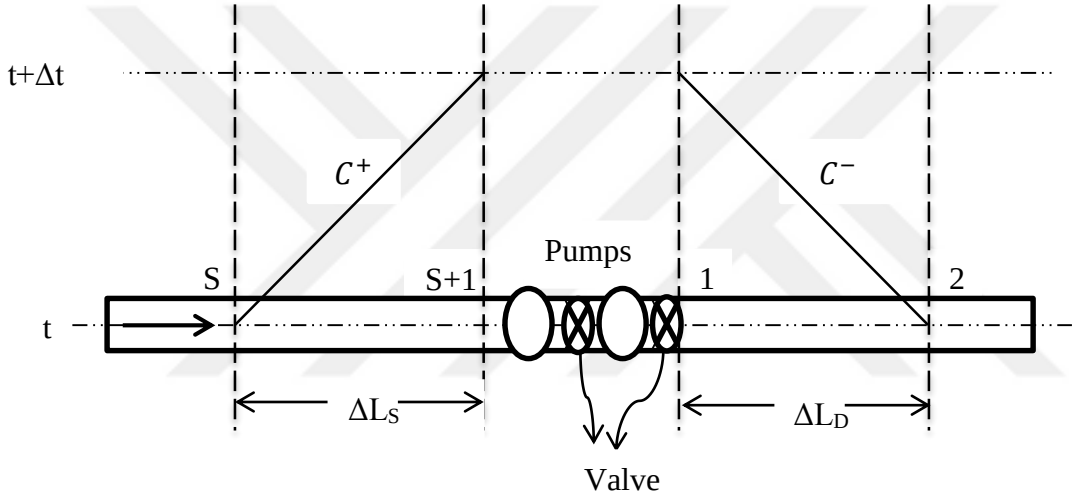

Figure 3-9: Grids for series connected pump boundary equations

Continuity relationships become;

$$QP(1) = QS(S+1) = \nu Q_{R_1} = \nu_2 Q_{R_2} \quad \textbf{(3.58)}$$

Head balance equation must be modified to satisfy this boundary;

$$HPM - BSQ.\nu + tdh_1 + tdh_2 - \frac{\Delta H_1 \nu|\nu|}{\tau_1^2} - \frac{\Delta H_1 c_1^2 \nu|\nu|}{\tau_2^2} = 0 \quad \textbf{(3.59)}$$

where;

$c_1 = \frac{Q_{R_1}}{Q_{R_2}}$ $\qquad$ $\nu_2 = c_1 \nu$

$\Delta H_1 =$ Head loss for valve 1 in front of pump 1

$\Delta H_2 =$ Head loss for valve 2 in front of pump 2

Modified F1 equation is shown below;

$$F1 = HPM - BSQ.\nu + H_{R_1}(\alpha_1^2 + \nu^2)\left[A_{01} + A_{11}(\pi + \tan^{-1}\frac{\nu}{\alpha_1})\right] + H_{R_2}(\alpha_2^2 + (c_1\nu)^2)\left[A_{02} + A_{12}(\pi + \tan^{-1}\frac{c_1\nu}{\alpha_2})\right] - \nu|\nu|\left(\frac{\Delta H_1}{\tau_1^2} + \frac{\Delta H_2}{\tau_2^2}c_1^2\right) = 0 \quad \textbf{(3.60)}$$

It should be noted that there are three unknowns on above equation α_1, α_2 and ν. Therefore, to solve this boundary, two more equations are required. Hence below two speed change equations are derived for each pump in series;

$$F2 = (\alpha_1^2 + \nu^2)\left[B_{01} + B_{11}\left(\pi + \tan^{-1}\frac{\nu}{\alpha_1}\right)\right] + \beta_{01} - C_{311}(\alpha_{01} - \alpha_1) = 0 \quad \textbf{(3.61)}$$

$$F3 = (\alpha_2^2 + (c_1\nu)^2)\left[B_{02} + B_{12}\left(\pi + \tan^{-1}\frac{c_1\nu}{\alpha_2}\right)\right] + \beta_{02} - C_{312}(\alpha_{02} - \alpha_2) = 0 \quad \textbf{(3.62)}$$

Extra subscript refers to pump number.

Again the same Newton-Raphson method can be used to solve these equations simultaneously for unknown variables.

3.6.6 Pump Boundary with Pumps Connected in Parallel

Solution of parallel connected pumps are similar to series and single pumps. Previously on series connection there were a single head balance equation and each pumps had their own speed change equation for solution. However, on parallel connected pump boundary there is a single head balance equation and speed change

equation for each pump. Therefore, number of equation to solve is equal to two times pump number which means there are more unknowns compared to previous solutions. A simple parallel connection is given on Figure 3-10;

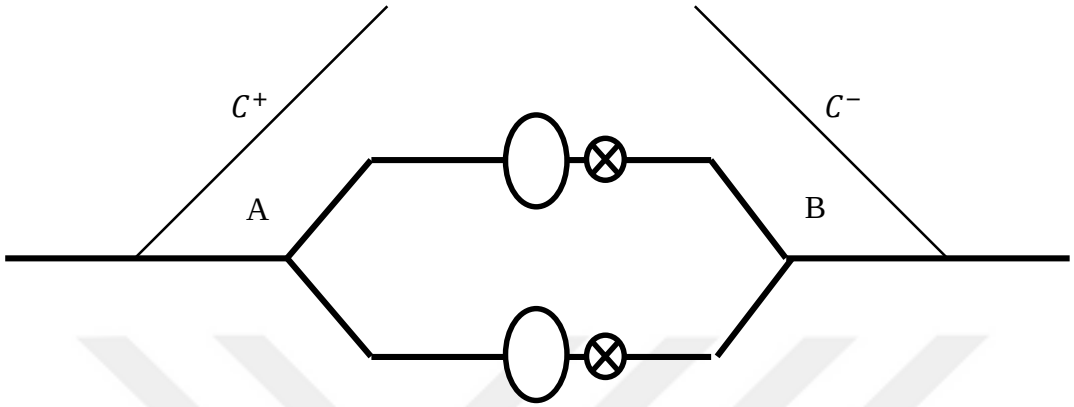

Figure 3-10: Grids for parallel connected pump boundary equations

Continuity relationship for parallel connected pumps becomes;

$$Q_{P_A} = Q_{P_B} = \nu_1 Q_{R_1} + \nu_2 Q_{R_2} \quad \textbf{(3.63)}$$

Head balance equation for each pump is given below;

$$F1 = H_{PA} + tdh_1 - \frac{\Delta H_1 \nu_1 |\nu_1|}{\tau_1^2} - H_{PB} = 0 \quad \textbf{(3.64)}$$

$$F2 = H_{PA} + tdh_2 - \frac{\Delta H_2 \nu_2 |\nu_2|}{\tau_2^2} - H_{PB} = 0 \quad \textbf{(3.65)}$$

Speed change equation for each pump is given below;

$$F3 = (\alpha_1^2 + \nu_1^2)\left[B_{01} + B_{11}\left(\pi + \tan^{-1}\frac{\nu_1}{\alpha_1}\right)\right] + \beta_{01} - C_{311}(\alpha_{01} - \alpha_1) = 0 \quad \textbf{(3.66)}$$

$$F4 = (\alpha_2^2 + \nu_2^2)\left[B_{02} + B_{12}\left(\pi + \tan^{-1}\frac{\nu_2}{\alpha_2}\right)\right] + \beta_{02} - C_{312}(\alpha_{02} - \alpha_2) = 0 \quad \textbf{(3.67)}$$

As a result there are four unknowns α_1, α_2, $\nu_1$and ν_2 and four equations. By using any iterative technique a simultaneous solutions of these variables can be obtained. It should be stressed that if a valve in front of a pump is closed than that pump should be omitted from the set of equations.

3.7 Air Chamber with Orifice

Air chambers are the most widely used protection method against water hammer. There are two functions of air chambers which are;

- To absorb high pressure in case of pressure increase in the line
- To discharge liquid into system to dampen negative pressures

Air inside water chambers acts as a cushion to the water that enters inside chamber in case of pressure rise. Moreover, in case pressure drops below the steady state level then the water stored inside an air chamber is discharged into the system increasing the pressure therefore preventing negative pressures and vacuum.

Optimal sizing and location of air chambers depend on trial and error process. Analysis should be executed for different location and sizes. In general almost half of the tank should be filled with air. Figure 3-11 illustrates grids for air chamber

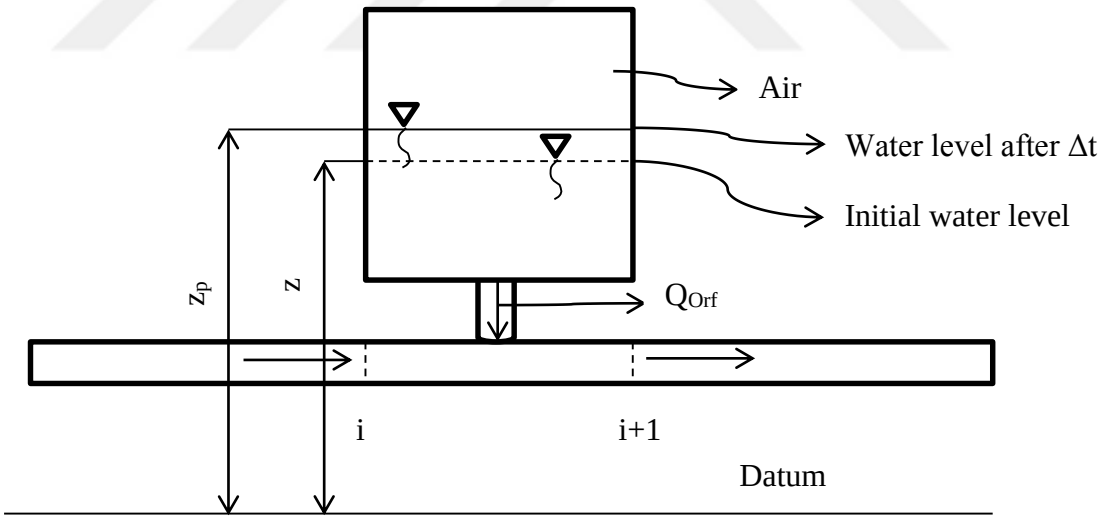

Figure 3-11: Grids for air chamber with orifice

To solve air chamber boundary polytropic relation for a perfect gas condition is assumed to be true. Below equation shows this relationship;

$$H_{0_{air}}^{*} V_{0_{air}}^{m} = C \qquad \textbf{(3.68)}$$

where;

$H^*_{0_{air}}$= Initial steady state absolute pressure head

$V^m_{0_{air}}$= Initial volume of the entrapped air inside chamber

m= Polytropic gas equation exponent (in between 1 – 1.4)

From Figure 3-11 continuity equation can be written as;

$$Q_i = Q_{i+1} + Q_{P_{Orf}} \tag{3.69}$$

where;

Q_{Orf} = Discharge that flows through orifice of air chamber at the beginning of time step Δt.

$Q_{P_{Orf}}$ = Discharge that flows through orifice of air chamber at the end of time step Δt

Positive values of orifice discharges mean there is a flow into the air chamber while negative means there is a flow outgoing from air chamber to the system.

To solve transient condition, heads before and after the connection point is assumed to be equal which means;

$$H_i = H_{i+1} \tag{3.70}$$

As a result of above assumptions unknown head value at the air chamber can be written by using Eq. (2.68 – 2.69) as;

$$H_i = H_{i+1} = \left(\frac{C_P + C_M - BQ_{P_{Orf}}}{2}\right) \tag{3.71}$$

By using the conservation of mass law, water level in the air chamber after Δt seconds can be written as;

$$z_p = z + 0.5\left(Q_{orf} + Q_{P_{orf}}\right)\frac{\Delta t}{A_c} \tag{3.72}$$

A_c= Cross sectional area of air chamber

One last equation is needed in order to solve air chamber since there are three unknowns which are Q_{porf}, H_i, z_p. Final relationship can be provided by an equation that describes air volume inside air chamber;

$$\forall_{P_{air}} = \forall_{air} - A_c(z_p - z) \qquad \textbf{(3.73)}$$

$\forall_{P_{air}}$= Air volume inside air chamber at the end of time step Δt

$\forall_{air}$= Air volume inside air chamber at the beginning of time step Δt

Through Eqs. (3.71 – 3.72 – 3.73) there are three unknowns and three equations therefore all variables can be solved by using an iterative technique. After each iteration value of C from Eq. (3.68) should be checked from the below equation;

$$\left(H_i + H_b - z_p - C_{orf} Q_{P_{orf}} \left|Q_{P_{orf}}\right|\right)\left[\forall_{air} - A_c(z_p - z)\right]^m = C_2 \qquad \textbf{(3.74)}$$

Finally it should be checked whether C_2=C or not and if they are equal then it means desired result is obtained.

3.8 Interior Valve

If there is a valve in between two pipe sections then the orifice equation must be treated simultaneously for end conditions of each pipe. When the valve motion starts there will be a pressure rise at the upstream and pressure drop at the downstream sides of the valve. Therefore, heads at upstream and downstream are not equal to each other but by assuming conservation of mass holds one can write the below equation;

$$Q_{P_{2,1}} = Q_{P_{1,NS}} = \frac{Q_0 \tau}{\sqrt{H_0}} \sqrt{H_{P_{1,NS}} - H_{P_{2,1}}} \; (For\ positive\ flow) \qquad \textbf{(3.75)}$$

$$Q_{P_{2,1}} = Q_{P_{1,NS}} = -\frac{Q_0 \tau}{\sqrt{H_0}} \sqrt{H_{P_{2,1}} - H_{P_{1,NS}}} \; (For\ reverse\ flow) \qquad \textbf{(3.76)}$$

In the above equations, first subscript denotes the pipe section and second subscript denotes the node number.

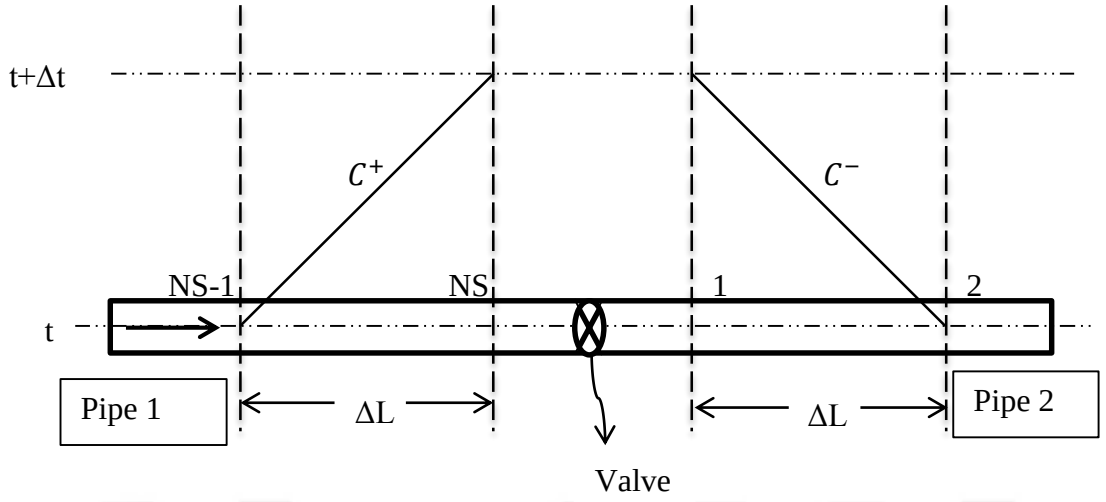

Figure 3-12: Grids for interior valve

When combined with Eqs. (2.68 – 2.69) below final equation can be obtained for discharge value;

$$Q_{P_{1,NS}} = -C_v(B_1 + B_2) + \sqrt{C_v^2(B_1 + B_2)^2 + 2C_v\left(C_{P_1} - C_{M_2}\right)} \quad \textbf{(3.77)}$$

$$Q_{P_{1,NS}} = C_v(B_1 + B_2) - \sqrt{C_v^2(B_1 + B_2)^2 - 2C_v\left(C_{P_1} - C_{M_2}\right)} \quad \textbf{(3.78)}$$

Eq. (3.77) is used for positive flow where as Eq. (3.78) is used for reverse flow conditions. In the above equations $C_v = (Q_0\tau)^2/2H_0$

H_0= Head loss across the valve

The result of Eqs. (3.77 – 3.78) can be used to find head values on both sides of interior valve by Eqs. (2.68 – 2.69).

It should be noted that when $C_{P_1} - C_{M_2} < 0$ then Eq. (3.77) and for $C_{P_1} - C_{M_2} > 0$ Eq. (3.78) should be used to find discharge value.

3.9 Downstream Valve

For downstream valve a simple orifice equation is used as shown below;

$$Q_0 = (C_D A_G)_0 \sqrt{2gH_0} \tag{3.79}$$

For another valve opening through time the above Eq. (3.79) can be generalized as;

$$Q_P = C_D A_G \sqrt{2g\Delta H} \tag{3.80}$$

To define valve opening below dimensionless equation is used;

$$\tau = \frac{C_D A_G}{(C_D A_G)_0} \tag{3.81}$$

By using Eqs (3.80 – 3.81) below relationship can be derived;

$$Q_P = \frac{Q_0}{\sqrt{H_0}} \tau \sqrt{\Delta H} \tag{3.82}$$

Where $\tau = 1$ shows that valve is at the steady-state setting and $\tau = 0$ shows that valve is closed. By substituting Eq. (3.82) into Eq. (2.68) a final equation for discharge through valve during transient event is obtained as;

$$Q_{P_{NS}} = -BC_v + \sqrt{(BC_v)^2 + 2C_v C_p} \tag{3.83}$$

In the above equations $C_v = (Q_0 \tau)^2 / 2H_0$

H_0= Steady state head value at downstream valve

Head value at the valve can be determined by substituting value of discharge into Eq. (2.68).

3.10 Surge Tank with Standpipe

Surge tank is one of the most commonly used protection devices against water hammer. It acts similar to air chamber. However, it is open on top and its height and area should be chosen large enough to satisfy pressure rises and prevent overflows from the top of the surge tank.

To illustrate surge tank in a mathematical form below assumptions are used;

$$Q_{P_{i,n+1}} = Q_{P_{i+1,1}} + Q_{P_{SP}} \quad \textbf{(3.84)}$$

$$H_{P_{i,n+1}} = H_{P_{i+1,1}} \quad \textbf{(3.85)}$$

where;

$Q_{P_{SP}}$= Discharge flowing into or out from stand pipe at the end of time step

By using above assumptions simultaneously with below equations discharge on stand pipe can be found numerically;

$$\gamma A_{SP} \frac{L_{SP}}{g A_{SP}} \frac{dQ_{SP}}{dt} = \gamma A_{SP}\left[H_{P_{i,n+1}} - (z_P - L_{SP})\right] - W - F_f \quad \textbf{(3.86)}$$

$$z_P = z + \frac{0.5\Delta t}{A_S}\left(Q_{P_{SP}} + Q_{SP}\right) \quad \textbf{(3.87)}$$

$$H_{P_{i,n+1}} = H_{P_{i+1,1}} = \frac{C_P + C_M - BQ_{P_{SP}}}{2} \quad \textbf{(3.88)}$$

where;

W= Weight of the liquid in the stand pipe

L_{SP}= Length of the stand pipe

F_f= Force due to friction in stand pipe

A_S= Area of surge tank

A_{SP}= Area of stand pipe

Q_{SP}= Discharge flowing into or out from stand pipe at the beginning of the time step

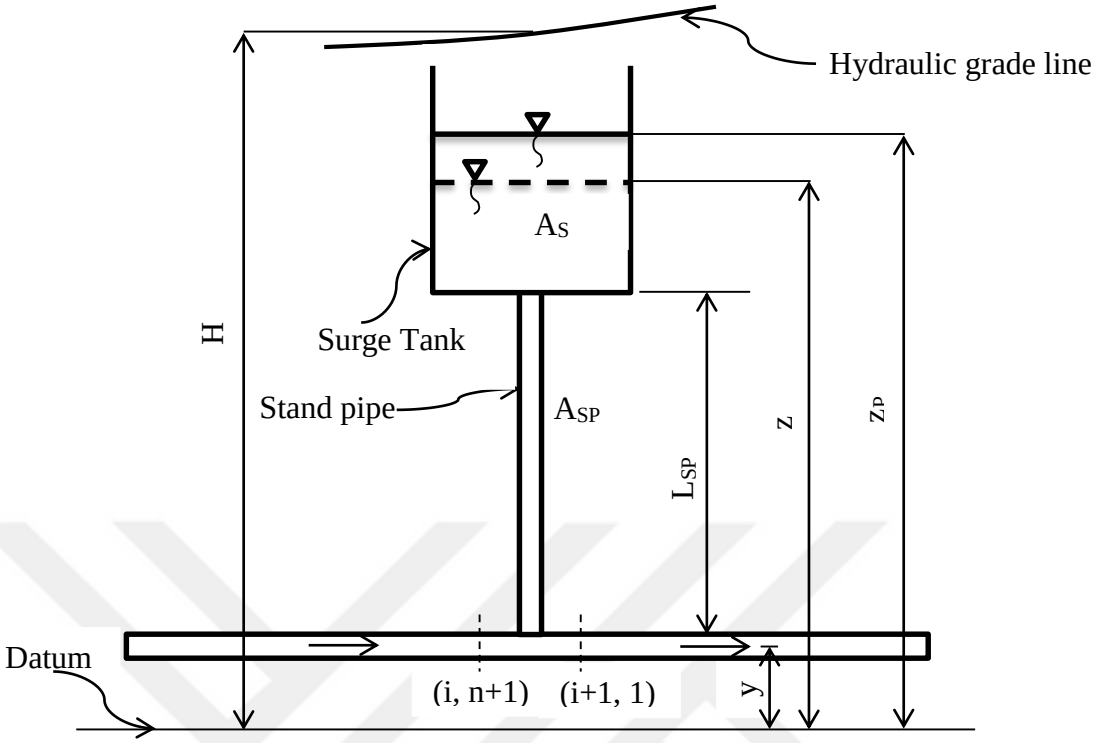

Figure 3-13: Grids for surge tank with standpipe

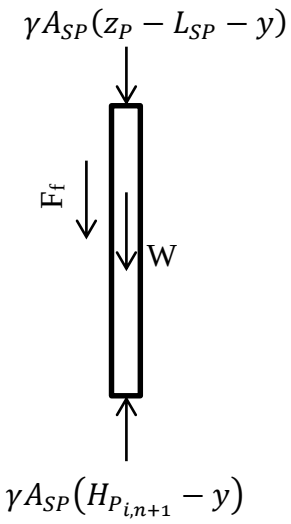

Figure 3-14: Free body diagram for stand pipe

Eq. (3.86) can be simplified by using below equations;

$$\frac{dQ_{SP}}{dt} = \frac{Q_{P_{SP}} - Q_{SP}}{\Delta t} \quad \textbf{(3.89)}$$

$$F_f = \frac{f L_{SP} Q_{SP} |Q_{SP}|}{2 g D_{SP} A_{SP}^2} \quad \textbf{(3.90)}$$

$$W = \gamma A_{SP} L_{SP} \quad \textbf{(3.91)}$$

Finally by simultaneous solution of Eqs. (3.86 – 3.87 – 3.88) yields below equation to find discharge through stand pipe;

$$Q_{P_{SP}} = \frac{g \Delta t A_{SP}}{L_{SP}} \left(H_{P_{i,n+1}} - z_P - F_f \right) + Q_{SP} \quad \textbf{(3.92)}$$

Above equation can be solved numerically and result of Eq. (3.92) can be put into Eq. (3.88) in order to find head value at the junction.

3.11 Air Valve

Air valves work hydraulically and main purpose of this valve is to reduce downsurge of pressures in the system and indirectly reduce pressure upsurges by introducing air into and out from the system.

In case of a pump shut down the air valve introduces air quickly into the pipe preventing a severe vacuum pocket formation. Vacuum pocket formation causes water column separation. Moreover, when this water column rejoins and pressure increases, the air valve discharges air that has entered into the system in order to suppress pressure upsurge.

There are four assumptions when using air valve boundary with method of characteristics;

- Air that enters into the pipe is isentropic
- The entrapped air inside pipe do not move with the flow but stays at the valve location.
- The expansion and contraction of the entrapped air is isothermal.
- Friction at junction is negligible therefore;

$$H_{P_{i,n+1}} = H_{P_{i+1,1}}$$

In most of the real life cases air valves are located on the highest point of a pipe system or on a vertical elbow points in which air is trapped as shown in Figure 3-15.

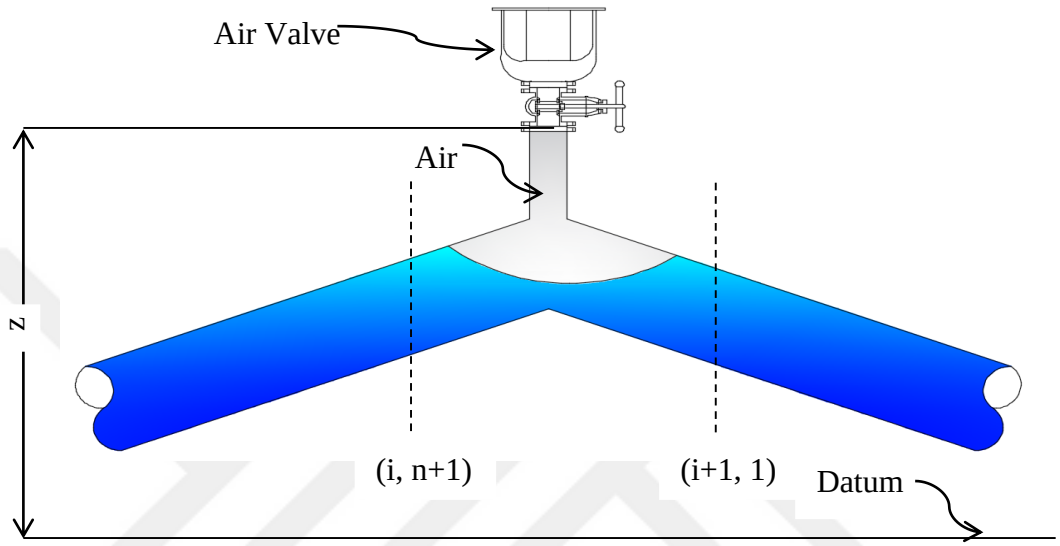

Figure 3-15: Grids for air valve

Net rate of change of air volume is found from below equation considering small time increment;

$$m_{P_a} = m_a + \frac{dm_a}{dt}\Delta t \qquad \textbf{(3.93)}$$

where,

m_a= Mass of air entrapped in the pipeline at the beginning of the time step

m_{P_a}= Mass of air entrapped in the pipeline at the end of the time step

In order to satisfy continuity equation below equation must be satisfied at each time increment;

$$\forall_{P_{air}} = \forall_{air} + 0.5\Delta t\left[\left(Q_{P_{i+1,1}} + Q_{i+1,1}\right) - \left(Q_{P_{i,n+1}} + Q_{i,n+1}\right)\right] \qquad \textbf{(3.94)}$$

Above Eq. (3.94) can be simplified using the equations shown below;

$$C_n = Q_{i+1,1} - \frac{gA}{a} H_{i+1,1} - \frac{f\Delta t}{2DA} Q_{i+1,1} \left| Q_{i+1,1} \right| \quad \textbf{(3.95)}$$

$$C_{n2} = Q_{i,n+1} + \frac{gA}{a} H_{i,n+1} - \frac{f\Delta t}{2DA} Q_{i,n+1} \left| Q_{i,n+1} \right| \quad \textbf{(3.96)}$$

$$C_{air} = \cancel{V}_{air} + 0.5\Delta t \left(C_n + Q_{i+1,1} - C_{n2} - Q_{i,n+1} \right) \quad \textbf{(3.97)}$$

Finally by using Eq. (2.77 – 2.78) compatibility equations final simplified form of air volume equation can be written as;

$$\cancel{V}_{P_{air}} = C_{air} + 0.5\Delta t \left(\frac{1}{B_i} + \frac{1}{B_{i+1}} \right) H_{P_{i,n+1}} \quad \textbf{(3.98)}$$

$$B = \frac{a}{gA}$$

At this point the assumption the expansion and contraction of air being isothermal must be described mathematically. Below equation gives this relation;

$$P\cancel{V}_{P_{air}} = m_{P_a} RT \quad \textbf{(3.99)}$$

Where;

R= Universal gas constant. For air it is 287.058 $Jkg^{-1}K^{-1}$

T= Absolute temperature of the air volume. For 25 ^{o}C it is 298.15 Kelvins.

P= Absolute pressure at junction

H_b= Atmospheric pressure head

$$P = \gamma \left(H_{P_{i,n+1}} - z - H_b \right) \quad \textbf{(3.100)}$$

By substituting head value $H_{P_{i,n+1}}$ from Eq. (3.100) into Eq. (3.98) a new form of Eq. (3.99) can be obtained as;

$$m_{P_a} RT = P \left[C_{air} + 0.5\Delta t \left(\frac{1}{B_i} + \frac{1}{B_{i+1}} \right) \left(\frac{P}{\gamma} + z - H_b \right) \right] \quad \textbf{(3.101)}$$

By substituting Eq. (3.93) into Eq. (3.101) final equation for air valve behaviour is obtained as;

$$\left(m_a + \frac{dm_a}{dt}\Delta t\right) RT = P\left[C_{air} + 0.5\Delta t\left(\frac{1}{B_i} + \frac{1}{B_{i+1}}\right)\left(\frac{P}{\gamma} + z - H_b\right)\right] \quad \textbf{(3.102)}$$

Eq. (3.102) is the main equation which describes air isothermal expansion and contraction in terms of two unknowns which are P and dm_a/dt . Therefore to solve it for two unknowns there is a need for another equation. This extra equations are provided by air valves behavioural patterns for inflow of air and outflow of air. This pattern can be divided into four zones;

- Subsonic air inflow

$$P_a > P > 0.53P_a \qquad \frac{dm_a}{dt} = C_d A_v \sqrt{7P_a\rho_a\left(\frac{P}{P_a}\right)^{1.43}\left[1 - \left(\frac{P}{P_a}\right)^{0.286}\right]} \quad \textbf{(3.103)}$$

- Sonic air inflow

$$P \leq 0.53P_a \qquad \frac{dm_a}{dt} = 0.686 C_d A_v \frac{P_a}{\sqrt{RT}} \quad \textbf{(3.104)}$$

Where;

P_a= Absolute atmospheric pressure. It is taken as 10.3 m or 101 kPa

ρ_a= Mass density of air at absolute atmospheric pressure. It is taken as 1.1839 kg/m^3 under 298.15 Kelvins

A_v= Area of the valve opening

C_d= Discharge coefficient of the valve

Now that inflow of air is derived but there is also requirement of equations for outflow of air in case pressure surges. Below two equations are used to simulate air outflow from pipe;

- Subsonic air outflow

$$\frac{P_a}{0.53} > P > P_a \qquad \frac{dm_a}{dt} = -C_d A_v \sqrt{7 P_a \rho_a \left(\frac{P}{P_a}\right)^{1.43} \left[1 - \left(\frac{P}{P_a}\right)^{0.286}\right]} \qquad \textbf{(3.105)}$$

- Sonic air velocity outflow

$$P > \frac{P_a}{0.53} \qquad \frac{dm_a}{dt} = -0.686 C_d A_v \frac{P_a}{\sqrt{RT}} \qquad \textbf{(3.106)}$$

Therefore, after determining zone of operation of air inflow or outflow Eq. (3.103) or (3.104) or (3.105) or (3.106) should be solved simultaneously with Eq. (3.102) in which only two unknowns are P and dm_a/dt. This two equation can be solved by any non linear solution technique such as Newton-Raphson or Bisection method.

3.12 Downstream Reservoir with a Constant Head

Downstream constant head boundary is solved by using the same principle as upstream constant head only for downstream case instead of C^- equation now a single C^+ equation will be used. Since head value is already known at the boundary then only unknown is discharge value which is found from below equtaion;

$$Q_{P_R} = (C_P - H_{P_R})/B \qquad \textbf{(3.107)}$$

3.13 Downstream Reservoir with a Dead End

Dead end have the meaning that the path is completely blocked and there are no discharge flowing through that boundary. In this case our discharge value at the boundary is known and equal to zero. In this case head value becomes equal to;

$$H_{P_R} = C_P \qquad \textbf{(3.108)}$$

3.14 Air Chamber with Standpipe

Unlike air chamber with orifice on this boundary chamber stands on top of a stand pipe as shown in Figure 3-16. An extra equation needs to be derived in order to account for liquid inside standpipe. Eq. (3.109) illustrates dynamic equation of standpipe;

$$\frac{\gamma L_{sp} A_{sp}}{g A_{sp}} \frac{dQ_{sp}}{dt} = \gamma A_{sp}\left[H_{P_{i,n+1}} - \left(H^{*}_{P_{air}} - H_b\right) - \left(Z_P - L_{sp}\right)\right] - F_f - W \qquad \textbf{(3.109)}$$

where;

F_f = Frictional forces ($\gamma h_{P_f} A_{sp}$) where h_{P_f}= Summation of all frictional head lossess in meters

W= Weight of the fluid inside standpipe ($\gamma L_{sp} A_{sp}$)

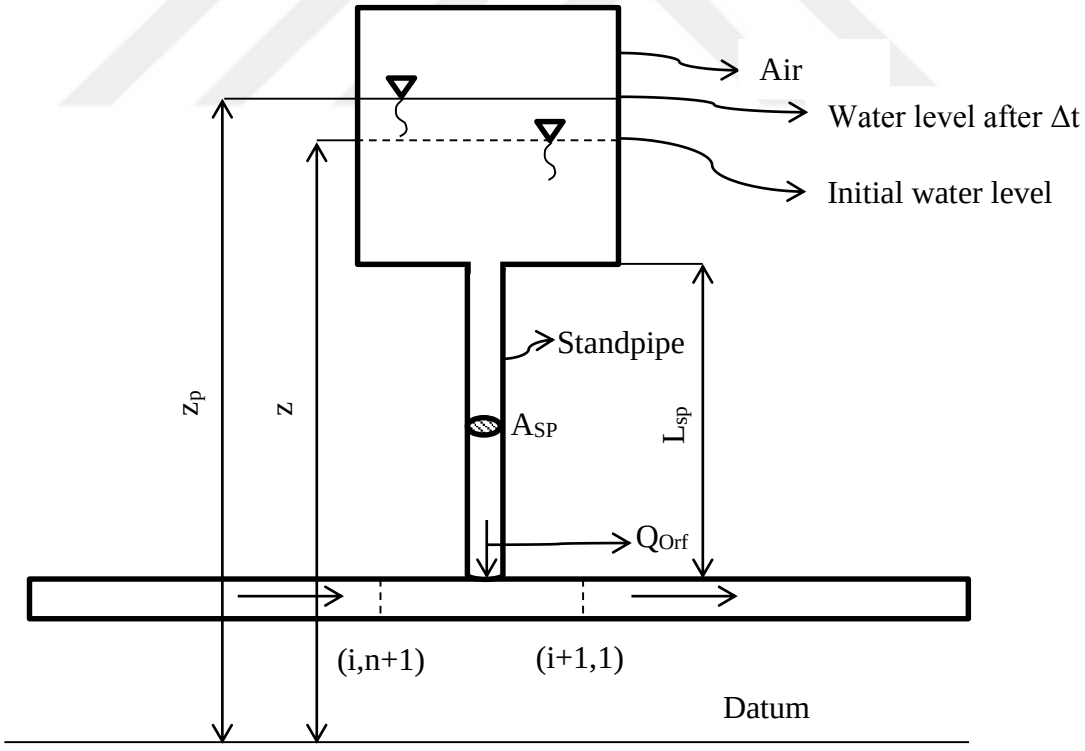

Figure 3-16: Grids for air chamber with standpipe

To calculate head losses Darcy-Weisbach friction loss formula can be used on standpipe and apart from this entrance losses can also be added into the equation. All losses are expressed as shown on Eq. (3.110).

$$h_{P_f} = kQ_{sp}|Q_{sp}| \tag{3.110}$$

Time rate of change of flow expression in Eq. (3.109) can be discretized as shown below;

$$\frac{dQ_{sp}}{dt} = \frac{\left(Q_{P_{sp}} - Q_{sp}\right)}{\Delta t} \tag{3.111}$$

By substituting expressions of F_f, W and Eq. (3.111) into Eq. (3.109) we can obtain equation of discharge through standpipe;

$$Q_{P_{sp}} = Q_{sp} + \frac{g\Delta t A_{sp}}{L_{sp}}\left(H_{P_{i,n+1}} - H^*_{P_{air}} - Z_P + H_b - kQ_{sp}|Q_{sp}|\right) \tag{3.112}$$

From previous Air chamber section;

$$H^*_{P_{air}}\left[\forall_{air} - A_c\left(z_p - z\right)\right]^m = C_2 \tag{3.113}$$

Now by using Eqs. (3.68 – 3.71 – 3.72 – 3.73 – 3.112 – 3.113) the set of equations can be solved for unknowns $Q_{P_{sp}}$, $H^*_{P_{air}}$, Z_P and $H_{P_{i,n+1}}$ by using any nonlinear equation solving method such as bisection method or newton-raphson.

An additional boundary condition can be add if any bypass line is required to be simulated. In such case set of equations should be written for two pipes one for inlet and other is for outlet pipe. As general form of the equations are known by changing diameter and length values in these equations new set of boundaries can be obtained.

It should be noted that selection of inlet and outlet pipe diameters affects overall effectiveness of air chamber. Moreover, outlet pipes take action during downsurges and in order to have quick reaction to downsurges this pipe should be selected larger than inlet pipe. On the other hand inlet pipe is responsible for inflow into the air

chamber during pressure upsurges and by selecting this pipe relatively smaller friction forces can be increased. Therefore, reducing the upsurge ratio. It should be noted though selecting too small or too high diameter values for pipes do not yield optimum values on the contrary selecting very little inlet pipe will prevent air chamber from receiving necessary inflow therefore it might lead to high pressure surges. All in all, different trials should be conducted to observe most optimum air chamber design.

Stephenson, D. (2002) developed an empirical model for optimisation of outlet and inlet pipe diameters. It is seen that results of his formula yields relatively optimised results.

3.15 Surge Tank with Throttled Orifice

Unlike previously solved surge tank with standpipe on this type of boundary we can't use pipe force balance equation that was shown on Eq. (3.86). However orifice flow equation can be used to compensate for this. General orifice flow equation is shown below;

$$Q_{P_{orf}} = C_D A_{orf} \sqrt{2gH} \tag{3.114}$$

This equation needs to be modified for a surge tank with throttled orifice and equation for positive flow into the tank and reverse flow out of the tank is defined as shown below;

For positive flow into the tank:

$$Q_{P_{orf}} = C_D A_{orf} \sqrt{H_p - Z_P} \tag{3.115}$$

For reverse flow out from the tank:

$$Q_{P_{orf}} = -C_D A_{orf} \sqrt{Z_p - H_P} \tag{3.116}$$

It is known from the Eq. (3.87) that one can describe Z_p in terms of discharge. Similarly, from Eq. (3.88) we can describe H_P in terms of unknown discharge as well. Upon substituting Eqs. (3.87 – 3.88) into Eqs. (3.115 – 3.116) a quadratic

equation is obtained which can be solved to obtain two roots. An algorithm can be written to discard one of those roots since it is very high chance that one of the roots would be either critically high or critically low which would indicate the correct root is the other one. Depending upon pressure and surge tank water elevation either Eq. (3.115) or Eq. (3.116) should be used to solve for required surge tank discharge.

Figure 3-17 illustrates variables in this section visually;

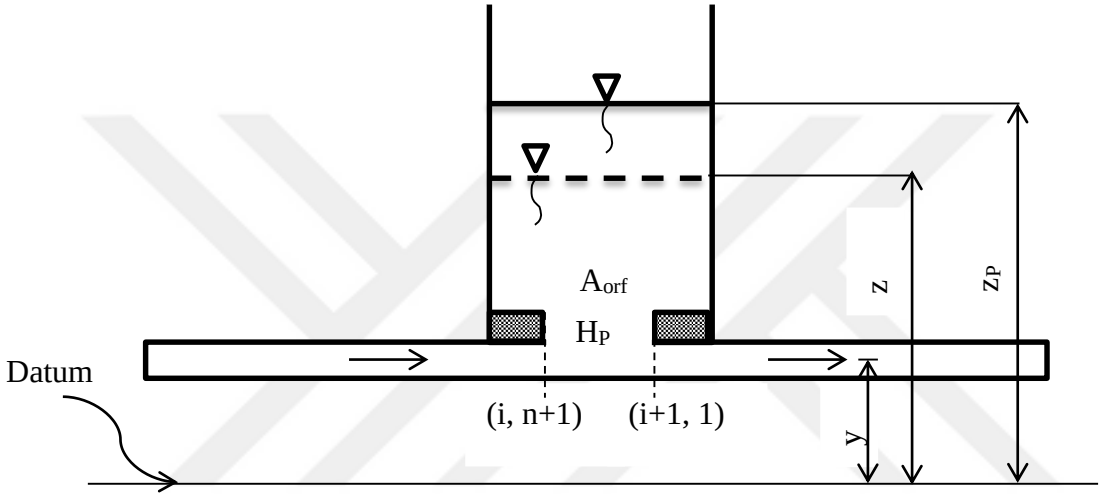

Figure 3-17: Grids for surge tank with throttled orifice

CHAPTER 4

H-HAMMER CODE

In this chapter graphical user interface and control functions of software is described. In addition, a users manual is provided in Appendix A.

4.1 Main User Interface

On main user interface all menus are available for usage. All of these menus serve to different purposes. Names of the menus are given below;

- Files
- Topography
- Material/Liquid Information
- Pressure Wave Speed Calculations
- Friction Factor Calculator
- Stress Analysis
- Pump Calculations
- Air Chamber Design
- Create Graph
- Animate

Functions of these menus are explained on below sub sections. Image of main screen can be seen on Figure 4-1.

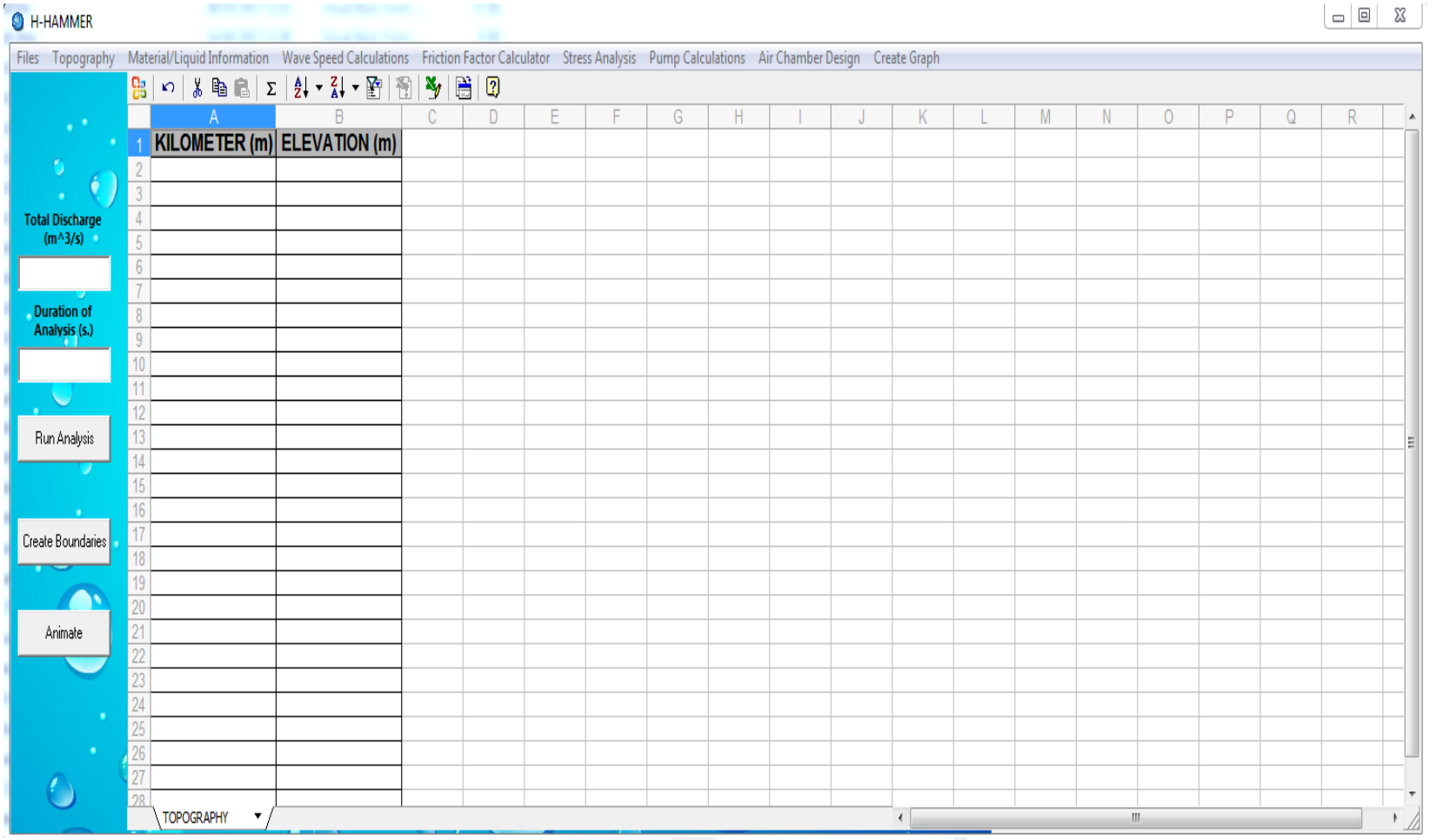

Figure 4-1: H-Hammer main interface

4.1.1 Files

Files menu is used for saving the results of analysis as an ".xls" file to the designated folder and exiting the program. Being able to save results as an ".xls" folder helps user create independent graphs and print out results from the ".xls" file with ease.

4.1.2 Topography

Topography is used to create profile view of the pipe route. It uses triangulated land model and calculates elevation points of land for each triangle. This menus final product is the profile view under which profile of pipe should be created by user. This profile views are later used in order to calculate pressures acting on each vertex of the pipe. Figure 4-2 shows an example topography output by H-Hammer.

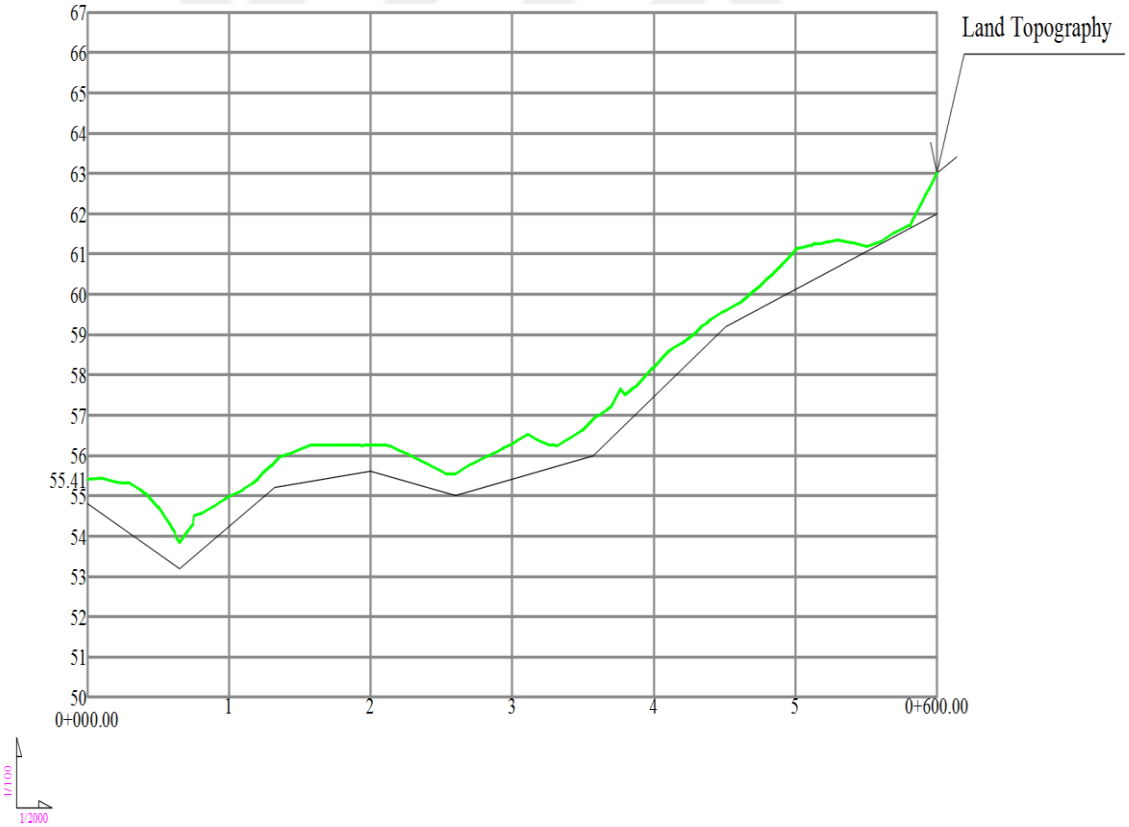

Figure 4-2: Example topography output

4.1.3 Material/Liquid Information

Under this menu modulus of elasticity and material roughness for variety of pipe materials are listed as well as bulk modulus of elasticity and density under atmospheric pressure values of different liquids are listed.

4.1.4 Pressure Wave Speed Calculations

This menu is used to calculate pressure wave speed for different support conditions. Moreover, it can calculate minimum time interval for a given pipe distance or maximum pipe distance for a given time interval which satisfies "Courant Condition".

Input values for this menu are;

- Pipe diameter
- Pipe thickness
- Pipe material modulus of elasticity
- Pipe material poisson's ratio
- Liquid bulk modulus of elasticity
- Support conditions
- Liquid density

Output values for this menu are;

- Pressure wave speed
- Minimum Δt value for given Δx that satisfies "Courant Condition"
- Maximum Δx value for given Δt that satisfies "Courant Condition"

4.1.5 Friction Factor Calculator

This menu solves "Colebrook-White" equation and finds friction factor which is required later on for water hammer analysis.

4.1.6 Stress Analysis

Stress analysis matches our pipe profile elevations with the elevation of hydraulic grade line and finds respective pipe thicknesses. Three different pipe thicknesses are found as a result of stress analysis:

- Thickness found from inner pressure
- Thickness found from exterior loads
- Minimum allowable thickness

Moreover, it will find maximum buckling pressure, deformation and ratio of change in shape. It should be noted at this point pipe material is assumed to be ductile and steel. Below techniques are used to find these values by reference of AWWA M11 Design of Steel Pipes Journal (2004);

$$T_{inner-pressure} = \frac{\gamma H_{max} D}{2\sigma_{hoop}} \quad \textbf{(4.1)}$$

$$T_{external-loads} = D\left(\frac{W_{ext.}(1-\mu^2)}{2E}\right)^{1/3} \quad \textbf{(4.2)}$$

where;

W_{ext}= External loads (Newtons)

E= Pipe material Young's Modulus of Elasticity (GPa)

σ_{hoop}= Pipe maximum hoop stress (MPa)

μ= Poisson ratio

γ= Specific weight of the fluid inside pipe (N/m^3)

As for minimum pipe thickness there are two conditions;

If $D \leq 54$ inches then

$$T_{min} = \frac{D}{288} \quad \textbf{(4.3)}$$

If $D > 54$ inches then

$$T_{min} = \frac{D + 20}{400} \quad \textbf{(4.4)}$$

Inches are used on Eq. (4.3 – 4.4).

Finally, by matching hydraulic grade line and pipe profile H-Hammer calculates head values acting on each pipe node.

4.1.7 Pump Calculations

This menu is used to calculate below values for a given pump;

- Rated torque (N.m)
- Radial speed (radian/s)
- Pump input power (kW.h)
- Pump inertia (Nm^2)

4.1.8 Air Chamber Design

This menu calculates diameter of air chamber inlet pipe. D. Stephenson (2002) developed the method to find optimised inlet diameter of air chamber depending on pressure surges and main pipe diameter;

$$D_i = D_p \left(\frac{2V_0^2}{2gh}\right)^{0.25} \quad \textbf{(4.5)}$$

Where;

D_i= Air chamber inlet pipe diameter

D_p= Diameter of the main pipe connected to air chamber

V_0= Initial velocity of fluid inside main pipe

h= Most critical drop or surge in pressure (Which ones absolute value is larger is considered in the calculations)

4.1.9 Create Graph

This menu can create below graphs for all of the selected nodes;

- HGL vs Time
- HGL vs Distance
- Discharge vs Time
- Discharge vs Distance

4.1.10 Animate

After completion of above procedures H-Hammer can now animate behaviour of HGL for better visualization of its motion. Animation time depends on the duration of simulation. Upon clicking on “Animate” button through main user interface recording option screen is displayed as shown on Figure 4-3.

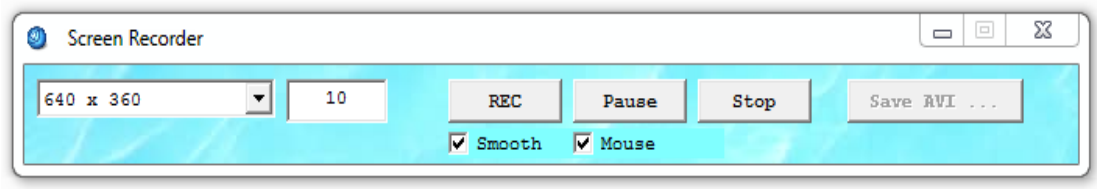

Figure 4-3: Screen recorder interface

Via screen recorder interface user can adjust video resolution and frame rate per second properties for the recording. After finishing recording by clicking on “Stop” button user can halt the recording process and save it as .avi file by clicking on “Save AVI” button. This tool is very useful for visualising the motion of HGL under transient events.

4.2 Boundary Elements and Property windows

4.2.1 Pipe Segment

Pipe segment is the main element of H-Hammer. This element connects all other boundaries to each other. Below Figure 4-4 illustrates symbol of pipe segment of H-Hammer.

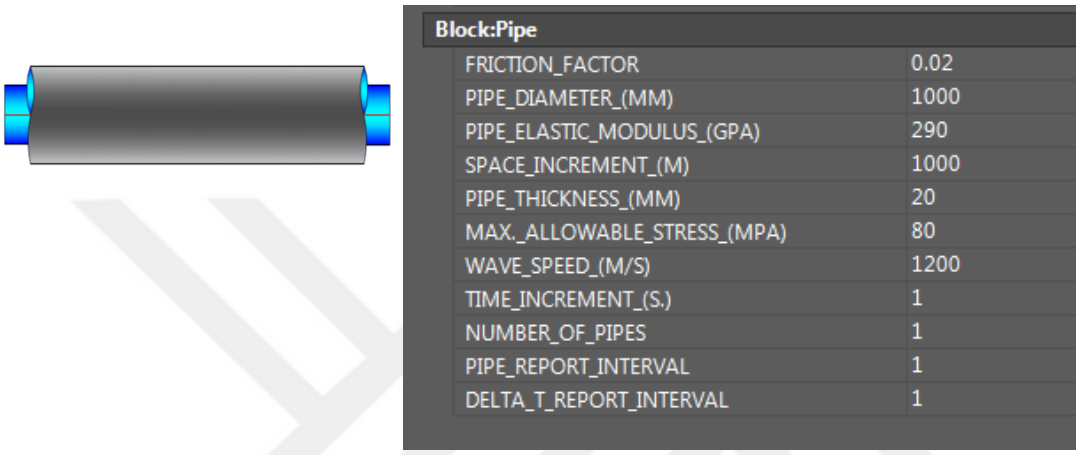

Figure 4-4: Pipe boundary symbol and Property window

This boundary has two connection points which are at the beginning and at the end of pipe. Usage of this element is a must in order to have any simulations. By setting number of pipes more than one unit, user can simulate longer pipelines without the necessity of connecting each one together. For example if number is set as “20” software will create 20 identical segments connected to each other and calculate accordingly.

Apart from that, user can change report intervals for space increments and Δt by setting “Pipe Report Interval” and “Delta T Report Interval” to a scale bigger than one. For example if our Δt value is equal to 0.5 and user set “Delta T Report Interval” as 2 then results will be tabulated with 2Δt time intervals although computations inside software will be conducted by using Δt time interval value. Similar adjustments can also be done for nodes. For example, if “Pipe Report Interval” is set to a scale more than 1 then software will not tabulate results of all

nodes but will step two by two for tabulation although computations are done for each node for high accuracy results. Only integer numbers can be set to the report interval segments.

4.2.2 Upstream Reservoir with a Constant Head

This is an upstream boundary that simulates a reservoir or a dam. Below Figure 4-5 illustrates upstream constant head symbol of H-Hammer.

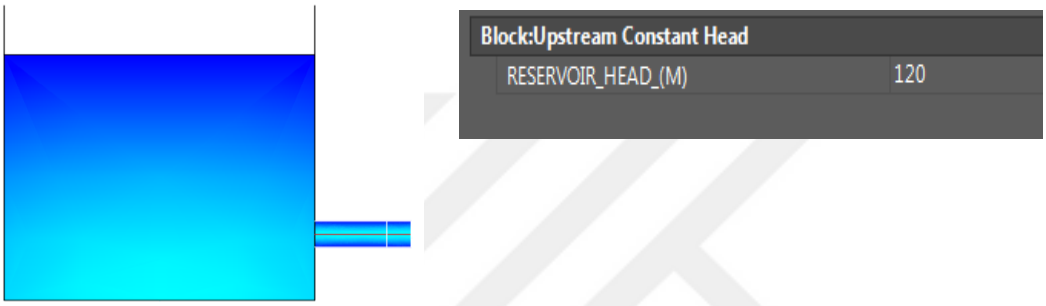

Figure 4-5: Upstream reservoir with constant head symbol and Property window

4.2.3 Upstream Reservoir with a Variable Head

Similar to upstream constant head this boundary also simulates a reservoir or a dam upstream but on this boundary sinusoidal waves cause changes in head value therefore it is named as upstream variable head. Figure 4-6 illustrates upstream variable head symbol of H-Hammer.

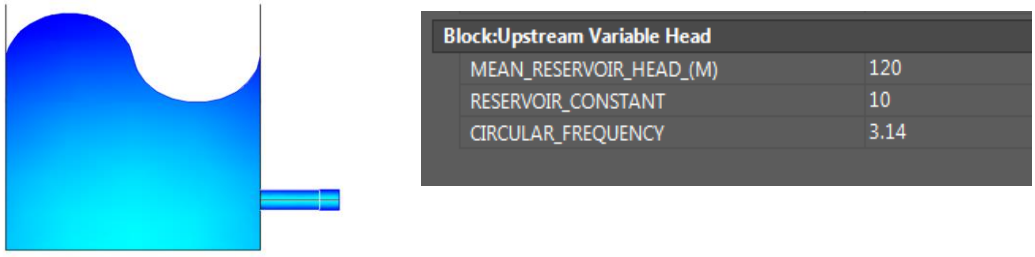

Figure 4-6: Upstream reservoir with variable head symbol and Property window

4.2.4 Pump Suction Pool

This boundary should be used with pump station boundary. It acts as a suction pool.

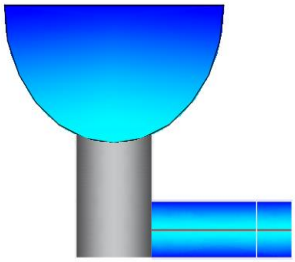

Block:Pump Suction Pool	
SUCTION_POOL_HEAD_(M)	1

Figure 4-7: Pump suction pool symbol and Property window

4.2.5 Series and Parallel Pumps

This is an upstream boundary that simulates behaviour of series and parallel connected identical pumps. Input variables for these pumps can be generated using pump calculations tab. Check or butterfly valve can be added in front of pump by typing “YES” or “NO” to the valve section of Property window.

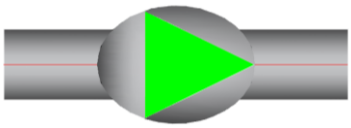

Block:Single Pump	
WRR_(NM^2)	1000
RATED_DISCHARGE_(M^3/S)	3
RATED_HEAD_(M)	150
RATED_SPEED_(RPM)	1100
RATED_TORQUE_(N.M)	1300
TIME_OF_FAILURE_(SEC.)	5000
NUMBER_OF_SERIES_PUMPS	1
HEAD_LOSS_COEFF.	1
PUMPING_ELEVATION_(M)	80
CHECK_VALVE_(YES/NO)	
RATED_EFFICIENCY	0.8
BUTTERFLY_VALVE_(YES/NO)	YES
BUTTERFLY_VALVE_CLOSURE_TIME_(SEC.)	250
SHUT_OFF_HEAD_(M)	85
A1_OF_HvsQ_CURVE_EQUATION	-1.87
A2_OF_HvsQ_CURVE_EQUATION	-1.14
A1_OF_EFFICIENCY_CURVE_EQUATION	-1.87
A2_OF_EFFICIENCY_CURVE_EQUATION	-1.14

Figure 4-8: Single or series pump symbol and Property window

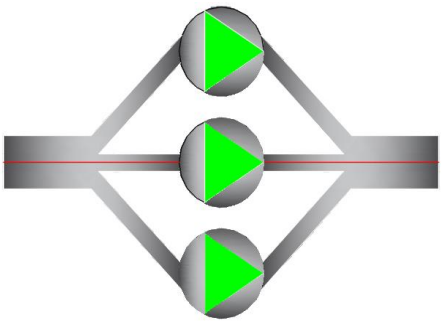

Block:Parallel Pump	
WRR_(NM^2)	1200
RATED_DISCHARGE_(M^3/S)	3
RATED_HEAD_(M)	150
RATED_SPEED_(RPM)	800
RATED_TORQUE_(N.M)	1200
TIME_OF_FAILURE_(SEC.)	5000
NUMBER_OF_PARALLEL_PUMPS	3
HEAD_LOSS_COEFF.	1
PUMPING_ELEVATION_(M)	85
CHECK_VALVE_(YES/NO)	NO
RATED_EFFICIENCY	0.85
BUTTERFLY_VALVE_(YES/NO)	NO
BUTTERFLY_VALVE_CLOSURE_TIME_(SEC.)	15
SHUT_OFF_HEAD_(M)	88
A1_OF_HvsQ_CURVE_EQUATION	-1.87
A2_OF_HvsQ_CURVE_EQUATION	-1.14
A1_OF_EFFICIENCY_CURVE_EQUATION	-1.87
A2_OF_EFFICIENCY_CURVE_EQUATION	-1.14

Figure 4-9: Parallel pump symbol and Property window

From Figure 4-8 and Figure 4-9 it can be seen that user is requested to enter curve equation constants for normal operation zone. This includes discharge-head curve and discharge-efficiency curve data. Finding these coefficients are quite an easy task and an example of how to find these coefficients are shown below by using an example pump curve.

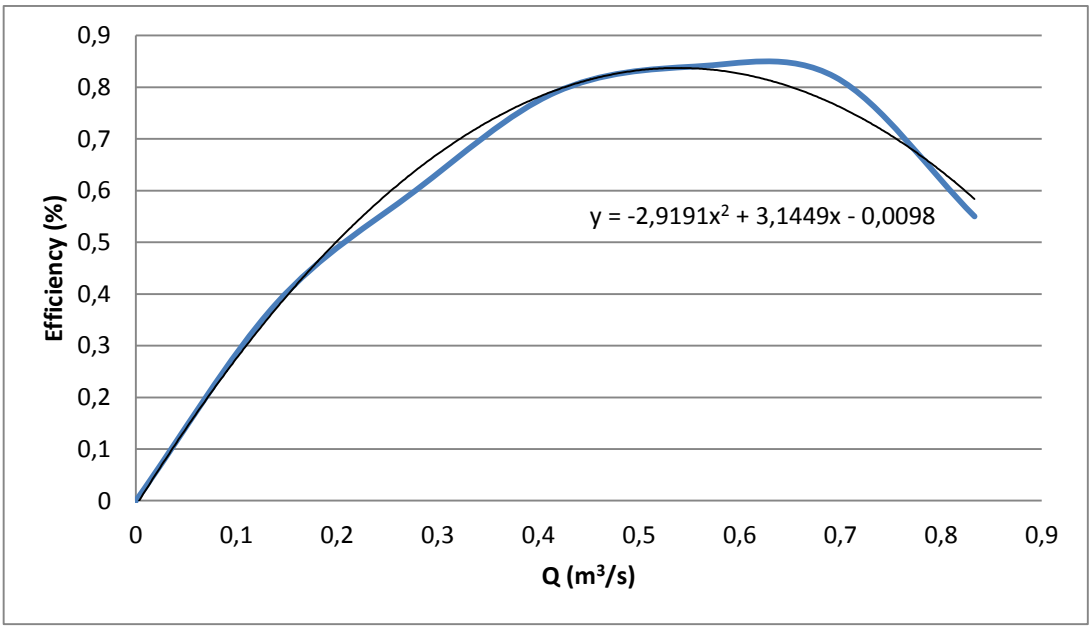

Figure 4-10: Discharge vs efficiency curve for normal operating zone

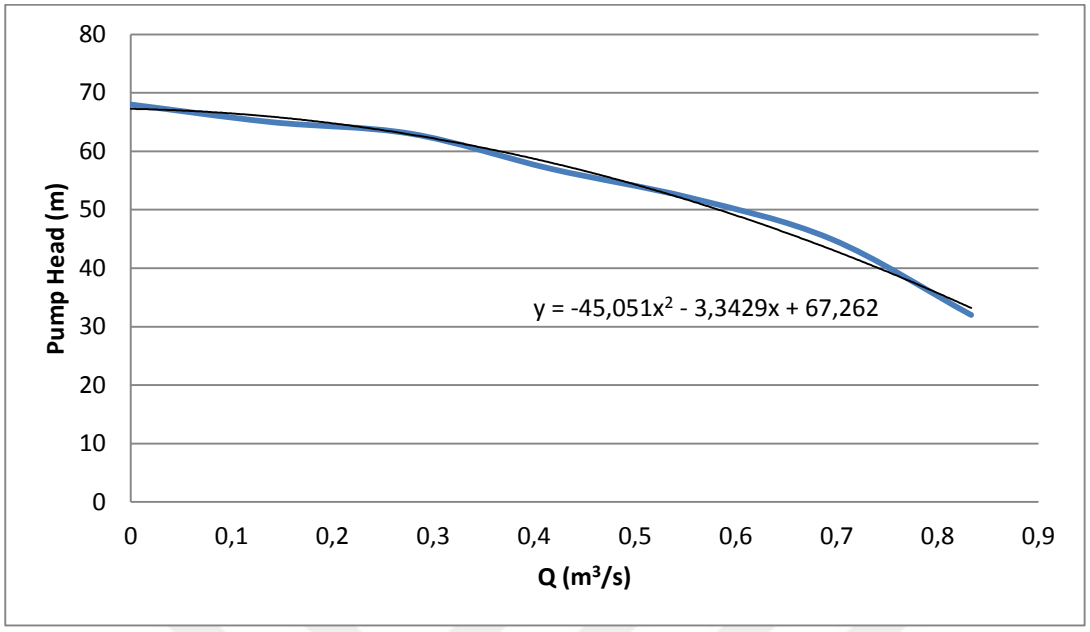

Figure 4-11: Pump head vs. discharge curve for normal operating zone

As shown in Figures 4-10 and 4-11 curve data is entered into MS Excel and an approximated curve is generated using this data. To find equation of this curve user should select "Polynomial" and should press on "Show equation on graph" option.

For the above curves the Property window input values are shown below;

A1_OF_HvsQ_CURVE_EQUATION= -3.3429

A2_OF_HvsQ_CURVE_EQUATION= -45.051

A1_OF_EFFICIENCY_CURVE_EQUATION= 3.1449

A2_OF_EFFICIENCY_CURVE_EQUATION= -2.9191

Shut off head= 68 m

Once above properties are entered software will simulate pump behaviour on normal zone according to above curves and develop curves for other zones of operation by using homologous pump characteristics.

4.2.6 Air Chamber

Air vessel boundary simulates a prevention system against pressure oscillations. This boundary usually is used to prevent downsurges that occur during pumping operations. In order to have quick and effective solution air vessels should be located as close as possible to the location of initial transient activity. Therefore, it will react faster preventing possible damage to the system.

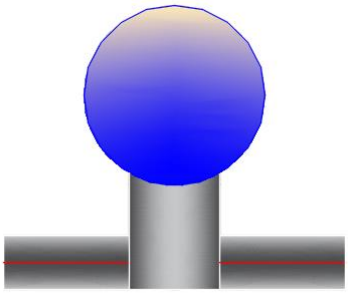

Block:Air Vessel	
BAROMETRIC_PRESSURE_(M)	10
CROSS_SECTIONAL_AREA_(M2)	5
INITIAL_AIR_VOLUME_(M3)	3
ORIFICE_CONSTANT	1
VESSEL_HEIGHT_(M)	2
DATUM_TO_BOTTOM	0
ORIFICE_AREA_(M^2)	0.2

Figure 4-12: Air chamber with orifice symbol and Property window

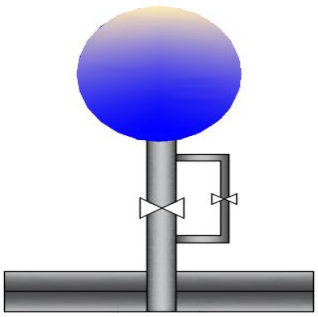

Block:Air Vessel-2	
BAROMETRIC_PRESSURE_(M)	10
CROSS_SECTIONAL_AREA_(M2)	5
INITIAL_AIR_VOLUME_(M3)	3
VESSEL_HEIGHT_(M)	2
DATUM_TO_BOTTOM	0
OUTLET_PIPE_DIAMETER_(MM)	800
INLET_PIPE_DIAMETER_(MM)	15
OUTLET_PIPE_LENGTH_(M)	0
INLET_PIPE_LENGTH_(M)	0
OUTLET_PIPE_FRICTION_FACTOR	0.02
INLET_PIPE_FRICTION_FACTOR	0.02
OUTLET_PIPE_MINOR_LOSS_COEFFICIENT	1
INLET_PIPE_MINOR_LOSS_COEFFICIENT	2.5

Figure 4-13: Air chamber with standpipe symbol and Property window

4.2.7 Surge Tank

Surge tank boundary represents a surge tank connected to the main system via a stand pipe. Surge tanks work in a similar manner to an air chamber but the main difference is that top of surge tank is open to atmosphere therefore, upsurges and downsurges are free to move inside tank.

Surge tanks should be located carefully and on higher points of topography if possible. Since water is free to surge upwards if surge tank is located close to datum elevation point one might have to build very tall surge tank. Therefore, making this solution cost ineffective. Different sizes and locations of surge tanks can be used to find optimum sizing and location.

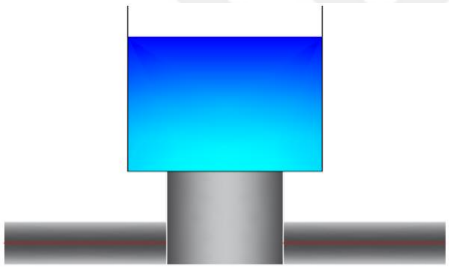

Custom	
Flow Orientation	Two Way
Block:Surge Tank	
CROSS_SECTIONAL_AREA_(M2)	380.13
STAND_PIPE_AREA_(M2)	35.18
STAND_PIPE_LENGTH_(M)	25
STAND_PIPE_FRICTION_FACTOR	0.017
DATUM_TO_BOTTOM	0

Figure 4-14: Surge tank with standpipe symbol and Property window

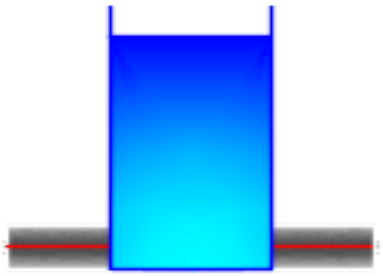

Custom	
Flow Orientation	Two Way
Block:Surge Tank-2	
CROSS_SECTIONAL_AREA_(M2)	380
ORIFICE_AREA_(M^2)	35
ORIFICE_DISCHARGE_COEFFICIENT	0.4
DATUM_TO_BOTTOM	0

Figure 4-15: Surge tank with throttled orifice symbol and Property window

Flow orientation of surge tank can be adjusted by user to;
-One Way – Inflow Only (Check valve to prevent outflow)

-One Way – Outflow Only (Check valve to prevent inflow)

-Two Way (No check valve)

4.2.8 Y-Junctions

This is a simple junction connector and divider boundary. An option to divide pipes into two or three sub-pipes are offered by software.

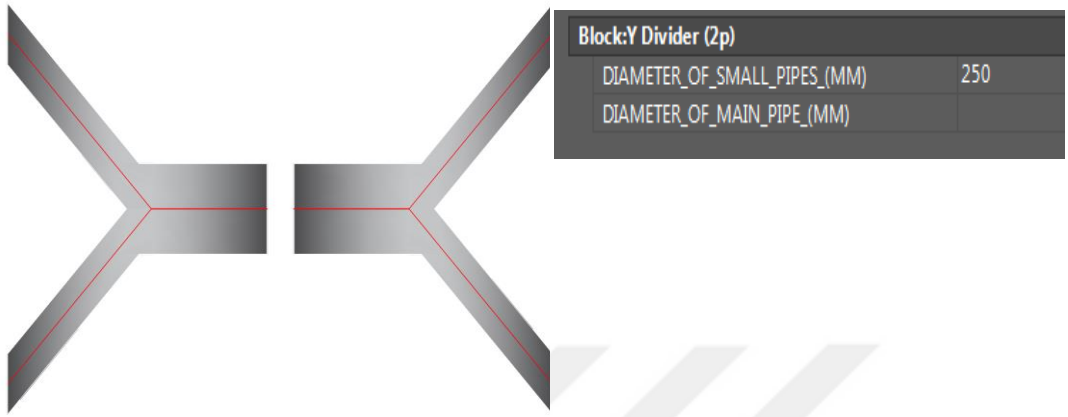

Figure 4-16: Y-junction(2p) symbol and Property window

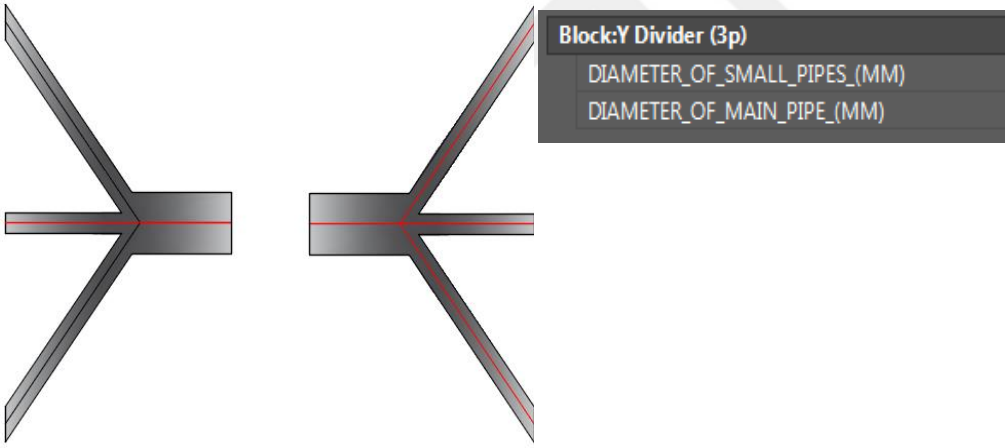

Figure 4-17: Y-junction(3p) symbol and Property window

4.2.9 Interior Valve and Downstream Valve

This is a simple valve boundary which are placed at the downstream and as interior to the system. Downstream valve has only one connection node to the left and interior valve has two connection points since it is interior boundary.

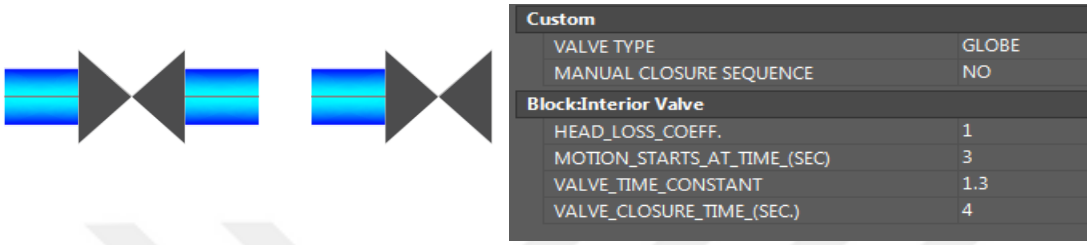

Figure 4-18: Valve symbol and Property window

By selecting "YES" from the "Manual Closure Sequence" dropdown menu, users are able to input their own valve operational closure sequence. If it is chosen as "NO" software will automatically calculate change in valve closure from a function of time given below;

$$Dimensionless\ Valve\ Closure = \left(1 - \frac{t}{t_c}\right)^{E_m}$$

Effective area of valve will be calculated dependent on the dimensionless valve closure and type of the valve using curves given on Figure 4-19.

Example data entry in case "Manual Closure Sequence" is set to "YES" is given below with its explanation;

Notation (t_c=total closure duration);

Manual Closure Sequence = 0-closure$_1$-time$_2$-closure$_2$-time$_3$-closure$_3$-t_c-closure$_3$

Example;

Manual Closure Sequence = 0-1-5-0.7-8-0

Above sequence illustrates that at the beginning of motion valve closure is set to '1' which means the system is at the initial steady state conditions after that it decreases (closure starts) linearly up to '0.7' in 5 seconds and finally it decreases to '0' in

another 3 seconds at 8th second valve is completely closed. Last closure need not to be ‘0’ but it can take any value between ‘0’ and ‘1’.

By using this sequencial entry user is able to open or close a valve partially or completely as desired. User can close the valve and then open it again by using sequencial entry system. Therefore, any valve operation can be simulated by using “Manual Closure Sequence” option.

User is also able to select type of the valve. H-Hammer includes;

- Globe Valve
- Butterfly Valve
- Circular Gate Valve
- Needle Valve
- Ball Valve

Code will calculate active opening of valve during closure operation by considering type of valve. Because some valves might have sudden decrease in their areas at the beginning of closure and then relatively slower reduction in the area after some percentage of closure. Therefore, relative closure of %70 may not mean that flow area of valve is only %30 of its original value. To describe this relationship Fok (1987) illustrated relative closure against valve area curves describing their patterns. Figure 4-19 illustrates relative closure against valve area curves for the valve types used in H-Hammer. Therefore, by selecting a valve type we can relate closure sequence and effective opening of the valve depending on the valve type.

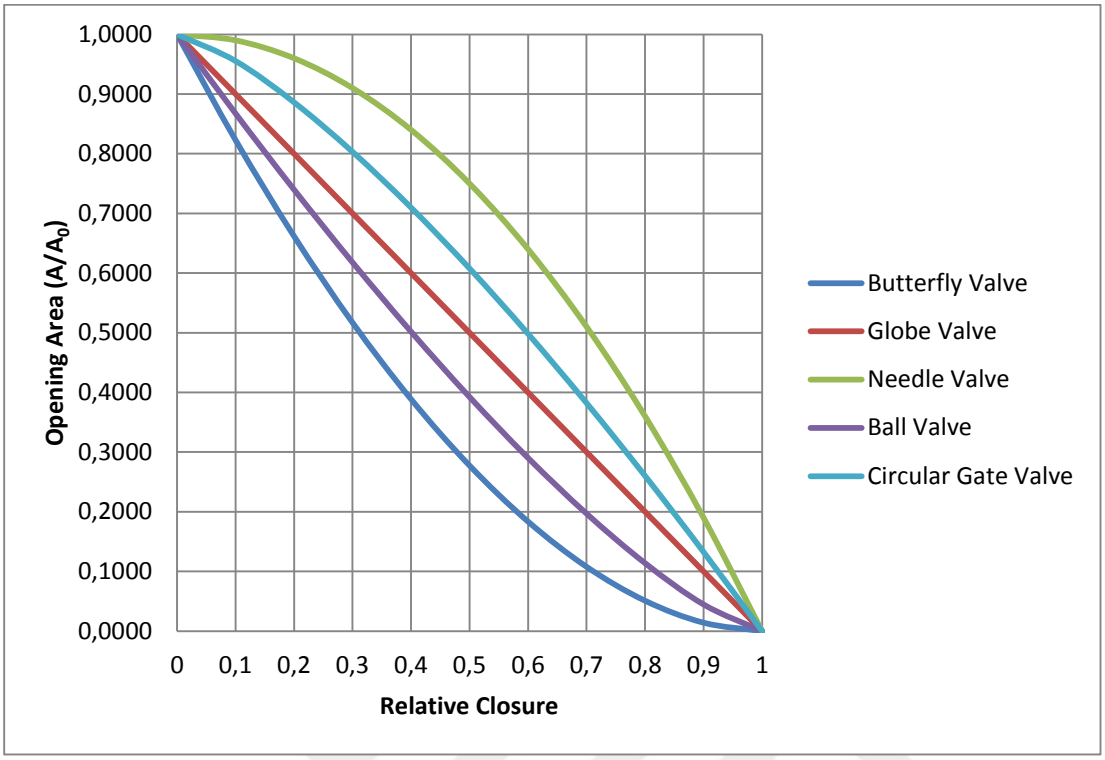

Figure 4-19: Valve operational closure ratio vs. effective valve area for different valve types

4.2.10 Downstream Reservoir with a Constant Head

This boundary is used at the downstream end of the pipe line attached to a constant head reservoir.

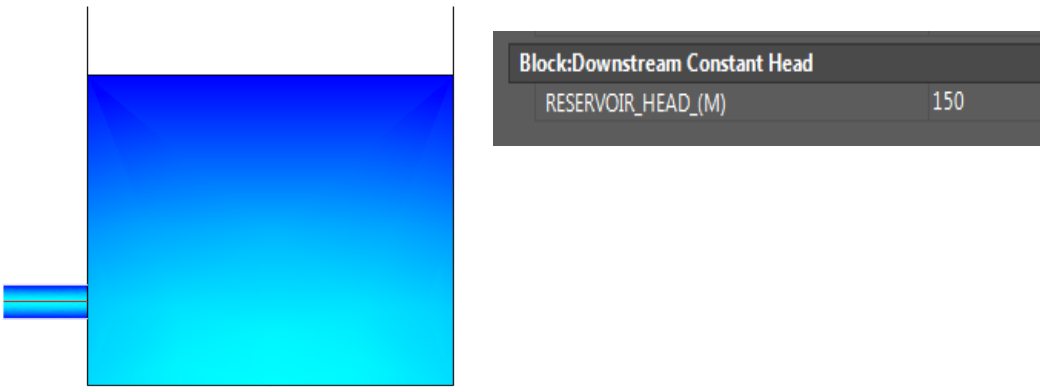

Figure 4-20: Downstream constant head symbol and Property window

4.2.11 Downstream Dead End

This boundary represents dead end conditions in which discharge amount is equal to zero. It should be used at downstream ends only as it has single connection point to the left. This boundary has no input requirement therefore has no Property window.

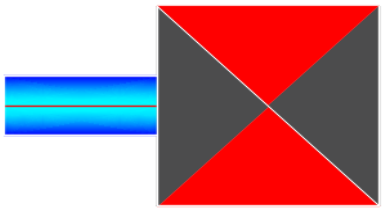

Figure 4-21: Dead end symbol

4.3 System Requirements for the Software

- AutoCAD 2015
- Visual Basic 6.0
- MS Excel
- Windows operating system (7 , 8 , 10)
- 64 bit processor system

CHAPTER 5

VERIFICATION OF THE CODE

Solution of seven different scenarios which were provided in some reputable sources are compared with the solution of the present study for verification purposes.

5.1 Pump Failure with Valve Scenario

In the first case the program titled Whammer and written by D.C. Wiggert (December, 1984) from Michigan State University will be compared with the program, H-Hammer developed in the present study. Whammer was written in Fortran programming language and is designed to analyse pump failure transients with or without a valve located just downstream of the pump. In this comparison output of Whammer is obtained by running it in executable format. At the end outputs of the two programs are compared. In this study two different scenarios will be simulated and compared;

- Pump trip with gradual valve closure
- Pump trip with check valve

Figure 5-1 illustrates schematic of pump trip scenario;

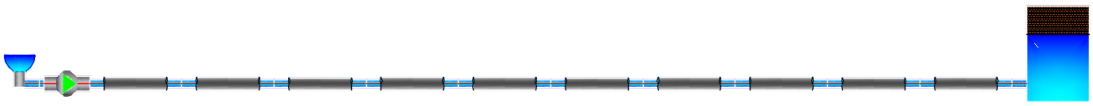

Figure 5-1: Schematic of pumping failure scenario

Table 5-1 illustrates general input data that were used on this simulations;

Table 5-1: General input data for pump (failure with valve in front scenario)

Pipe Length, L	10,000	m
Diameter of Pipe, D	0.65	m
Acoustic speed, a	1320.92	m/s
Friction Factor, f	0.022	
Density of Water, ρ	1000	kg/m^3
Hoop Stress of Pipe, σ	35	MPa
Rated Head of Pump, H_R	85	m
Rated Discharge of Pump, Q_R	0.10	m^3/s
Rated Speed of Pump, N_R	885	rpm
Rated Torque of Pump, T_R	1056.40	N.m
Rated Efficiency of Pump, η_R	0.85	
Valve Minor Loss Coeff.	3	
Value of D/e	20	
Value of WR^2	200	Nm^2
Elasticity Modulus of Pipe Material	170	GPa
Bulk Modulus of Elasticity of Fluid	2.19	GPa

5.1.1 Pump Trip with Globe Valve Closure

Simulation data is given below;

Pump trip starts at "t"= 10 second.

Chosen Δt= 0.38 seconds.

Valve closure time: 8 seconds after the pump trip

In both cases a scenario is solved where pump trip occurs at 10th second of operation and upon this failure a globe valve starts closing to protect turbo pump from reverse flow conditions preventing possible damage to the machine.

Results are compared on the following graphs;

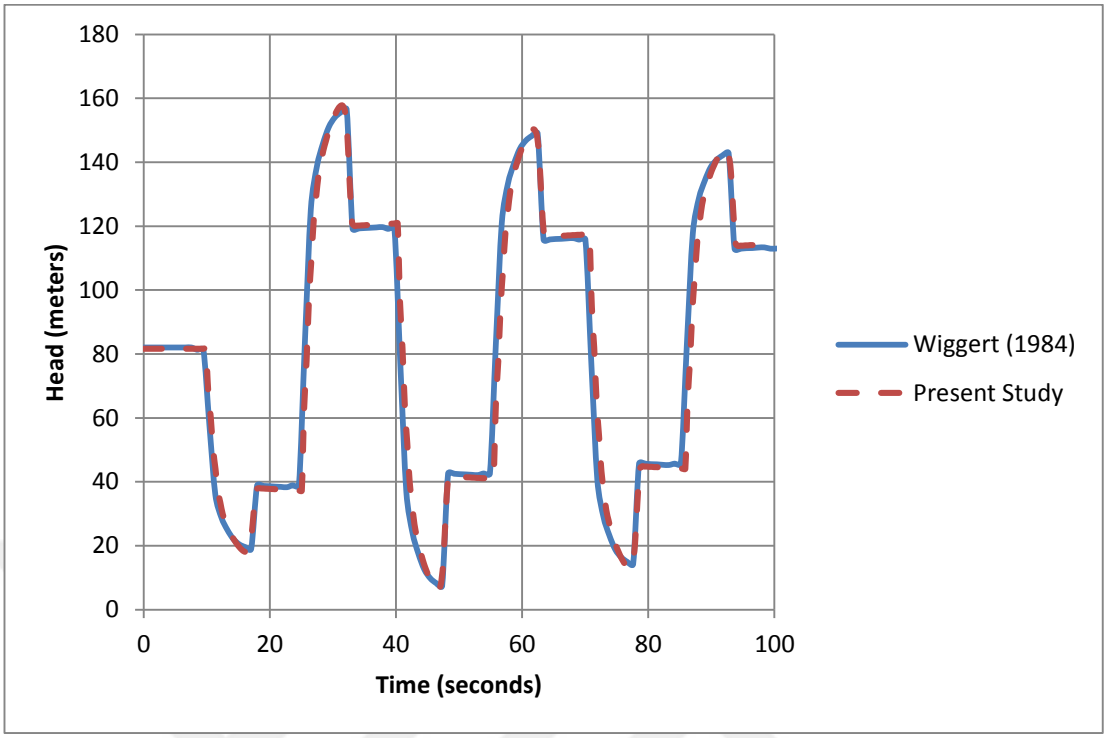

Figure 5-2: Head vs time graph for pump trip with valve at x=0+000 m

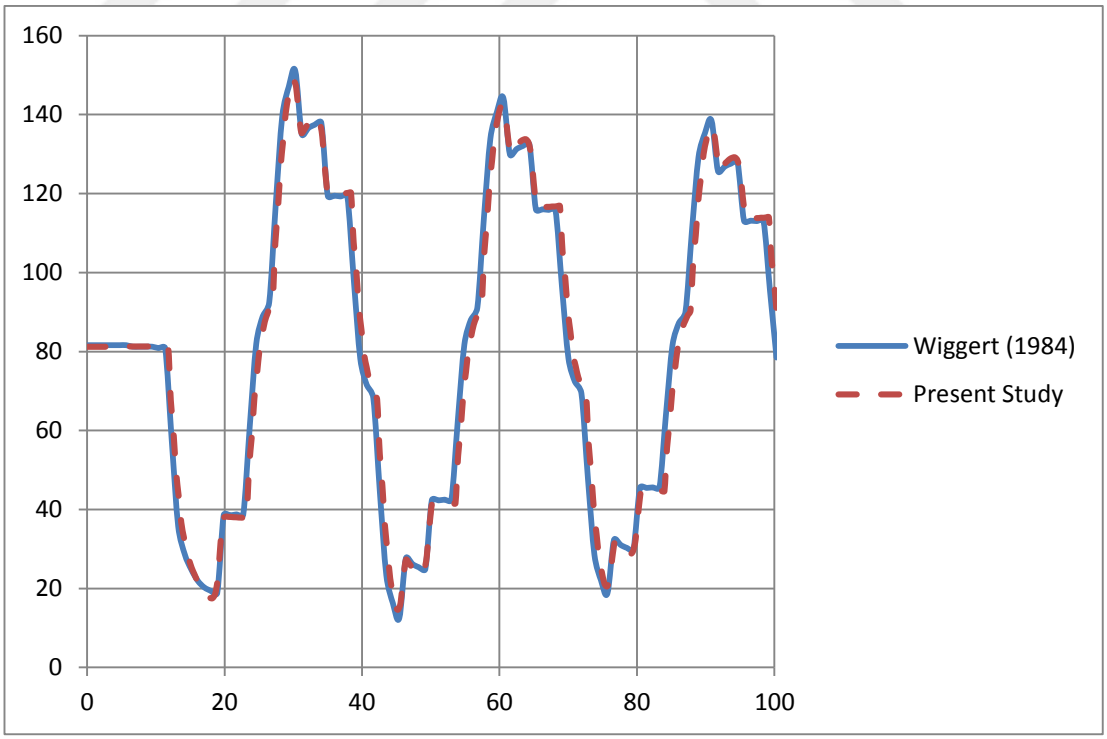

Figure 5-3: Head vs time graph for pump trip with valve at x=2+500 m

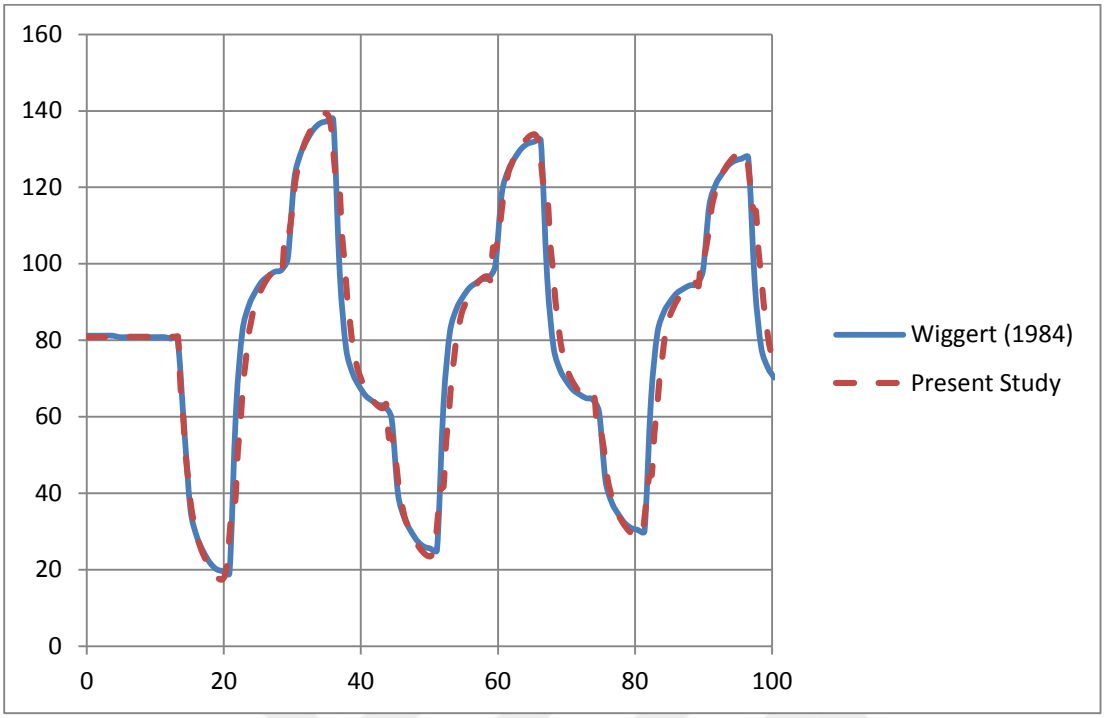

Figure 5-4: Head vs time graph for pump trip with valve at x=5+000 m

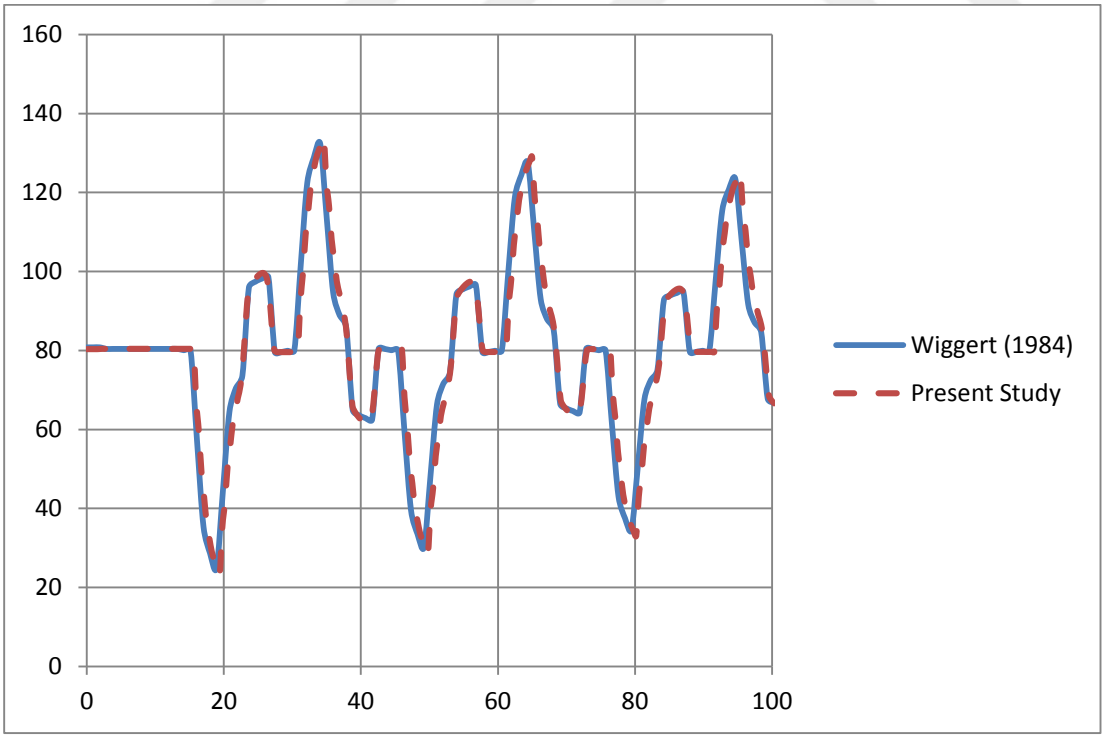

Figure 5-5: Head vs time graph for pump trip with valve at x=7+500 m

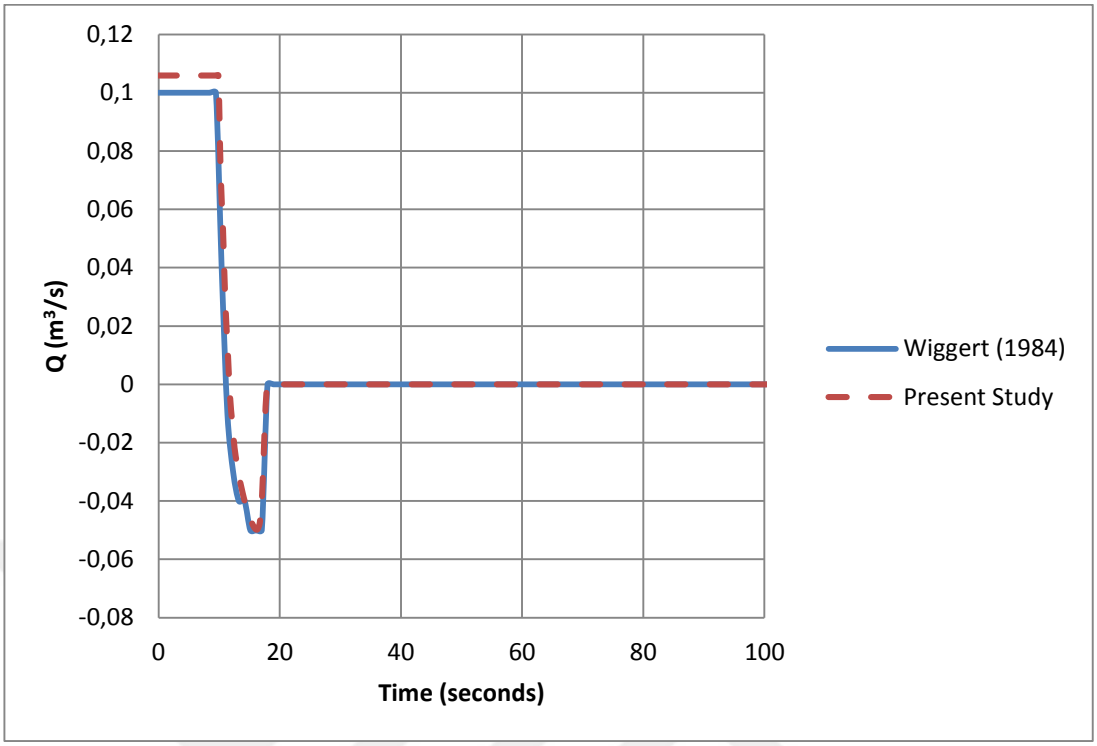

Figure 5-6: Discharge vs time graph for pump trip with valve at x=0+000 m

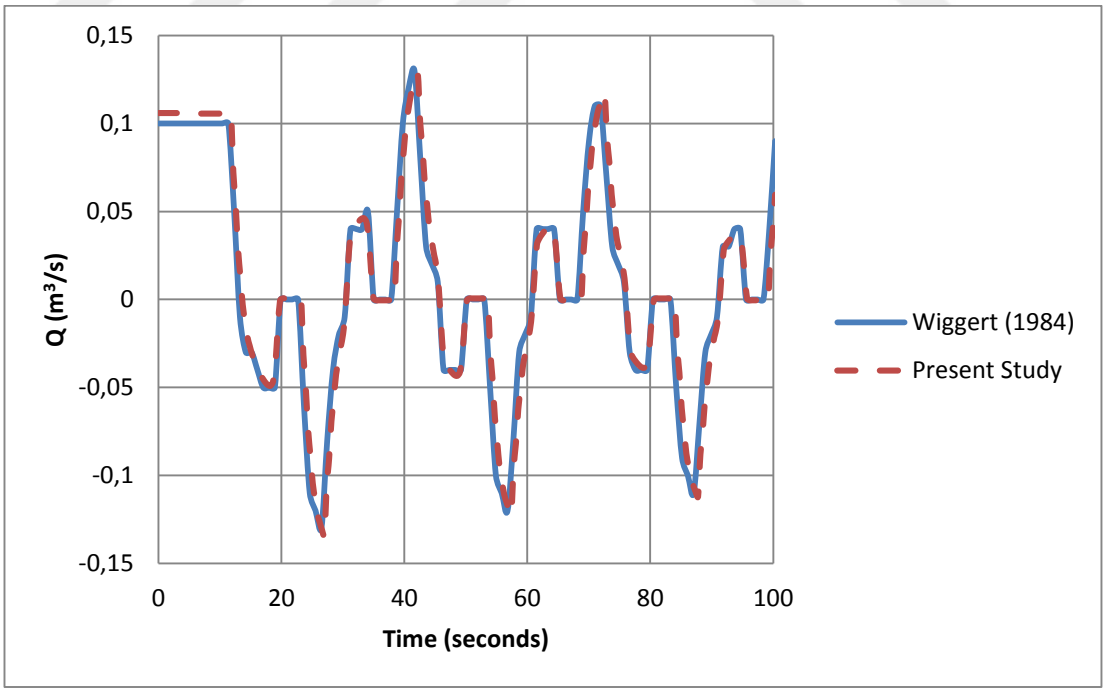

Figure 5-7: Discharge vs time graph for pump trip with valve at x=2+500 m

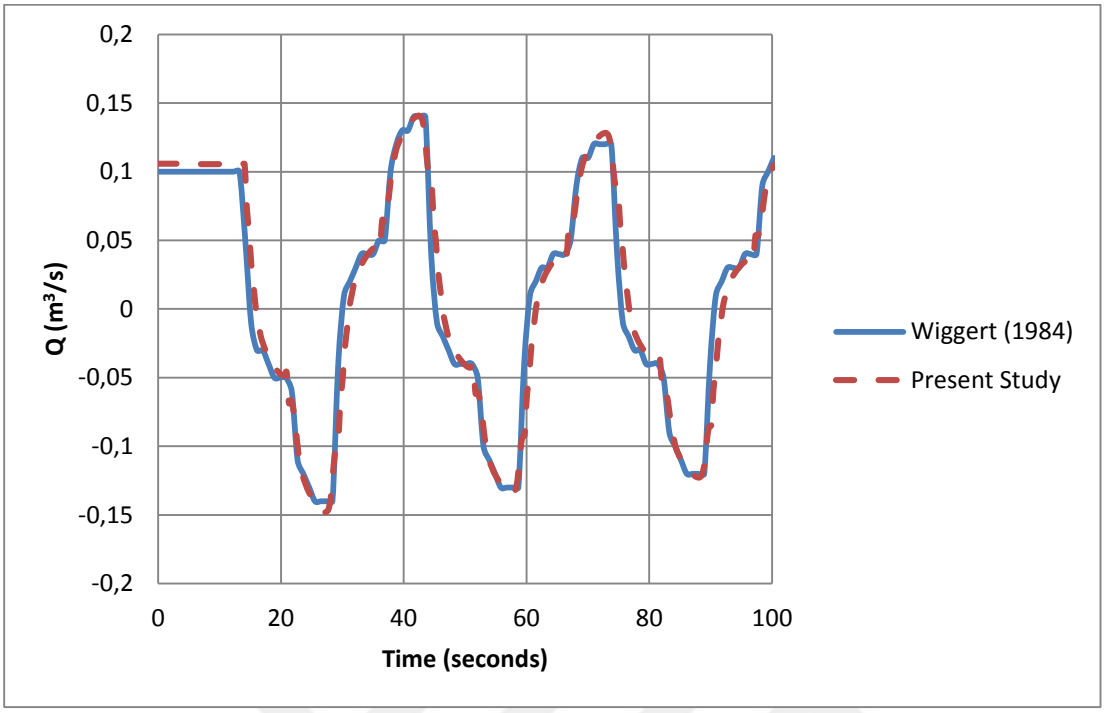

Figure 5-8: Discharge vs time graph for pump trip with valve at x=5+000 m

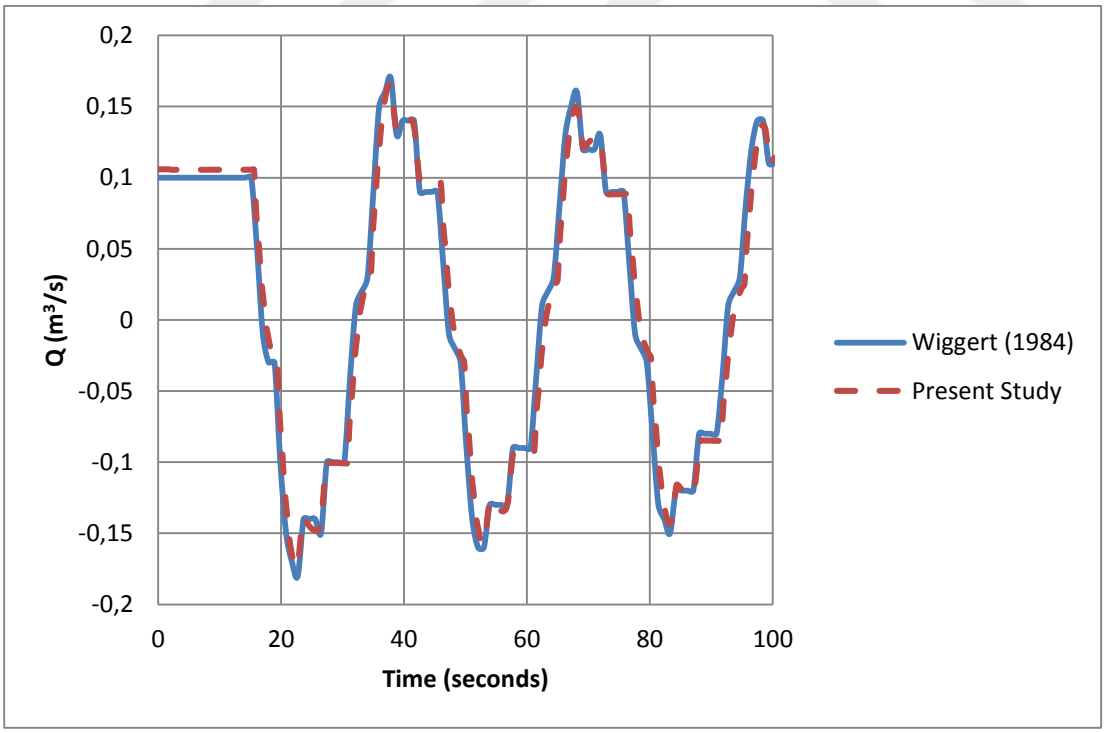

Figure 5-9: Discharge vs time graph for pump trip with valve at x=7+500 m

From above graphs it is visible that quite close results are obtained. By using smaller Δt time and Δx space intervals more accurate results can be obtained at the cost of increasing computer time. But 0.38 seconds time interval yields quite accurate results in terms of head and discharge values in this example.

5.1.2 Pump Trip with Check Valve

Unlike butterfly valve, check valve will close instantly upon arrival of reverse flow on pump boundary location causing a sudden pressure variations. It is a highly undesired situation which often causes check valve slam but these valves are necessary to protect turbo pumps from the effects of reverse flows.

Simulation data is given below;

Pump trip starts at “t”= 3 second.

Chosen Δt= 0.38 seconds.

Valve closure time: 0.01 seconds after the pump trip (instantly)

Results are compared on the following graphs;

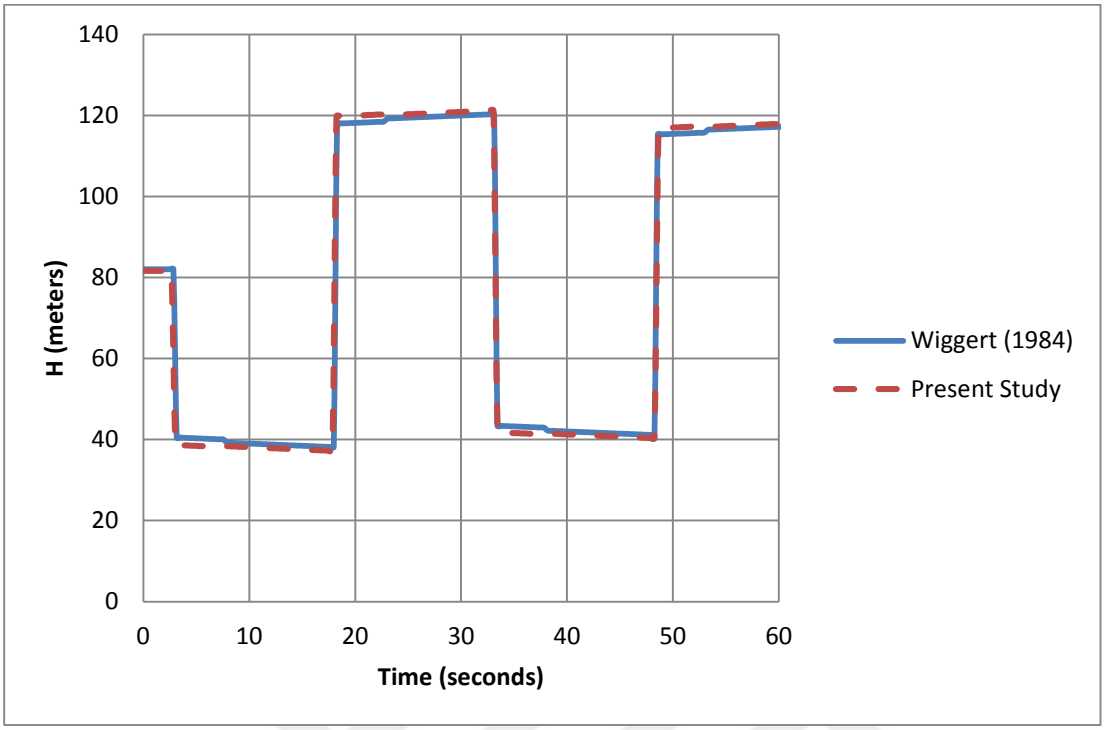

Figure 5-10: Head vs time graph for pump trip with check valve at x=0+000 m

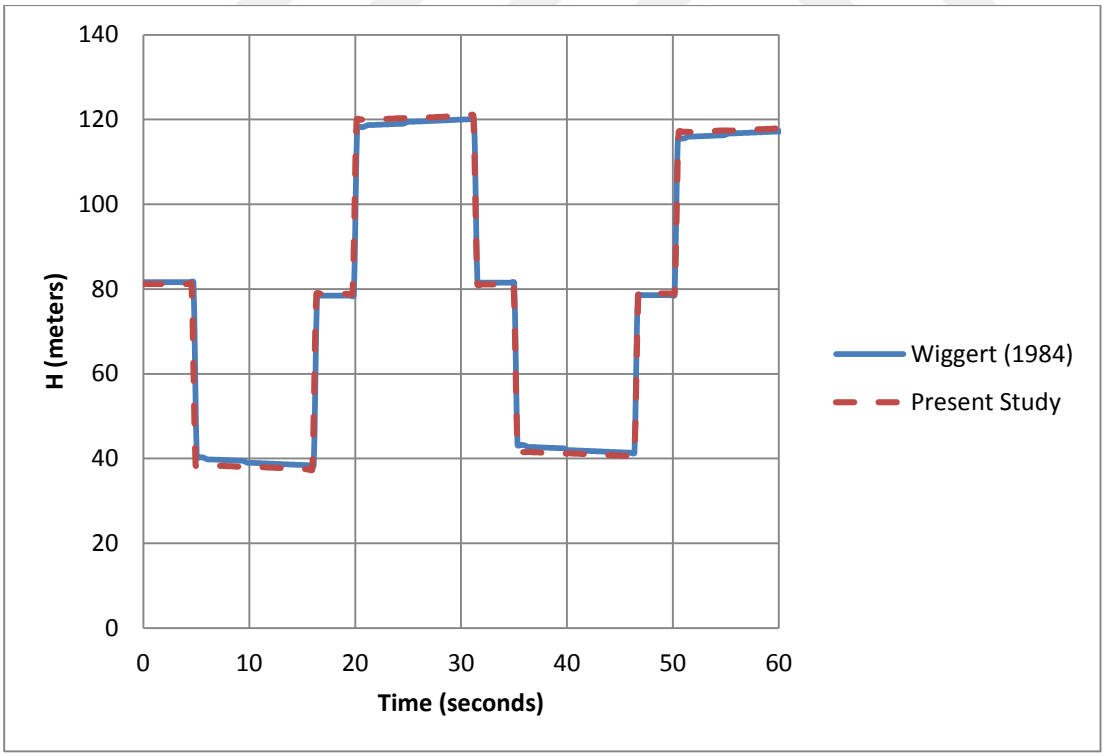

Figure 5-11: Head vs time graph for pump trip with check valve at x=2+500 m

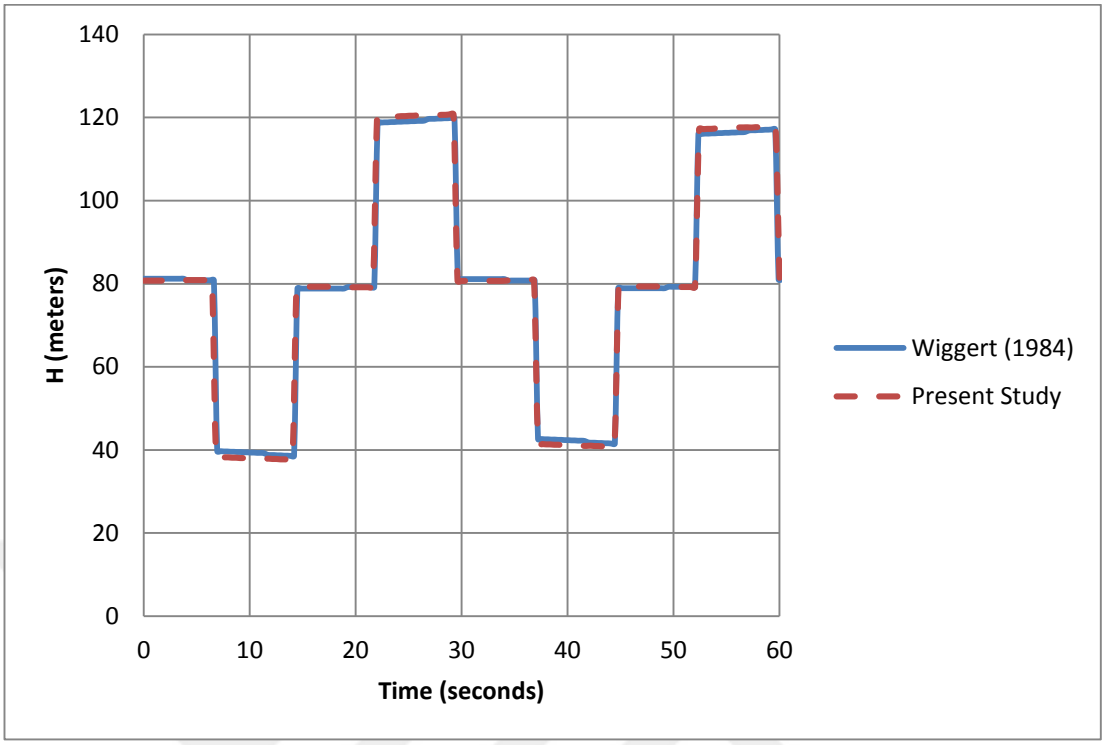

Figure 5-12: Head vs time graph for pump trip with check valve at x=5+000 m

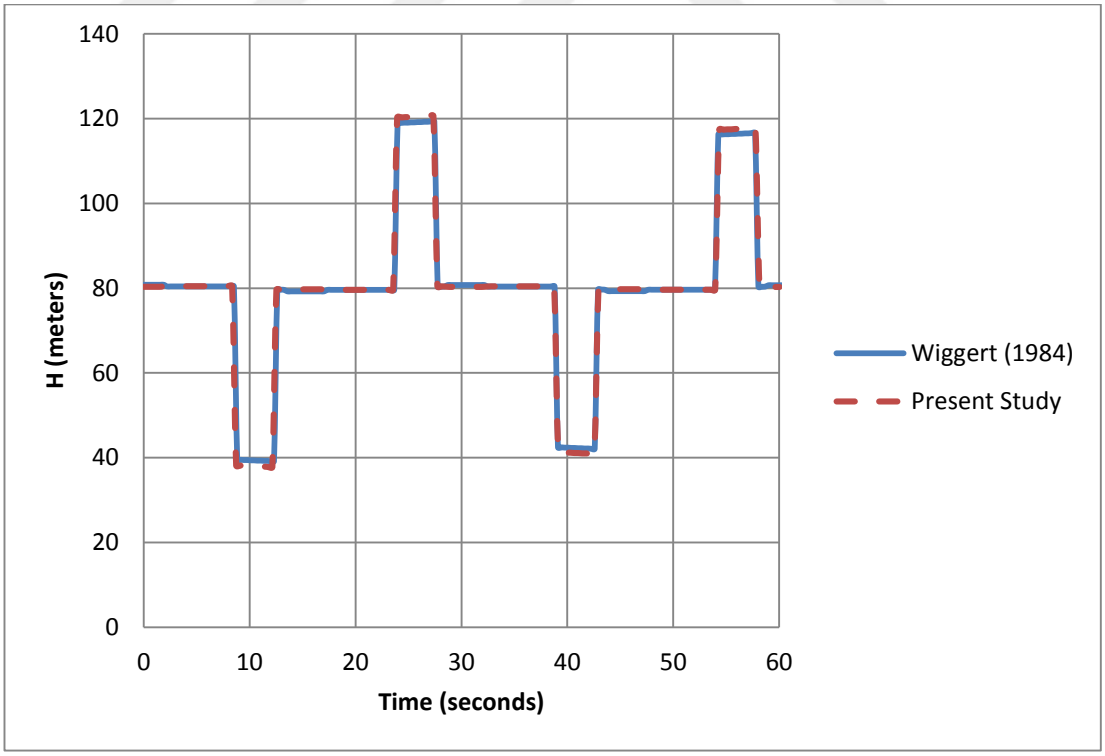

Figure 5-13: Head vs time graph for pump trip with check valve at x=7+500 m

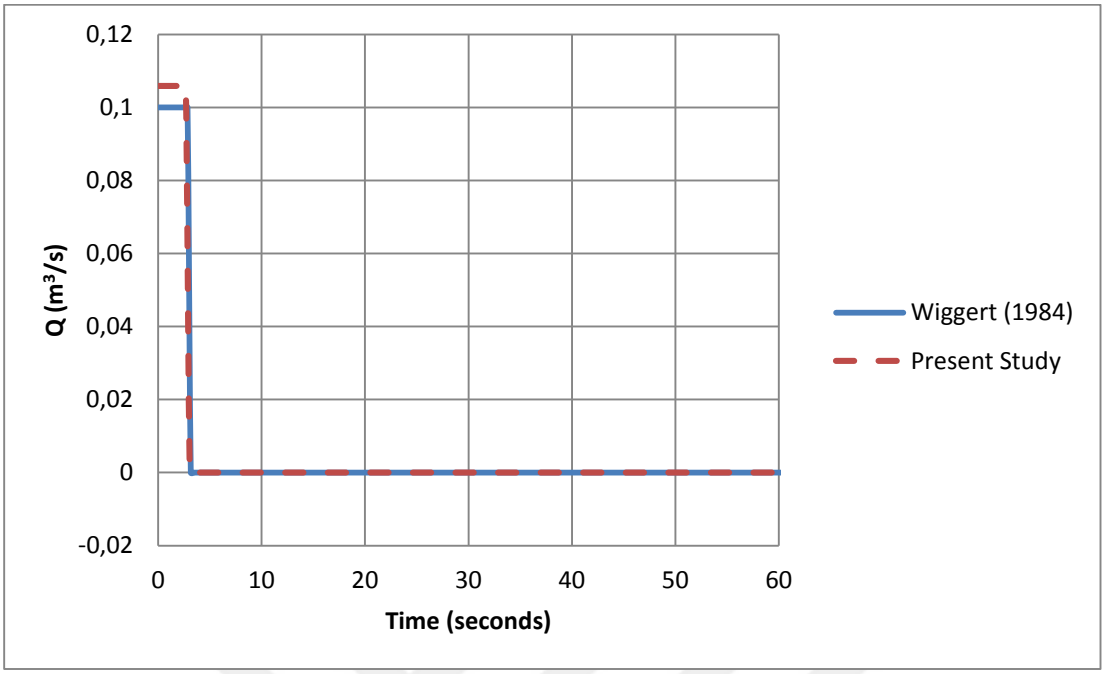

Figure 5-14: Discharge vs time graph for pump trip with check valve at x=0+000 m

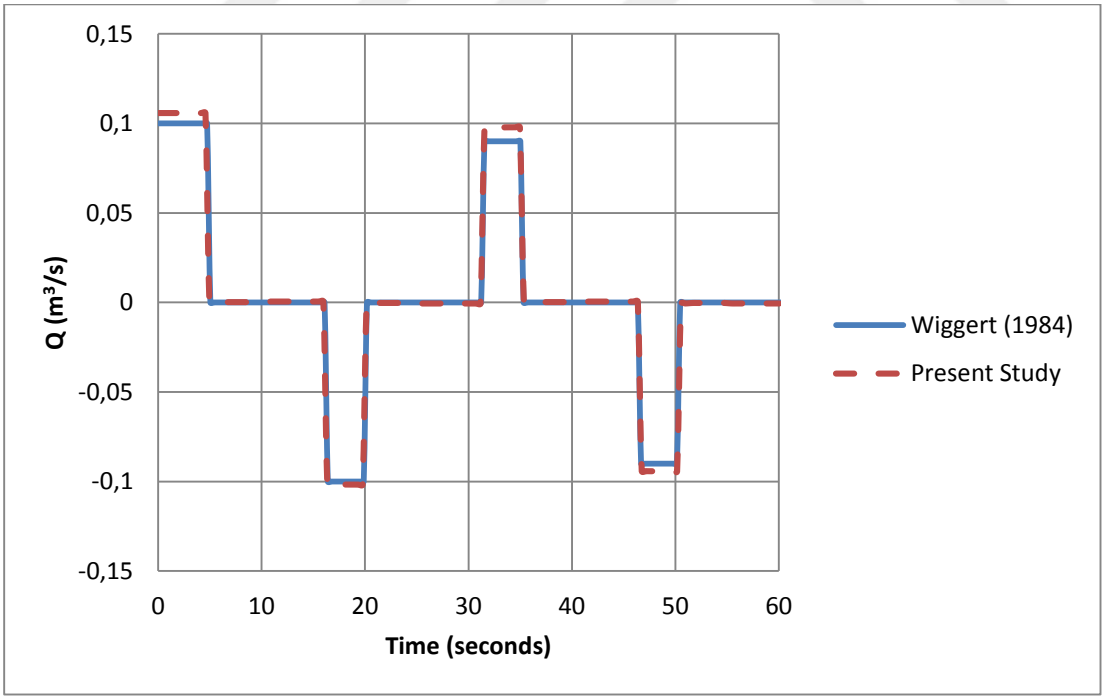

Figure 5-15: Discharge vs time graph for pump trip with check valve at x=2+500 m

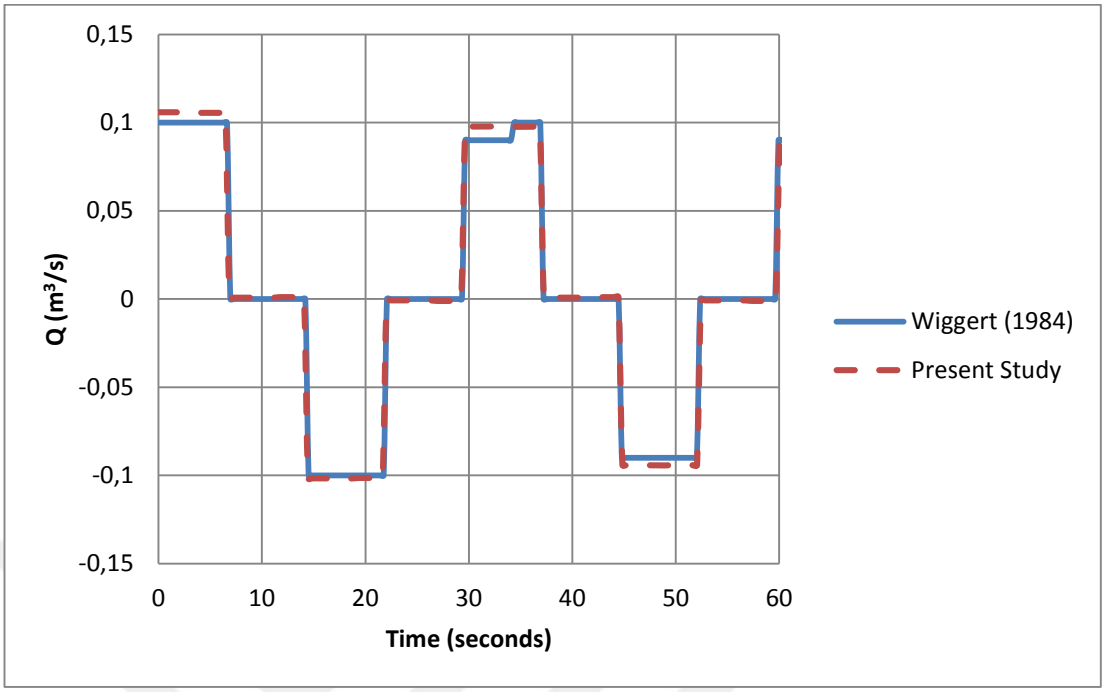

Figure 5-16: Discharge vs time graph for pump trip with check valve at x=5+000 m

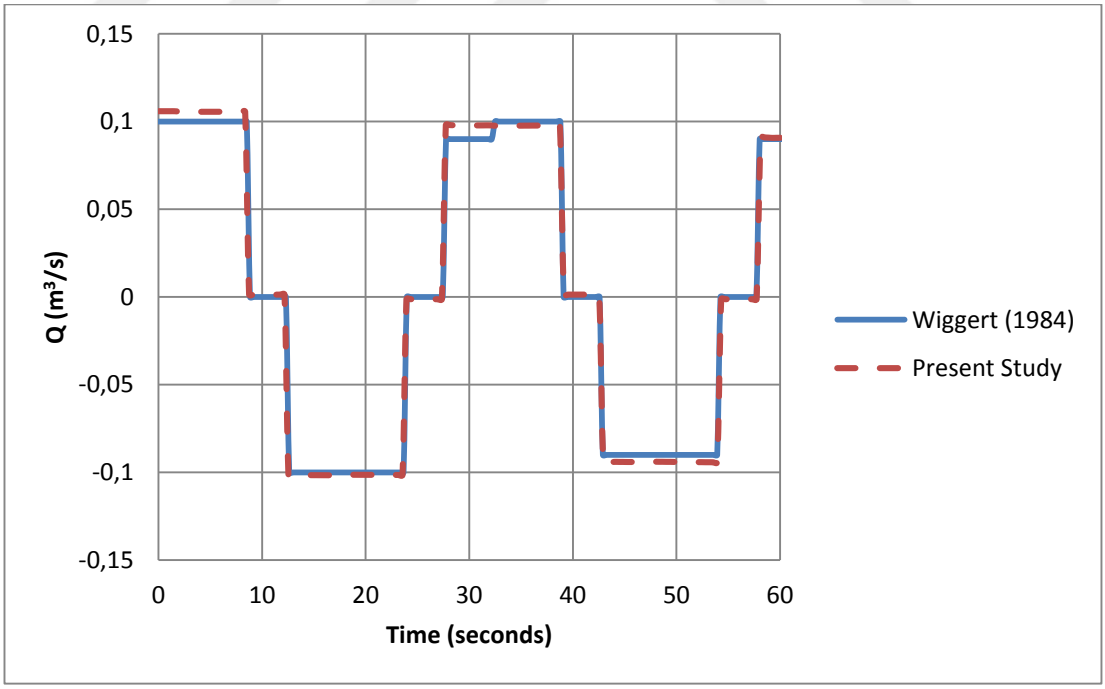

Figure 5-17: Discharge vs time graph for pump trip with check valve at x=7+500 m

5.2 Series Connection with Downstream Valve Scenario

5.2.1 Comparison to Series Junction Case Study by Wylie & Streeter

Another trial is made by comparing results of H-Hammer with results of case study conducted by Wylie and Streeter (1978). The details and results of his study were obtained from "Fluid Transients (1978)" book "Appendix C (p.340-342)" section.Figure 5-18 illustrates definition of the system simulated.

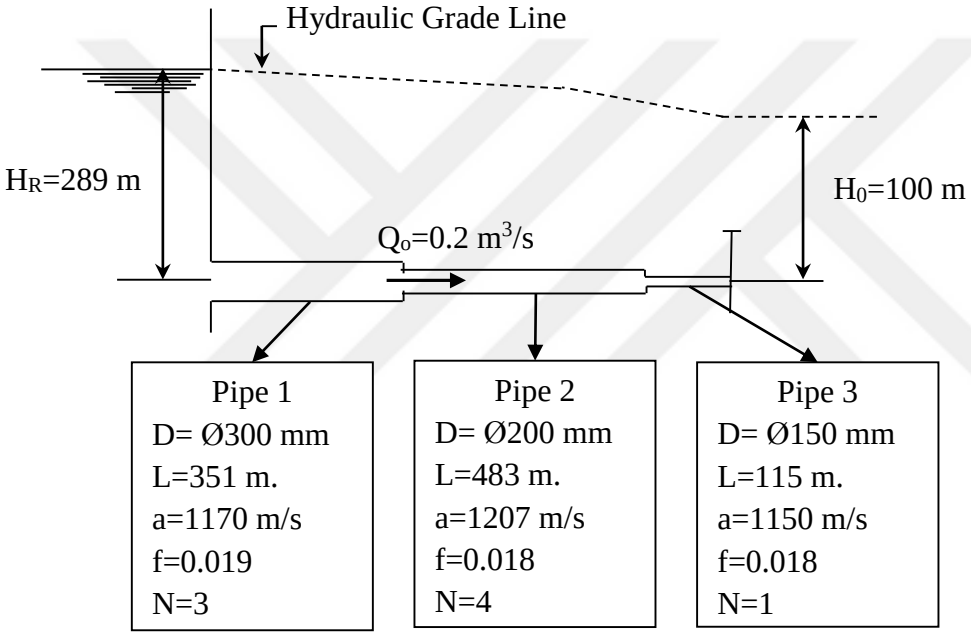

Figure 5-18: Series connected pipes transient problem definition (Wylie-Streeter, 1978)

Δt is chosen as 0.1 seconds to match case study identically.

To solve this problem by using above time interval one need to divide those pipes into pieces in order to satisfy Courant condition. Therefore, pipe 1 is divided into 3 parts, pipe 2 is divided into 4 parts and pipe 3 is not divided since it already satisfies Courant condition as it is. Figure 5-19 illustrates schematic of the problem created H-Hammer.

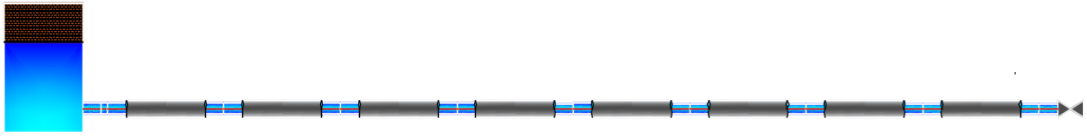

Figure 5-19: H-Hammer schematic of series junction case study by Wylie & Streeter

Custom built τ values of downstream valve are used in the problem to have identical conditions for the sake of comparison. Simulation time is 2.1 seconds.

Head and discharge values at the end of each pipe (junctions) are given and compared to the results obtained by Wylie and Streeter on the Table 5-2 and Table 5-3.

Table 5-2: Series junction simulation head comparison (H-Hammer & Wylie-Streeter)

		H (Head Values in meters)							
		WYLIE-STREETER (1978)				PRESENT STUDY			
Time(s.)	Tau	Reservoir	Pipe 1	Pipe 2	Pipe 3	Reservoir	Pipe 1	Pipe 2	Pipe 3
0.00	1.000	289.04	279.96	190.13	100.00	289.04	279.93	190.09	99.96
0.10	0.867	289.04	279.96	190.13	127.65	289.04	279.93	190.09	127.52
0.20	0.733	289.04	279.96	209.29	167.51	289.04	279.93	209.18	167.58
0.30	0.600	289.04	279.96	236.95	224.67	289.04	279.93	236.97	224.61
0.40	0.467	289.04	279.96	280.29	311.71	289.04	279.93	280.21	311.32
0.50	0.333	289.04	279.96	346.37	448.71	289.04	279.93	346.07	449.05
0.60	0.200	289.04	290.24	451.27	668.7	289.04	290.17	451.45	668.63
0.70	0.183	289.04	305.14	621.16	673.58	289.04	305.14	620.97	674.07
0.80	0.167	289.04	328.37	646.61	651.84	289.04	328.32	646.95	650.83
0.90	0.150	289.04	364.09	667.97	690.25	289.04	363.93	667.18	689.81
1.00	0.133	289.04	421.37	693.87	736.11	289.04	421.49	693.63	737.04
1.10	0.117	289.04	516.21	720.75	764.86	289.04	516.15	721.20	763.76
1.20	0.100	289.04	515.51	736.44	790.15	289.04	515.80	735.57	789.50
1.30	0.083	289.04	505.57	743.16	805.23	289.04	505.13	742.92	806.45
1.40	0.067	289.04	491.17	728.44	805.76	289.04	491.10	729.02	804.70
1.50	0.050	289.04	461.26	679.15	773.19	289.04	461.79	678.30	772.30
1.60	0.033	289.04	398.87	666.19	684.02	289.04	398.21	665.67	685.48
1.70	0.017	289.04	283.49	627.78	683.85	289.04	283.43	628.87	682.50
1.80	0.000	289.04	282.49	598.18	686.38	289.04	282.56	597.29	686.11
1.90	0.000	289.04	281.68	546.49	570.22	289.04	281.74	546.23	570.89
2.00	0.000	289.04	275.5	395.07	407.59	289.04	275.38	395.36	407.35
2.10	0.000	289.04	260.99	165.77	221.48	289.04	260.97	165.78	221.41

Table 5-3: Series junction simulation discharge comparison (H-Hammer & Wylie-Streeter)

		Q (Discharge Values in m^3/s)							
		WYLIE-STREETER (1978)				PRESENT STUDY			
Time(s.)	Tau	Reservoir	Pipe 1	Pipe 2	Pipe 3	Reservoir	Pipe 1	Pipe 2	Pipe 3
0.00	1.000	0.200	0.200	0.200	0.200	0.200	0.200	0.200	0.200
0.10	0.867	0.200	0.200	0.200	0.196	0.200	0.200	0.200	0.196
0.20	0.733	0.200	0.200	0.195	0.190	0.200	0.200	0.195	0.190
0.30	0.600	0.200	0.200	0.188	0.180	0.200	0.200	0.188	0.180
0.40	0.467	0.200	0.200	0.177	0.165	0.200	0.200	0.177	0.165
0.50	0.333	0.200	0.200	0.161	0.141	0.200	0.200	0.161	0.141
0.60	0.200	0.200	0.194	0.135	0.103	0.200	0.194	0.135	0.103
0.70	0.183	0.200	0.185	0.093	0.095	0.200	0.185	0.093	0.095
0.80	0.167	0.200	0.171	0.088	0.085	0.200	0.171	0.088	0.085
0.90	0.150	0.188	0.150	0.085	0.079	0.188	0.150	0.085	0.079
1.00	0.133	0.171	0.117	0.077	0.072	0.171	0.117	0.077	0.072
1.10	0.117	0.144	0.061	0.068	0.065	0.144	0.061	0.068	0.065
1.20	0.100	0.103	0.051	0.059	0.056	0.103	0.050	0.059	0.056
1.30	0.083	0.037	0.040	0.048	0.047	0.037	0.041	0.048	0.047
1.40	0.067	-0.074	0.023	0.035	0.038	-0.074	0.023	0.035	0.038
1.50	0.050	-0.084	0.001	0.018	0.028	-0.084	0.000	0.018	0.028
1.60	0.033	-0.088	-0.028	0.011	0.017	-0.087	-0.028	0.011	0.017
1.70	0.017	-0.095	-0.070	0.009	0.009	-0.096	-0.070	0.009	0.009
1.80	0.000	-0.101	-0.079	-0.004	0.000	-0.101	-0.079	-0.004	0.000
1.90	0.000	-0.092	-0.082	-0.021	0.000	-0.092	-0.082	-0.021	0.000
2.00	0.000	-0.065	-0.087	-0.026	0.000	-0.066	-0.087	-0.026	0.000
2.10	0.000	-0.074	-0.083	-0.036	0.000	-0.074	-0.084	-0.036	0.000

From the comparison it can be stated that results of H-Hammer is highly accurate and it yielded similar results to Wylie-Streeter's case study.

5.2.2 Comparison to Series Junction Case Study by Chaudhry

Second comparison is made between analysis conducted by Chaudhry (1979) and H-Hammer. The details and results of his study were obtained from "Applied Hydraulic Transients (1979)" book "Appendix B (p.469-473)" section. Figure 5-20 illustrates definition of the system simulated.

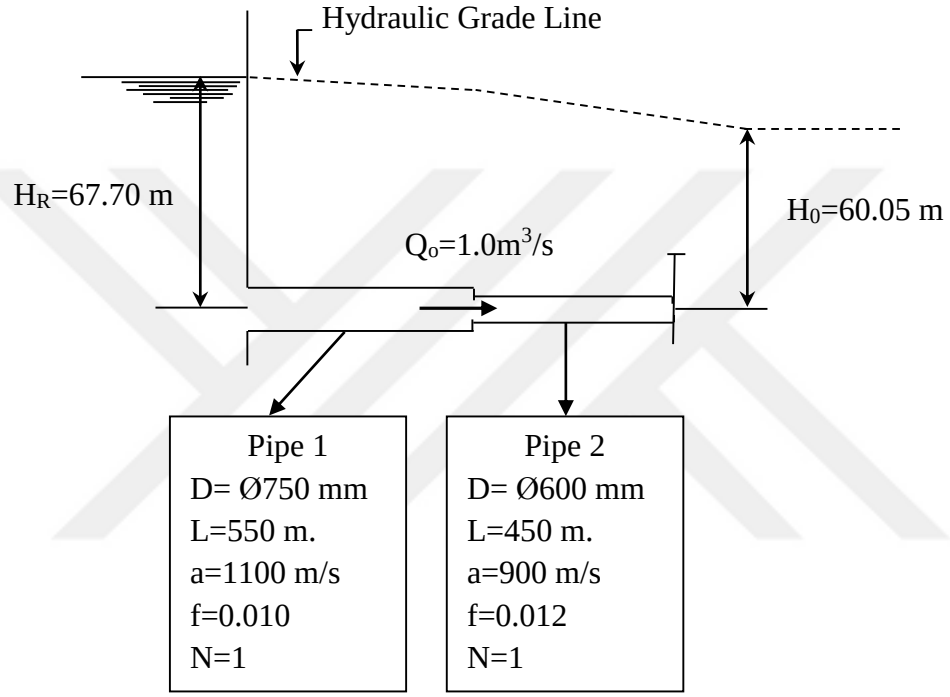

Figure 5-20: Series connected pipes transient problem definition (Chaudhry, 1979)

Δt= 0.5 seconds

Figure 5-21 illustrates H-Hammer schematic of the case studied by Chaudhry;

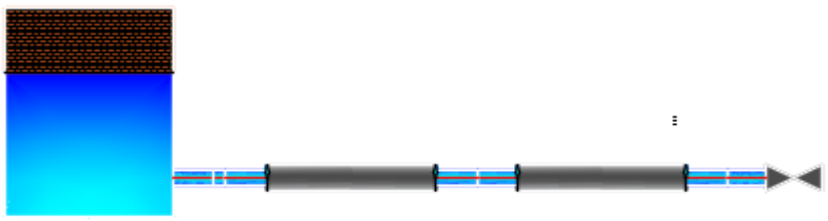

Figure 5-21: H-Hammer schematic of series junction case study by Chaudhry

Custom built τ values of downstream valve are used in the problem to have identical conditions for the sake of comparison. Simulation time is 10 seconds.

Head and discharge values at each node are given and compared to the results obtained by Chaudhry in Table 5-4 and Table 5-5.

Table 5-4: Series junction simulation head comparison (H-Hammer & Chaudhry)

		H (Head Values in meters)					
		CHAUDHRY (1979)			PRESENT STUDY		
Time(s.)	Tau	Reservoir	Pipe 1	Pipe 2	Reservoir	Pipe 1	Pipe 2
0.000	1.000	67.70	65.78	60.05	67.70	65.78	60.04
0.500	0.963	67.70	65.78	63.46	67.70	65.78	63.41
1.000	0.900	67.70	68.73	69.78	67.70	68.69	69.76
1.500	0.813	67.70	74.16	79.88	67.70	74.16	79.78
2.000	0.700	67.70	79.92	95.83	67.70	79.91	95.75
2.500	0.600	67.70	88.25	110.41	67.70	88.24	110.32
3.000	0.500	67.70	94.95	125.13	67.70	94.99	124.94
3.500	0.400	67.70	99.18	139.2	67.70	99.13	139.02
4.000	0.300	67.70	104.4	149.14	67.70	104.33	148.84
4.500	0.200	67.70	108.47	158.61	67.70	108.36	158.27
5.000	0.100	67.70	111.20	165.65	67.70	111.06	165.37
5.500	0.038	67.70	113.07	149.46	67.70	112.98	149.04
6.000	0.000	67.70	96.01	114.28	67.70	95.79	114.30
6.500	0.000	67.70	63.25	61.79	67.70	63.36	62.02
7.000	0.000	67.70	34.25	12.33	67.70	34.66	12.56
7.500	0.000	67.70	23.55	6.75	67.70	23.62	7.33
8.000	0.000	67.70	47.63	34.76	67.70	47.74	34.68
8.500	0.000	67.70	82.89	88.45	67.70	82.75	88.06
9.000	0.000	67.70	105.95	130.93	67.70	105.51	130.69
9.500	0.000	67.70	108.01	123.42	67.70	107.97	122.94
10.000	0.000	67.70	78.38	85.12	67.70	78.40	85.28

Table 5-5: Series junction simulation discharge comparison (H-Hammer & Caudhry)

		Q (Discharge Values in m^3/s)					
		CHAUDHRY (1979)			PRESENT STUDY		
Time(s.)	Tau	Reservoir	Pipe 1	Pipe 2	Reservoir	Pipe 1	Pipe 2
0.000	1.000	1.000	1.000	1.000	1.000	1.000	1.000
0.500	0.963	1.000	1.000	0.989	1.000	1.000	0.990
1.000	0.900	1.000	0.988	0.97	1.000	0.989	0.970
1.500	0.813	0.977	0.967	0.937	0.977	0.967	0.937
2.000	0.700	0.935	0.922	0.884	0.934	0.922	0.884
2.500	0.600	0.867	0.847	0.814	0.867	0.847	0.813
3.000	0.500	0.761	0.755	0.722	0.761	0.754	0.721
3.500	0.400	0.643	0.633	0.609	0.643	0.633	0.609
4.000	0.300	0.506	0.496	0.473	0.506	0.495	0.472
4.500	0.200	0.35	0.344	0.325	0.349	0.344	0.325
5.000	0.100	0.183	0.177	0.166	0.183	0.177	0.166
5.500	0.038	0.006	0.004	0.059	0.006	0.004	0.060
6.000	0.000	-0.175	-0.106	0.000	-0.174	-0.104	0.000
6.500	0.000	-0.217	-0.157	0.000	-0.215	-0.157	0.000
7.000	0.000	-0.139	-0.085	0.000	-0.140	-0.084	0.000
7.500	0.000	0.047	0.035	0.000	0.046	0.034	0.000
8.000	0.000	0.208	0.126	0.000	0.208	0.124	0.000
8.500	0.000	0.205	0.148	0.000	0.203	0.148	0.000
9.000	0.000	0.088	0.054	0.000	0.089	0.054	0.000
9.500	0.000	-0.097	-0.071	0.000	-0.095	-0.070	0.000
10.000	0.000	-0.229	-0.139	0.000	-0.229	-0.137	0.000

As previously results are observed to be very close to each other.

5.3 Pump Failure without Valve Scenario

In this case we will compare results of a study conducted by M. Hanif Chaudhry. The details and results of his study were obtained from "Applied Hydraulic Transients (1979)" book "Appendix C (p.474-480)" section. He simulated a pump failure scenario without any check or butterfly valve for 15 seconds and tabulated the results. Figure 5-22 below illustrates details of the system that is simulated;

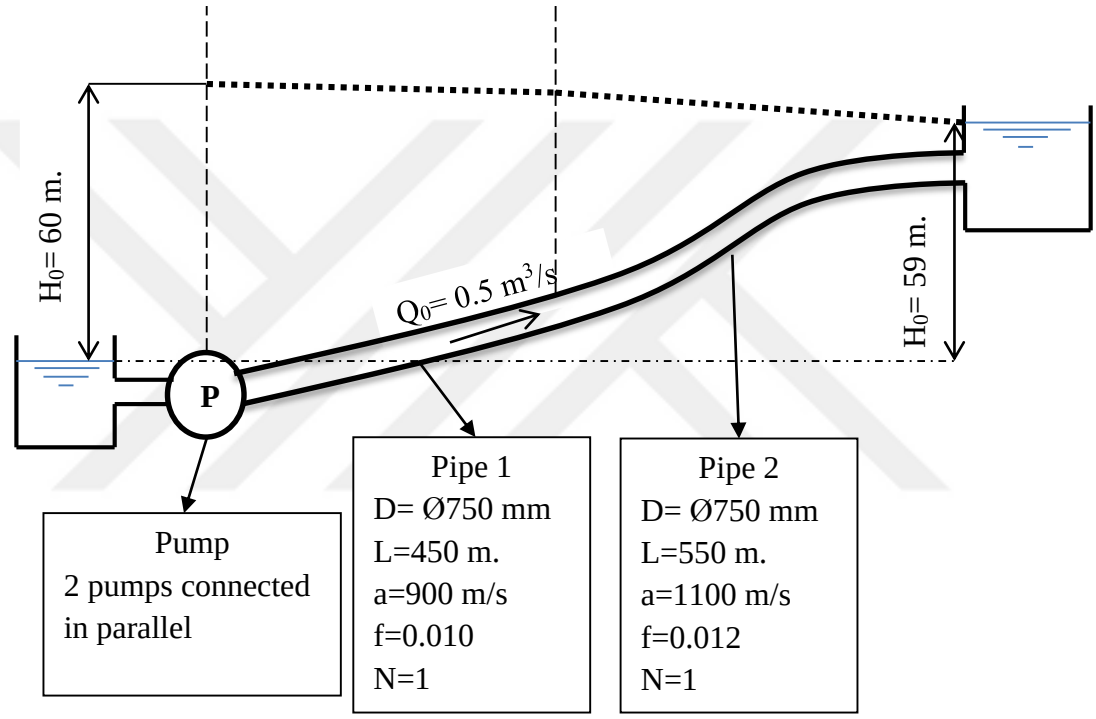

Figure 5-22: Pump failure transient problem definition (Chaudhry, 1979)

Table 5-6: General input data for pump (failure without valve in front scenario)

Rated Head of Pump, H_R	60	m
Rated Discharge of Pump, Q_R	0.25	m^3/s
Rated Speed of Pump, N_R	1100	rpm
Rated Torque of Pump, T_R	1520.02	N.m
Rated Efficiency of Pump, η_R	0.84	
Value of WR^2	16.85	$kg.m^2$ per pump

The same problem is solved using H-Hammer. It should be noted that pump curves are derived by using homologous relationships on H-Hammer.

Δt= 0.02 seconds

Figure 5-23 illustrates H-Hammer schematic of this problem. Total of 40 nodes are used.

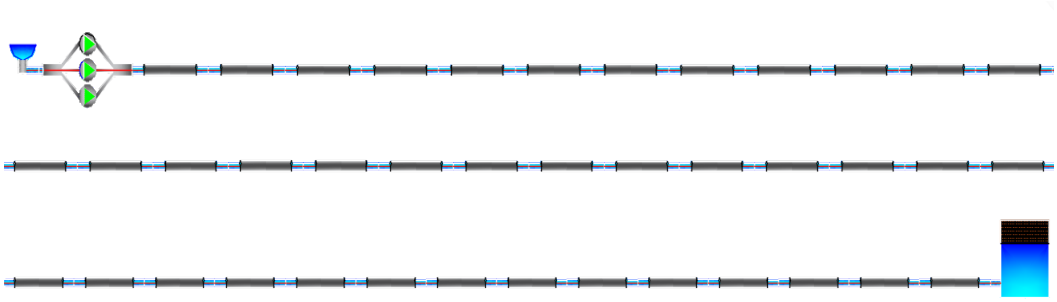

Figure 5-23: H-Hammer schematic of pump failure case study by Chaudhry (1979)

Graphs compare head and discharge results at the pump location and at the end points of each pipe.

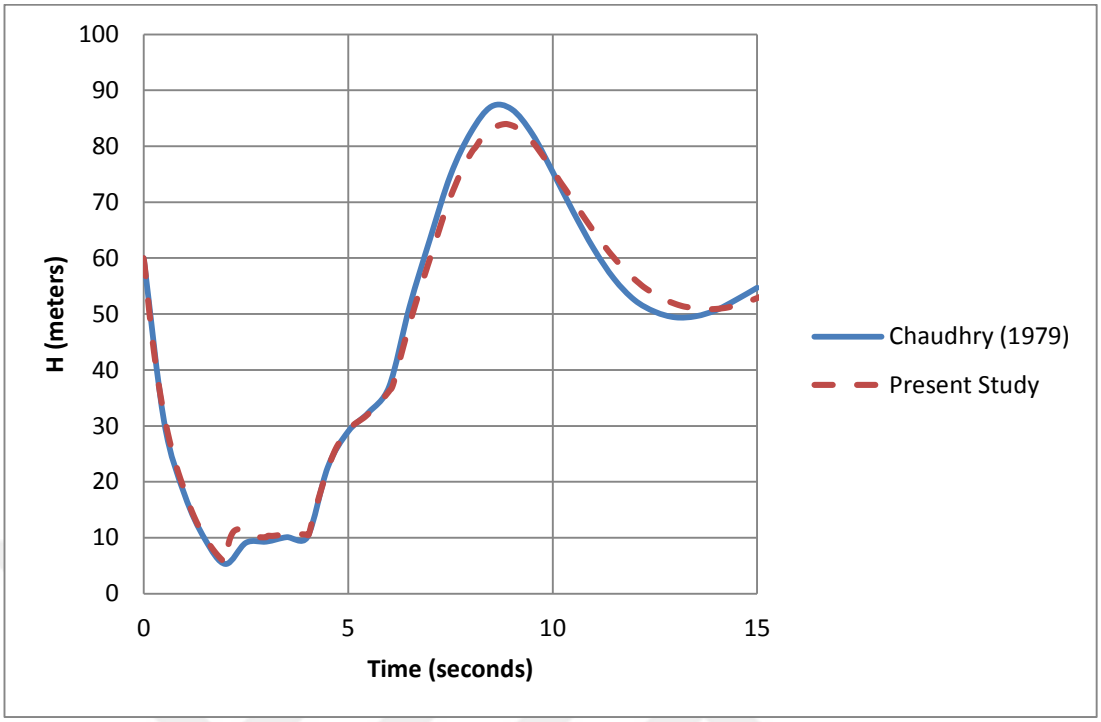

Figure 5-24: Head vs time graph for pump trip without valve at x=0+000 m

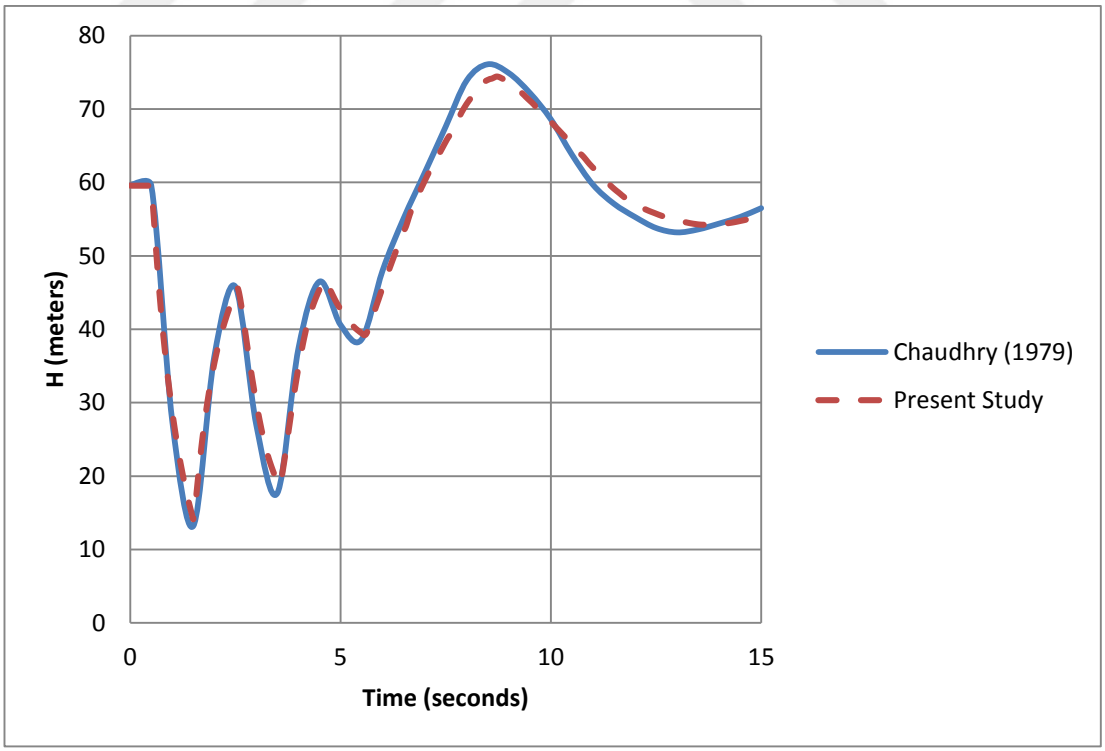

Figure 5-25: Head vs time graph for pump trip without valve at x=0+450 m

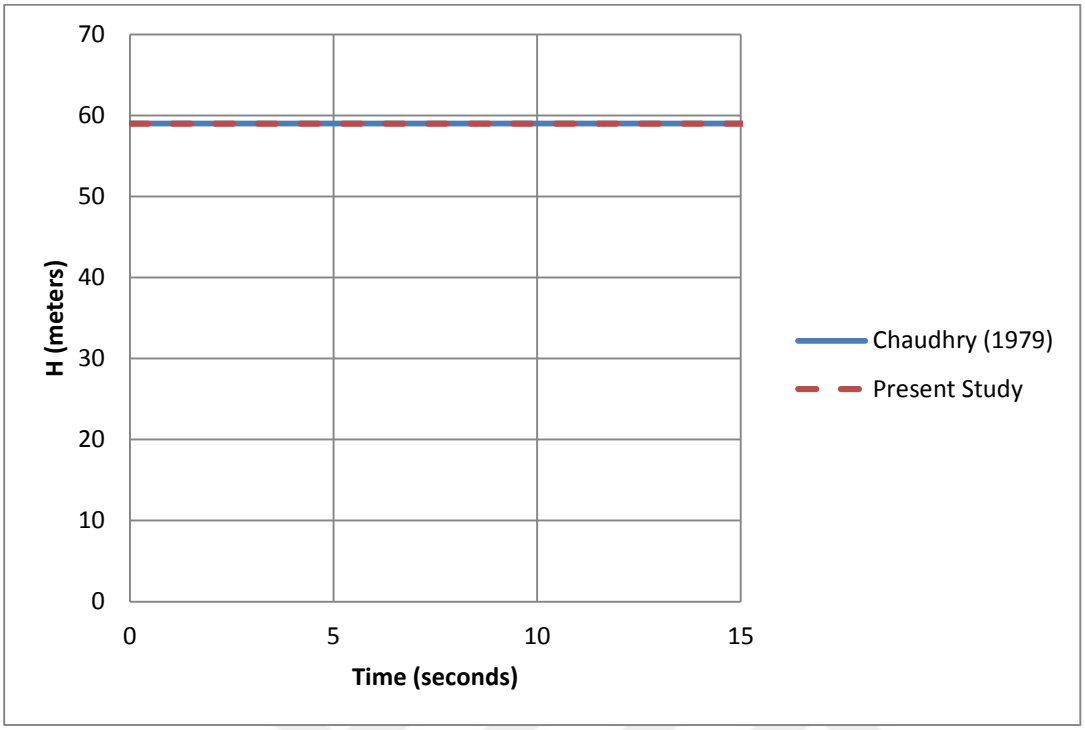

Figure 5-26: Head vs time graph for pump trip without valve at x=1+000 m

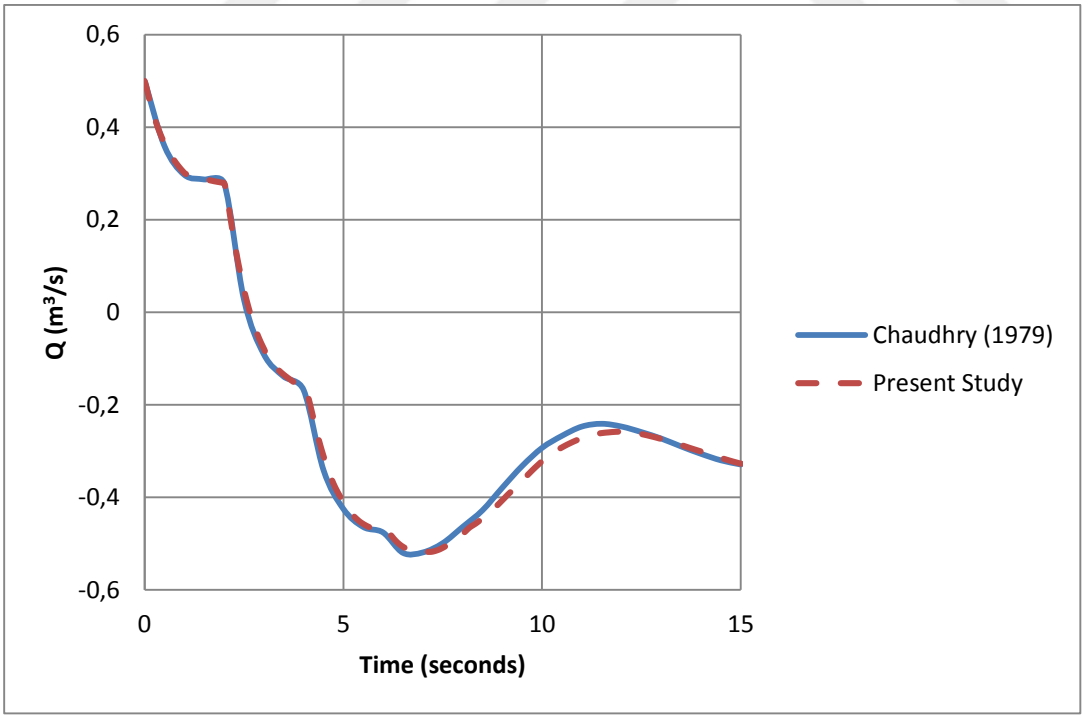

Figure 5-27: Discharge vs time graph for pump trip without valve at x=0+000 m

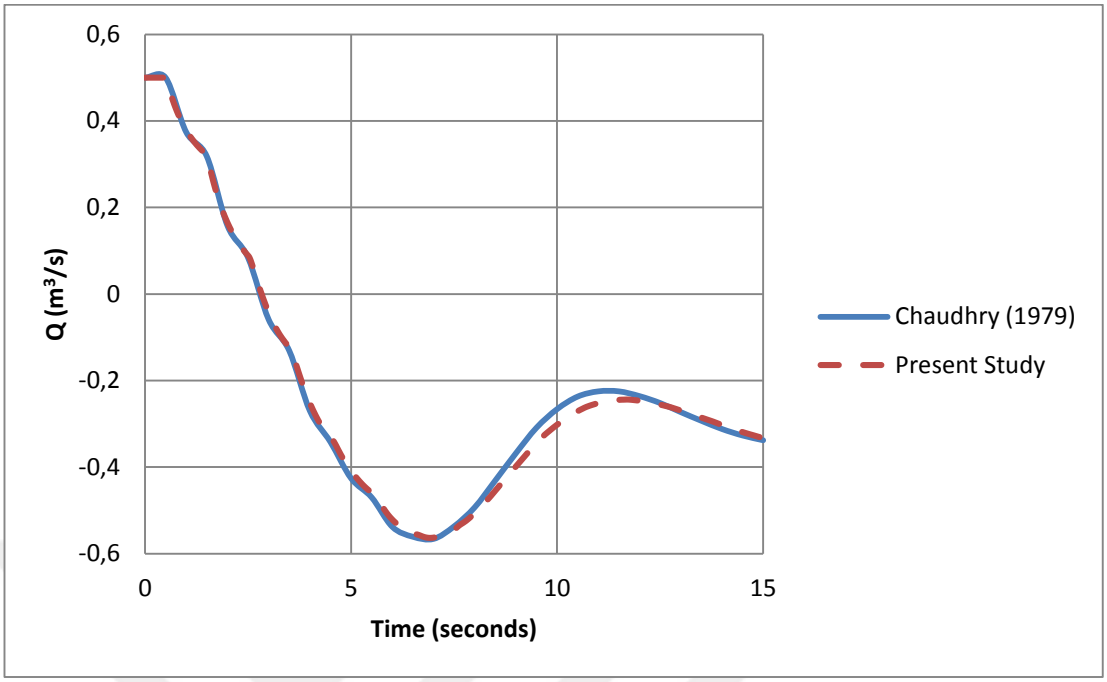

Figure 5-28: Discharge vs time graph for pump trip without valve at x=0+450 m

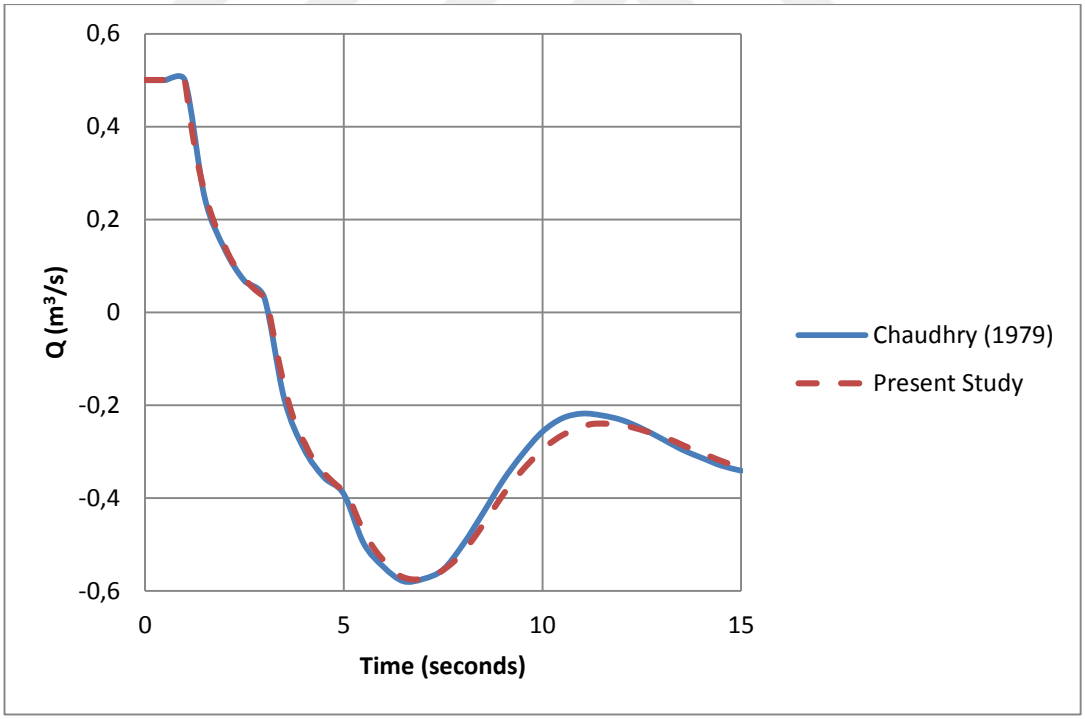

Figure 5-29: Discharge vs time graph for pump trip without valve at x=1+000 m

Fairly similar results are obtained by doing analysis for pump failure on H-Hammer.

5.4 Surge Tank Scenario

In this chapter two example surge tank scenarios that were solved by Şefik COFCOF will be solved on H-Hammer and results will be compared. The details and results of his study were obtained from “Denge Bacaları (2011)” book “ (p.22-33)”.

5.4.1 Surge Tank with Standpipe Scenario

In this section surge tank with standpipe will be located at the end of an energy tunnel and case for complete load rejection will be solved. The same scenario is repeated for normal water elevation and maximum discharge values on H-Hammer. Details of the scenario are illustrated on Figure 5-30.

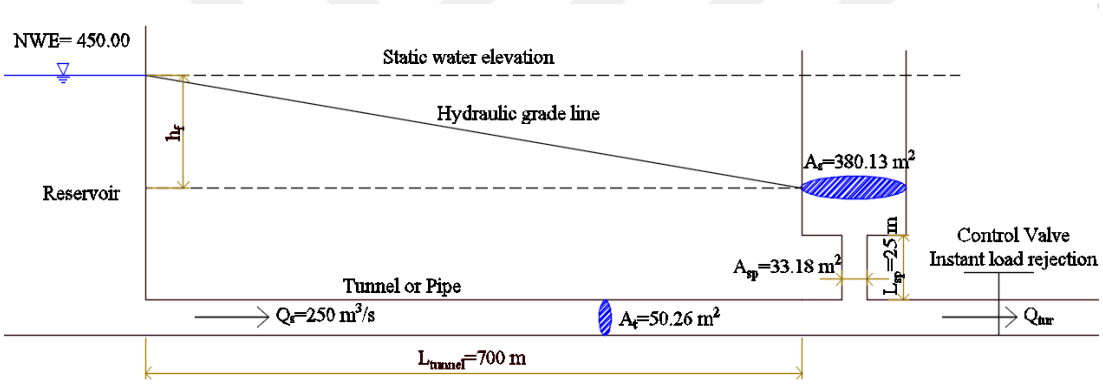

Figure 5-30: Surge tank with standpipe scenario

In brief simulation parameters are given below;

NWE= 450.00

Q= 250 m^3/s

A_{st}= 380.13 m^2

A_{tunnel}= 50.26 m^2

L_{tunnel}= 700 m

A_{sp}= 33.18 m^2

L_{sp}= 25 m

Figure 5-31: Surge tank with standpipe H-Hammer schematic

Energy tunnel is divided into 7 segments of 100 m space increments as it can be seen from above Figure 5-31 and at the end after surge tank 2 segments of 5 m space increments are placed to connect downstream instant load rejection to tank. Simulation was done using;

a= 500 m/s

Δt= 0.2 seconds.

On his study by using empirical formulas below results are obtained for this scenario;

Y_{max}=14.36 meters

Y_1= 11.97 meters according to Jeagar method

Y_1= 11.00 meters according to Parmakian Charts

Y_2= 15.00 meters according to Forcheimer

Y_2= 12.10 meters according to Parmakian Charts

Where;

Y_{max}= Maximum water level increase in tank measured from steady state water height of tank

Y_1= Maximum water level increase in tank measured from static water height

Y_2= Maximum water level decrease in tank measured from static water height

Results of H-Hammer:

As it can be seen from the Figure 5-32 results of analysis yields for surge tank elevations are;

Steady state water elevation= 448.61

Static water elevation= 450.00

Maximum uprise elevation= 463.02

Maximum downsurge elevation= 438.41

Therefore H-Hammer results are;

Y_{max}= 463.02 - 448.61= 14.41 meters

Y_1= 463.02 - 450.00= 13.02 meters

Y_2= 450.00 - 438.41 = 11.58 meters

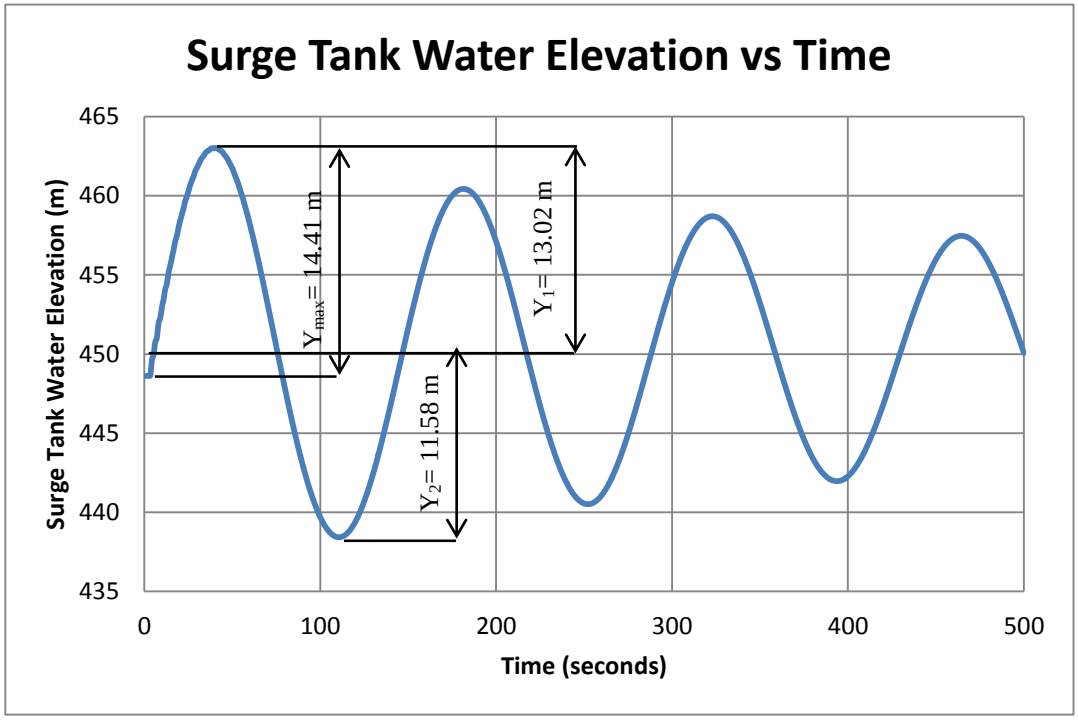

Figure 5-32: Surge tank with standpipe water elevation changes

As it can be seen from the Figure 5-32 the comparison of results are tabulated on below Table 5-7 in units of meters;

Table 5-7: Surge tank with standpipe result comparisons

	EMPIRICAL		GRAPHICAL	MOC
	Jeager	Forcheimer	Parmakian	H-Hammer
Y_{max} (m)	14.36	-	-	14.41
Y_1 (m)	11.97	-	11.00	13.02
Y_2 (m)	-	15.00	12.10	11.58

Table 5-7 shows that all in all results are fairly similar to each other.

5.4.2 Surge Tank with Throttled Orifice Scenario

On this section surge tank with throttled orifice will be located at the end of an energy tunnel downstream side of surge tank continue with branched junction connection. The same scenario is repeated for normal water elevation and maximum discharge values on H-Hammer. Details of the scenario are illustrated on Figure 5-33.

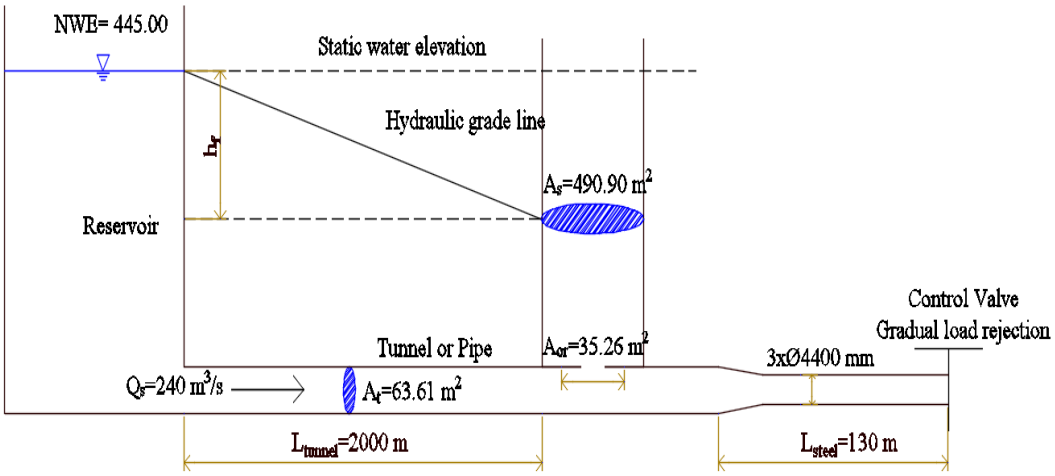

Figure 5-33: Surge tank with throttled orifice scenario

In brief simulation parameters are given below;

NWE= 445.00

Q= 240 m^3/s

A_{st}= 490.90 m^2

A_{tunnel}= 63.61 m^2

L_{tunnel}= 2000 m

$A_{steel\ pipes}$= 15.20 m^2

$L_{steel\ pipe}$= 130 m

Steel pipe consists of 3xΦ4400 mm pipes. Therefore it is a branching junction with 3 division.

Gate closure time= 6 seconds (not instantly)

H-Hammer schematic of this scenario is given on Figure 5-34.

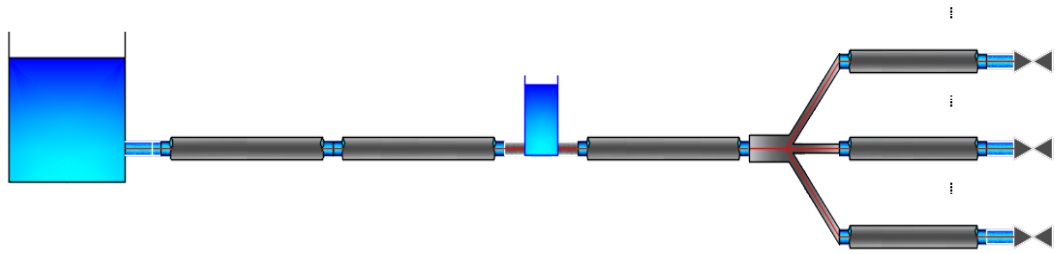

Figure 5-34: Surge tank with throttled orifice H-Hammer schematic

a_{tunnel}= 500 m/s

a_{steel}= 700 m/s

Δt= 0.05 seconds.

On his study by using empirical formulas below results are obtained for this scenario;

Y_{max}=19.40 meters

Y_1= 15.83 meters according to Jeagar method

Y_1= 17.22 meters according to Parmakian Charts

Y_2= 20.43 meters according to Forcheimer

Y_2= 16.80 meters according to Parmakian Charts

Results of H-Hammer:

As it can be seen from the Figure 5-35 results of analysis yields for surge tank elevations are;

Steady state water elevation= 442.90

Static water elevation= 445.00

Maximum uprise elevation= 462.43

Maximum downsurge elevation= 429.65

Therefore H-Hammer results are;

Y_{max}= 462.43 - 442.90= 19.53 meters

Y_1= 462.43 - 445.00= 17.43 meters

Y_2= 445.00 - 429.65 = 15.35 meters

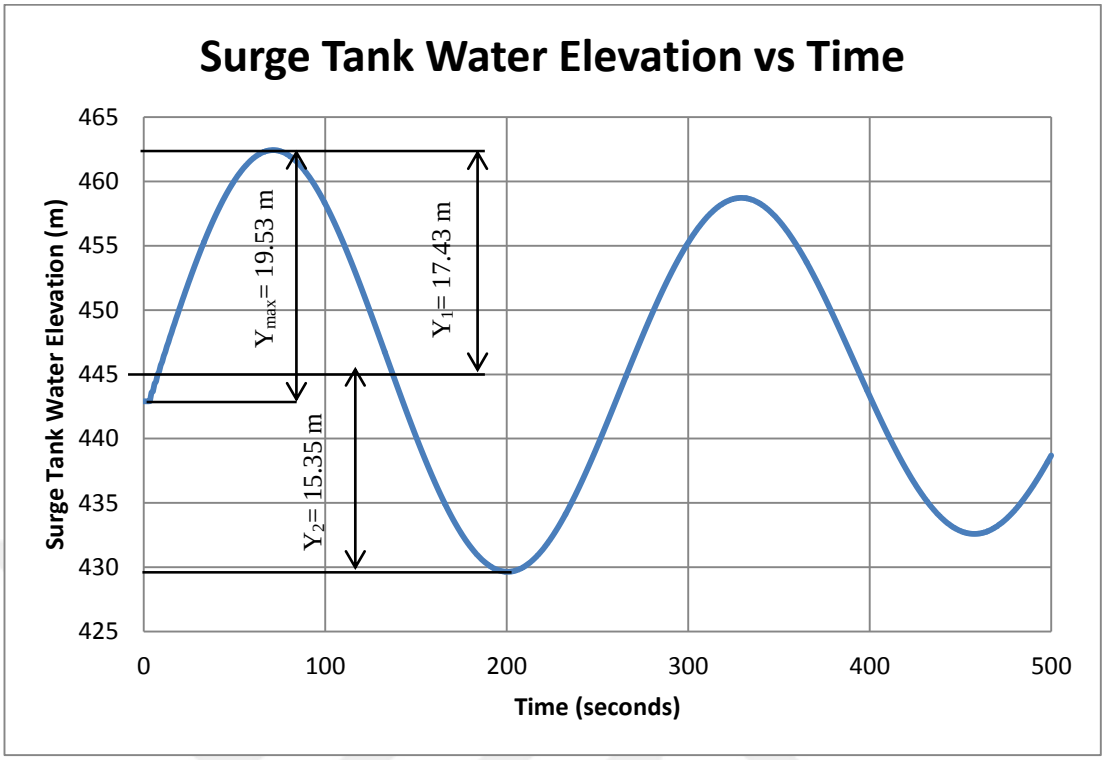

Figure 5-35: Surge tank with throttled orifice water elevation changes

Below Table 5-8 compares results of other studies (all units are measured in meters);

Table 5-8: Surge tank with throttled orifice result comparisons

	EMPIRICAL		GRAPHICAL	MOC
	Jeager	Forcheimer	Parmakian	H-Hammer
Y_{max} (m)	19.40	-	-	19.53
Y_1 (m)	15.83	-	17.22	17.43
Y_2 (m)	-	20.43	16.80	15.35

Again with throttled orifice boundary simulation results are fairly similar to the results of empirical formulas.

CHAPTER 6

CONCLUSIONS

In the present study, a code was developed to solve a large variety of fluid transient problems. The method of characteristics was used to solve the basic unsteady pipe flow equations. The theoretical background was explained in detail in the early chapters of the thesis. Most commonly encountered boundary conditions were inserted into the code, which are: Series Junction, Branching Junction, Upstream Reservoir with Constant Head, Upstream Reservoir with Variable Head, Centrifugal Pumps (Single-Series-Parallel Connected), Air Chamber with Orifice, Interior Valve, Downstream Valve, Surge Tank with Standpipe, Air Valve, Downstream Reservoir with a Constant Head, Downstream Dead End, Air Chamber with Standpipe and Surge Tank with Throttled Orifice, etc.

The code requires and makes use of Autocad, MS Excel and Visual Basic 6.0 programs together to perform the simulations and present the output in a professional-looking way. The accuracy of the code was verified by performing a number of simulations of the problems found in some well-known fluid transient textbooks. Comparisons showed that the results of the code developed in the present study are in good agreement with those of the textbooks.

The program capabilities were detailed in the relevant chapters. A user manual was also prepared to guide the potential users to use the program efficiently. Needless to say, the code still requires further improvements, new boundary elements and other contributions that can be added in the future by others. It is deemed that a good step was taken in the right direction to develop eventually a relatively sophisticated fluid transient code that it would be beneficial to the design engineers working in this field.

REFERENCES

1. Allievi, L. (1902). General theory of the variable motion of watere in pressure conduits. *Annali della Societa degli Ingegneri ed Architetti Italiani* 17(5): 285-325 (in Italian). (French translation by Allievi, in Revue Me' canique, Paris, 1904) (Discussed by Bergant et al., 2006).

2. Allievi, L. (1913). Teoria del colpo d'ariete (Theory of water-hammer.). *Atti del Collegio degli Ingegneri ed Architetti Italiani*, Milan, (in Italian) (Discussed by Bergant et al., 2006).

3. Bergeron, L. (1935). Estude des variations de re' gime dans les conduites d'eau-Solution graphique ge' ne' rale (Study on the Steady-State Variations in Water-Filled Conduits-General Graphical Solution) (in French). *Revue Ge' ne' rale de l'Hydraulique* 1(1): 12-25. (Discussed in Saikia and Sarma, 2006).

4. Bergeron, L. (1936). Estude des coups de beler dans les conduits, nouvel exose' de la methodegraphique. *La Technique Moderne* 28: 33. (Discussed in Saikia and Sarma, 2006).

5. Kepkep, Z. (1976). *Solution of Hydraulic Transients in Closed Conduit Systems. M.S. Thesis, METU*

6. Wiggert, D.C., and Sandquist, M.J. (1977). "Fixed-grid characteristics for pipeline transients." *Journal of Fluids Engineering*, ASCE, 103(12), 1403-1415

7. Streeter, V.L., Wylie, E.B. (1978). *Fluid Transients*. McGraw Hill, New York.

8. Wiggert, D.C., and Sandquist, M.J. (1979). "The effect of gaseous cavitation on fluid transients." *Journal of Fluids Engineering*, ASME, 101(3), 79-86.

9. Chaudhry, H.M. (1979). *Applied Hydraulic Transients*. VNR Company.

10. Özer, M. (1980). *Solution of Transient Flow in Pipe Networks. M.S. Thesis, METU*

11. Wylie, E.B. (1984), Simulation of Vaporous and Gaseous Cavitation, *Journal of Hydralic Engineering,* ASME, 106, 307-311.

12. Wiggert, D.C. (1984). *Single Pipeline Water Hammer Program. Michigan State University.*

13. Karley, B.W. (1984), *"Analysis of Fluid Transients in Large Distribution Networks"*

14. Shimada, M., Okushima, S. (1984). New Numerical Model and Technique for Water Hammer. *Journal of Hydraulic Engineering* 110(6): 736-748.

15. Chaudhry, H.M., Hussaini, M.Y. (1985). Second-order Accurate Explicit Finite-Difference Schemes for Water Hammer Analysis. *Journal of Fluids Engineering* 107: 523-529.

16. Fok, A.T.K., *"A Contribution to the Analysis of Energy Losses in Transient Pipe Flow",* Ph.D. Thesis, University of Ottawa, 1987

17. Streeter, V.L., Wylie, E.B. (1993). *Fluid Transients 2nd edition*. McGraw Hill, New York.

18. Silva-Araya, W., Chaudhry, M.F. (1997). Computation of Energy Dissipation in Transient Flow. *Journal of Hydraulic Engineering* 123(2): 108-115.

19. Pezzigan, G. (1999). "Quasi-2D model for unsteady flow in pipe networks." *Journal of Hydralic Engineering* 125(7), 676-685.

20. Larock, B.E., Jeppson, R.W., Watters, G.Z. (2000). *Hydraulics of Pipeline Systems.* CRC Press

21. Saral, F. İ. (2000). *Hydraulic Transients in Closed Pipe Circuits. M.S. Thesis, METU*

22. Ramezani, L. (2001). *"A Computer Model as Surge Preventive Measure in Small Hydropower Schemes"*

23. Stephenson, D. (2002). "Simple Guide for Design of Air Vessels for Water Hammer Protection of Pumping Lines." *Journal of Hydralic Engineering*, ASCE, 128: 792-797.

24. Ghidaoui, M.S., Mansour, G.S., Zhao, M. (2002). Applicability of Quasi Steady and Axisymmetric Turbulence Models in Water Hammer. *Journal of Hydralic Engineering* 128(10): 917-924.

25. Zhao, M., Ghidaoui, M.S. (2003). Efficient Quasi Two Dimensional Model for Water Hammer Problems. *Journal of Hydraulic Engineering* 1129(12): 1007-1013.

26. Zhao, M., Ghidaoui, M.S. (2004). Godunov-type Solutions for Water Hammer Flows. *Journal of Fluids Engineering* 130(4):341-348.

27. AWWA M11, (2004), *Steel Pipe: A Guide for Design and Installation 4th Edition*

28. Kolev, N. I (2004), *Multiphase Flow Dynamics 1.*

29. Cannizzaro, D., and Pezzinga, G. (2005). "Energy Dissipation in Transient Gaseous Cavitation." *Journal of Fluids Engineering.*, 724-732.

30. Greyvenstein, G.P. (2006). An Implicit Method for Analysis of Transient Flows in Piping Networks. *International Journal for Numerical Methods in Engineering* 53: 1127-1148.

31. Bozkuş, Z. (2008). Water Hammer Analyses of Çamlıdere-İvedik Water Treatment Plant (IWTP) Pipeline. *Teknik Dergi Vol. 19, No. 2 April 2008, pp:4409-4422*

32. Afshar. M.H., Rohani, M. (2008). Water Hammer Simulation by Implicit Method of Characteristics. *International Journal of Pressure Vessels and Piping* 85: 851-859.

33. Koç, G. (2007). *Simulation of Flow Transients in Liquid Pipeline Systems. M.S. Thesis, METU*

34. Cofcof, Ş. (2011). *Denge Bacaları*

35. Bozkuş, Z., Dursun, S. (2014). *Numerical Investigation of Protection Measures Against Water Hammer in the Yesilvadi Hydropower Plant.*

36. Bozkuş, Z. (2016). *Fluid Transients in Closed Conduits Lecture Note. Middle East Technical University*

37. Bozkuş, Z., Çalamak, M., Rezaei, V. (2016). Performance of a Pumped Discharge Line with Combined Application of Protection Devices Against Water Hammer. *KSCE Journal of Civil Engineering (2017)21(4):1493-1500*

38. Bozkuş, Z., Dinçer, A.E. (2016). Investigation of Water Hammer Problems in Wind-Hydro Hybrid Power Plants. *Arabian Journal for Science and Engineering DOI 10.1007/s13369-016-2142-2*

39. Bentley Hammer. Hammer Water Hammer and Transient Analysis Software. http://www.bentley.com/en/US/Products/HAMMER/Product

40. Wanda transient simulation software. https://www.deltares.nl/en/software/wanda/

APPENDIX A

A.1 USERS MANUAL

In this section, step by step instructions on how to use software will be provided. Figure A-1 illustrates main user interface of the code.

1. Open AutoCAD
2. Click on create boundaries and click on an empty space on AutoCAD drawing. Figure A-1 illustrates how to create boundaries on AutoCAD interface.

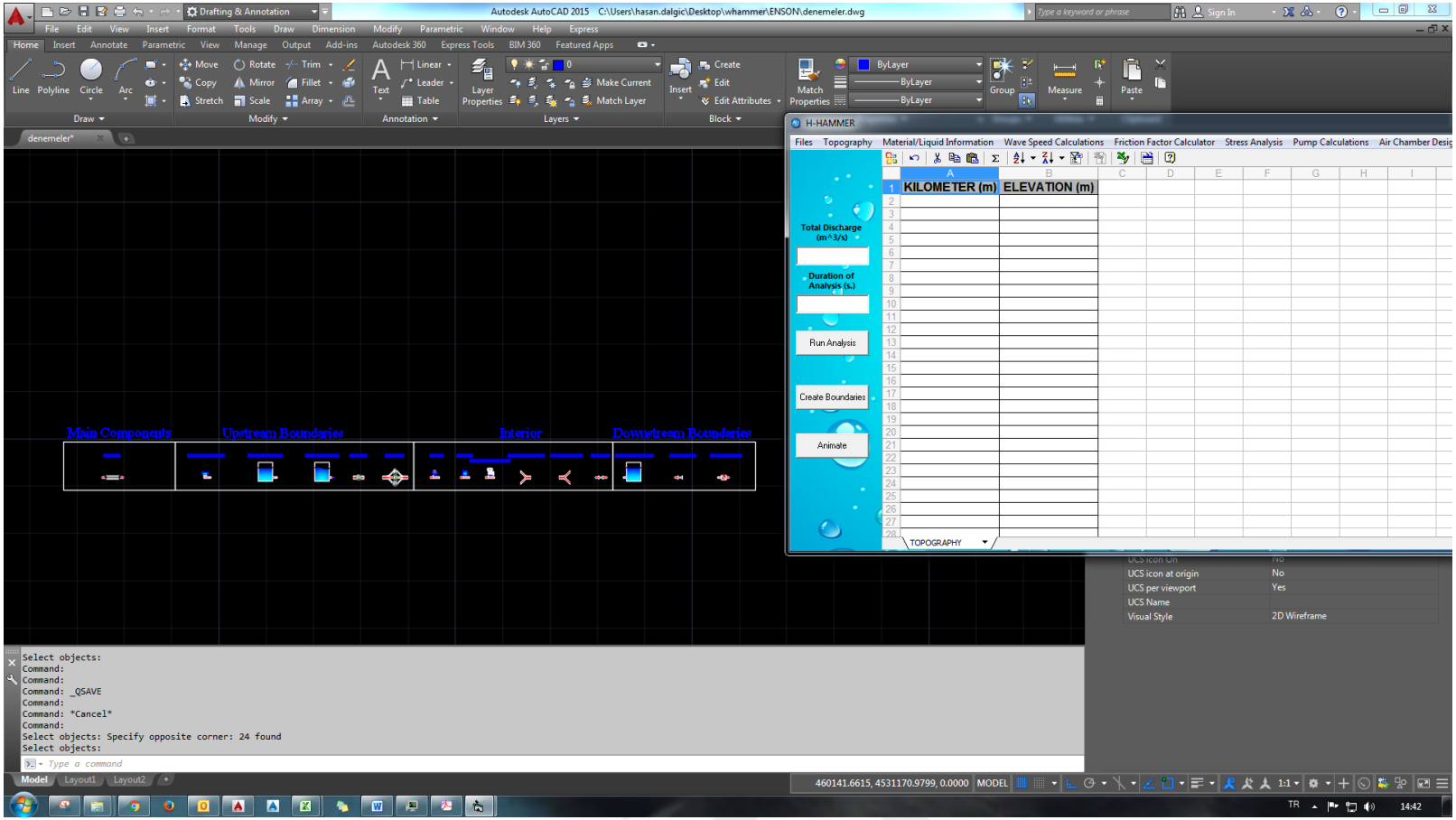

Figure A-1: Creating Boundaries

Now create a topography view of your pipeline by using Topography from main interface. In order to create a topography you need to have triangulation model of the land as shown below. Triangulation models consist of 3dFace objects which have elevation data of topography stored inside them. H-Hammer is able to obtain this elevations at all intersections along the pipe plan view and create a profile view of land using these data. Figure A-2 illustrates pipe plan view and triangulation model.

Figure A-2: Pipe plan view and triangulation model

Steps for creating a topography is listed below;

- Click on “Topography” button from main menu.
- Click on pipeline plan view which resides on triangulation model (Figure A-2)
- In around 20-30 seconds it will finish calculations (Depending on the length of the pipeline) and when the signal for finish is given then user should click on an empty space on AutoCAD. End product of this step is shown on below figure.

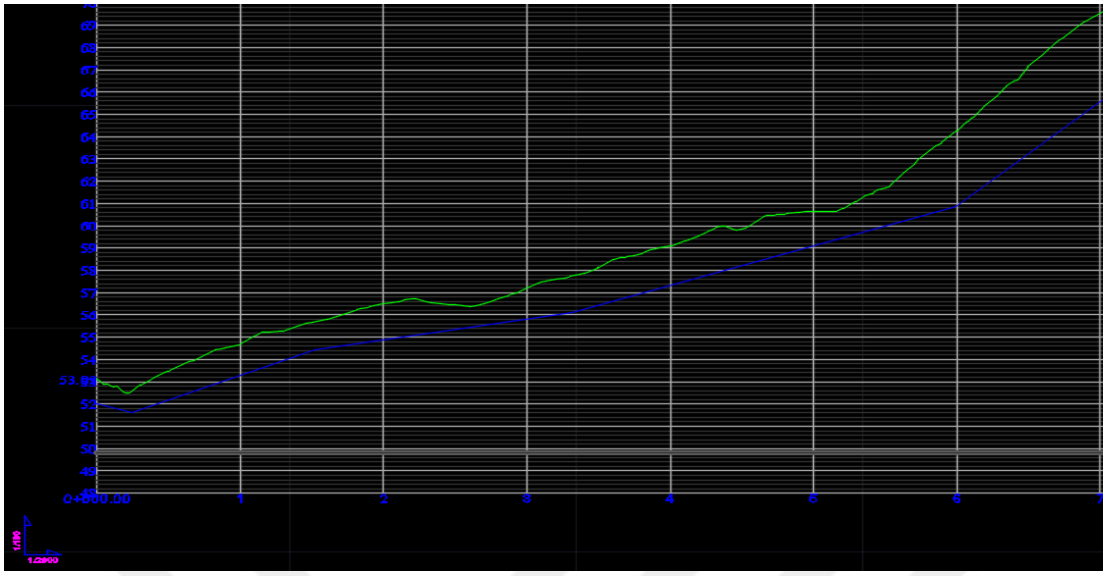

Figure A-3: Complete profile view created by H-Hammer

3. Next visualize your scenario and start creating it by connecting boundary parts. In order to create a scenario below AutoCAD commands must be used;

a. Copy command= “Co”

b. Move command = “M”

By using “Co” command multiple boundaries can be copied and pasted on to the same space and by using “M” command that boundary can be moved and connected to each other in order to create a scenario.

4. As it was mentioned on section 3 connect boundaries and create a scenario as shown on below figure. Note that all boundaries should be connected to each other from their end point.

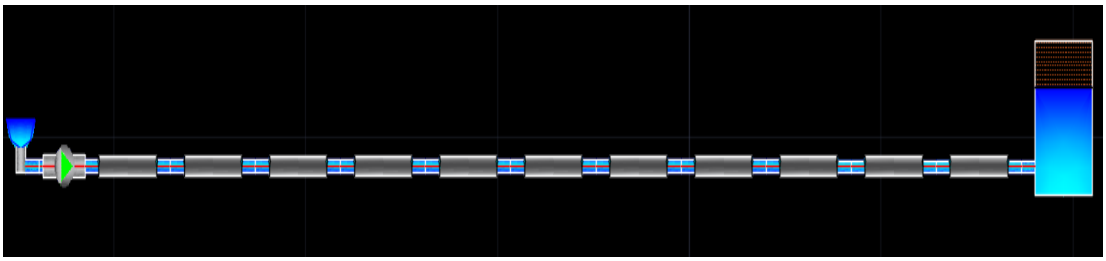

Figure A-4: Example pump failure scenario

5. In order to continue with analysis user should input necessary data into boundary objects which will determine the course of the scenario. Property window should be filled for analysis. An example of pump property window is shown below.

Block:Single Pump	
WRR_(NM^2)	150
RATED_DISCHARGE_(M^3/S)	0.555
RATED_HEAD_(M)	26
RATED_SPEED_(RPM)	885
RATED_TORQUE_(N.M)	1056.39
TIME_OF_FAILURE_(SEC.)	50
NUMBER_OF_SERIES_PUMPS	2
HEAD_LOSS_COEFF.	3
PUMPING_ELEVATION_(M)	52
CHECK_VALVE_(YES/NO)	NO
RATED_EFFICIENCY	0.85
BUTTERFLY_VALVE_(YES/NO)	NO
BUTTERFLY_VALVE_CLOSURE_TIME_(SEC.)	250
SHUT_OFF_HEAD_(M)	34
A1_OF_HvsQ_CURVE_EQUATION	-1.6714
A2_OF_HvsQ_CURVE_EQUATION	-22.526
A1_OF_EFFICIENCY_CURVE_EQUATION	3.1449
A2_OF_EFFICIENCY_CURVE_EQUATION	-2.9191

Figure A-5: Example for full pump boundary property window

6. Now user should input steady state discharge and time duration of the analysis in the main interface and click on "Run Analysis".
7. After clicking on "Run Analysis" program will direct you to select the scenario which you already created on AutoCAD model space. This analysis will result showing below data which includes "HGL Values (m)" which are measured from the beginning elevation of pipe profile and "Discharge values (m^3/s)". Results are listed as shown in below figure.

	A	B	C	D	E	F	G	H	I	J	K	L	M	N	O	P	Q	R	S	T
1	HGL VALUES (m)										DISCHARGE VALUES (m^3/s)									
2	DISTANCE (m.)	0.000	0.000	100.000	200.000	300.000	400.000	500.000	600.000	700.000	DISTANCE (m.)	0.000	0.000	100.000	200.000	300.000	400.000	500.000	600.000	700.000
3	TIME (s.)	NODE 1	NODE 2	NODE 3	NODE 4	NODE 5	NODE 6	NODE 7	NODE 8	NODE 9	TIME (s.)	NODE 1	NODE 2	NODE 3	NODE 4	NODE 5	NODE 6	NODE 7	NODE 8	NODE 9
4	0.00	0.000	114.980	114.904	114.828	114.751	114.675	114.599	114.523	114.447	0.00	1.000	1.020	1.020	1.020	1.020	1.020	1.020	1.020	1.020
5	0.08	0.000	114.980	114.904	114.828	114.751	114.675	114.599	114.523	114.447	0.08	1.020	1.020	1.020	1.020	1.020	1.020	1.020	1.020	1.020
6	0.16	0.000	114.980	114.904	114.828	114.751	114.675	114.599	114.523	114.447	0.16	1.020	1.020	1.020	1.020	1.020	1.020	1.020	1.020	1.020
7	0.24	0.000	114.980	114.904	114.828	114.751	114.675	114.599	114.523	114.447	0.24	1.020	1.020	1.020	1.020	1.020	1.020	1.020	1.020	1.020
8	0.32	0.000	114.980	114.904	114.828	114.751	114.675	114.599	114.523	113.378	0.32	1.020	1.020	1.020	1.020	1.020	1.020	1.020	1.020	1.030
9	0.40	0.000	114.980	114.904	114.828	114.751	114.675	114.599	113.455	112.310	0.40	1.020	1.020	1.020	1.020	1.020	1.020	1.020	1.030	1.040
10	0.48	0.000	114.980	114.904	114.828	114.751	114.675	113.532	112.388	112.310	0.48	1.020	1.020	1.020	1.020	1.020	1.020	1.030	1.040	1.040
11	0.56	0.000	114.980	114.904	114.828	114.751	113.608	112.465	112.388	112.310	0.56	1.020	1.020	1.020	1.020	1.020	1.030	1.040	1.040	1.040
12	0.64	0.000	114.980	114.904	114.828	113.685	112.543	112.465	112.388	112.310	0.64	1.020	1.020	1.020	1.020	1.030	1.040	1.040	1.040	1.040
13	0.72	0.000	114.980	114.904	113.762	112.620	112.543	112.465	112.388	112.310	0.72	1.020	1.020	1.020	1.030	1.040	1.040	1.040	1.040	1.040
14	0.80	0.000	114.980	113.839	112.698	112.620	112.543	112.465	112.388	112.310	0.80	1.020	1.020	1.030	1.040	1.040	1.040	1.040	1.040	1.040
15	0.88	0.000	114.980	112.775	112.698	112.620	112.543	112.465	112.388	112.310	0.88	1.020	1.020	1.040	1.040	1.040	1.040	1.040	1.040	1.040
16	0.96	0.000	114.980	112.776	112.698	112.620	112.543	112.465	112.388	112.310	0.96	1.020	1.020	1.040	1.040	1.040	1.040	1.040	1.040	1.040
17	1.04	0.000	114.980	112.777	112.699	112.620	112.543	112.465	112.388	112.310	1.04	1.020	1.020	1.040	1.040	1.040	1.040	1.040	1.040	1.040
18	1.12	0.000	114.980	112.778	112.699	112.621	112.543	112.465	112.388	112.310	1.12	1.020	1.020	1.040	1.040	1.040	1.040	1.040	1.040	1.040
19	1.20	0.000	114.980	112.778	112.700	112.622	112.543	112.465	112.388	112.310	1.20	1.020	1.020	1.040	1.040	1.040	1.040	1.040	1.040	1.040

Figure A-6: Example full results table (HGL and Discharge)

8. It should be noted that these HGL values are measured from the origin of the profile and in order to better understand what happens during transients "Head Values" acting on various parts of the pipe should be calculated and this can be achieved by matching profile view elevations and HGL. To do this software offers "Stress Analysis". Upon finishing "Transient Analysis" a new "Stress Analysis" should be conducted to find acting head values along various points of pipeline profile. First form on next page should be filled to start this analysis which includes;

- Pipe section diameters (mm)
- Max. hoop stres of pipe material (MPa)
- Specific weight of the fluid flowing inside pipe (N/m^3)
- External loads (Pa)
- Pipe material modulus of elasticity (GPa)

An example form for stress analysis can be seen from the Figure A-7 on next page.

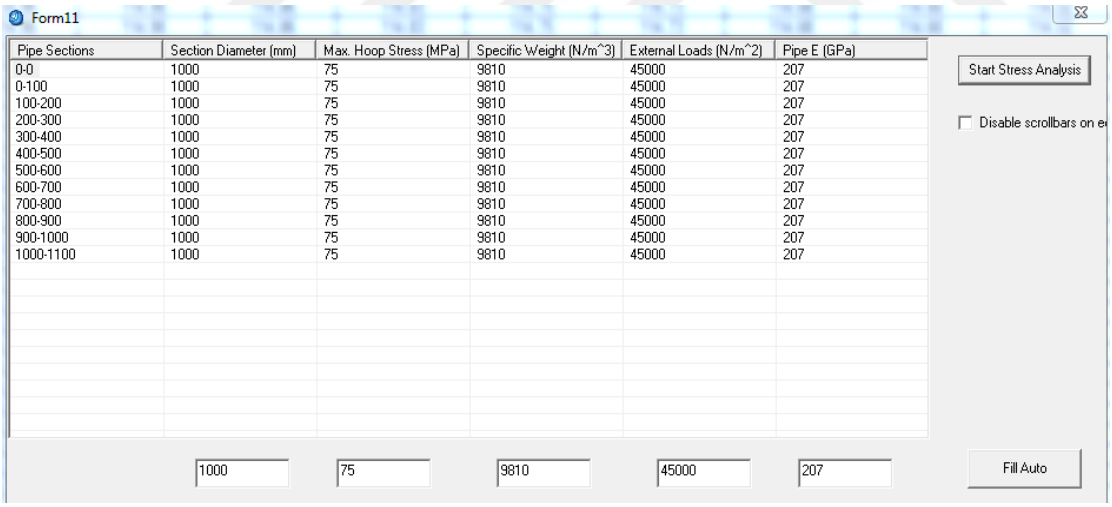

Figure A-7: Example fully filled stress analysis form

After starting analysis it will ask user to select land profile and then pipeline profile. An example is shown below (pipeline profile should be drawn by user considering topographical features);

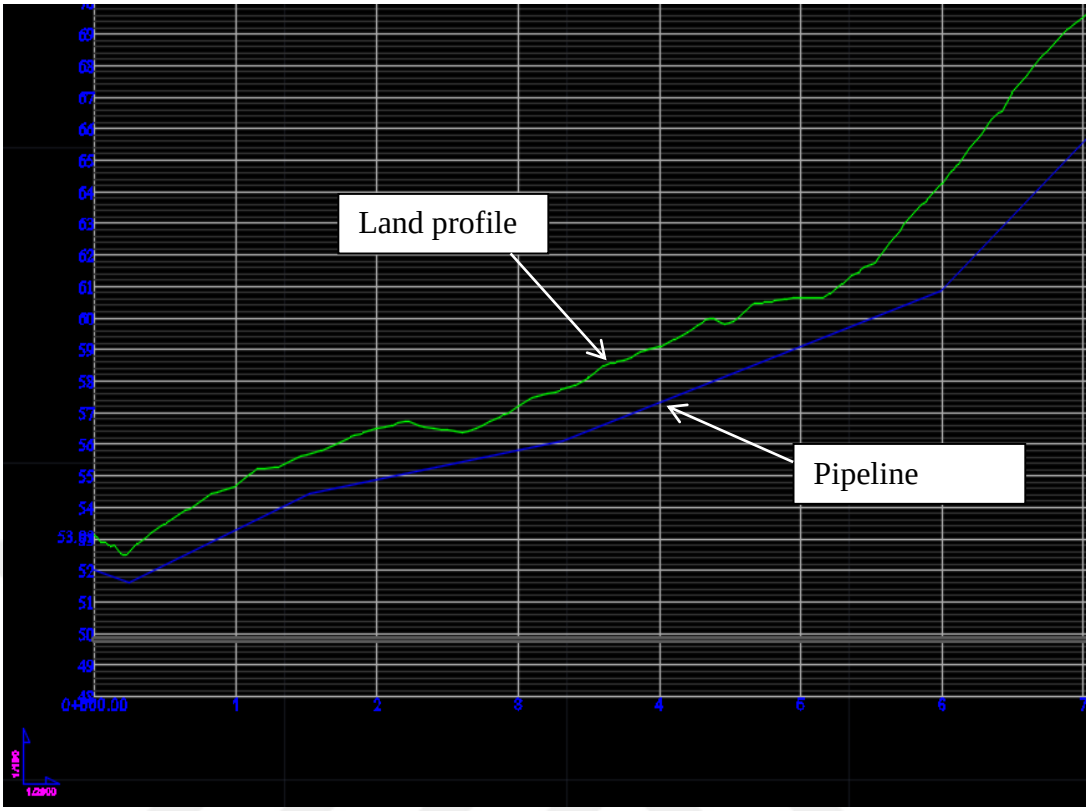

Figure A-8: Example pipeline profile drawn by user

After selecting profiles user need to select upstream boundary of their scenario and rest of the calculations will be done by software.

9. As a result of this analysis below data are calculated;

- Head values acting along pipe on different nodes (m)
- Pipe thicknesses calculated from inner pressure (mm)
- Minimum required pipe thicknesses (mm)
- Pipe thicknesses calculated from external loads (mm)
- Total deformation of pipe (cm)
- Percentage of change in cross sectional area of pipe (%)
- Maximum external load that pipe can carry without bending (Pa)

	DISTANCE INTERVALS (m)											
	0-0	0-100	100-200	200-300	300-400	400-500	500-600	600-700	700-800	800-900	900-1000	1000-1100
Max. Hydraulic Grade Line Elevation Inside Interval (m)	151.47	151.47	149.72	149.72	149.69	149.63	149.52	149.31	149.00	148.71	145.67	133.98
Min. Pipe Elevation Inside Interval (m)	52.00	51.60	53.32	54.89	55.83	57.36	59.15	61.01	65.68	70.34	75.00	91.69
Origin Elevation (m)	52.00	52.00	52.00	52.00	52.00	52.00	52.00	52.00	52.00	52.00	52.00	52.00
Pressure Acts on Section (m) (Max. HGL-(Min Elev.-Origin Elev.))	151.47	151.87	148.41	146.83	145.86	144.27	142.38	140.30	135.33	130.37	122.66	94.29
Max Hoop Stress (Mpa)	75.00	75.00	75.00	75.00	75.00	75.00	75.00	75.00	75.00	75.00	75.00	75.00
Pipe Diameter (mm)	1000.00	1000.00	1000.00	1000.00	1000.00	1000.00	1000.00	1000.00	1000.00	1000.00	1000.00	1000.00
Calculated Pipe Thickness for Transient Inner Pressure (mm)	9.91	9.93	9.71	9.60	9.54	9.44	9.31	9.18	8.85	8.53	8.02	6.17
Min Required Pipe Thickness (mm)	3.47	3.47	3.47	3.47	3.47	3.47	3.47	3.47	3.47	3.47	3.47	3.47
Calculated Pipe Thickness from External Loads (mm)	5.46	5.46	5.46	5.46	5.46	5.46	5.46	5.46	5.46	5.46	5.46	5.46
Deformation (cm)	0.21	0.21	0.21	0.21	0.21	0.21	0.21	0.21	0.21	0.21	0.21	0.21
Change in Cross Sectional Area (%)	2.06	2.06	2.06	2.06	2.06	2.06	2.06	2.06	2.06	2.06	2.06	2.06
Max External Pressure Durability without Bending (N/m^2)	86602.55	86602.55	86602.55	86602.55	86602.55	86602.55	86602.55	86602.55	86602.55	86602.55	86602.55	86602.55

Figure A-9: Example result of stress analysis

10. After all above steps are completed user can click on animate button from main user interface and visualize the motion of the HGL through given time duration.

APPENDIX B

B.1 RESTRICTIONS

NOTE: All boundaries should be connected from their snapping points. Figure B-1 illustrates snapping point of pipe segment;

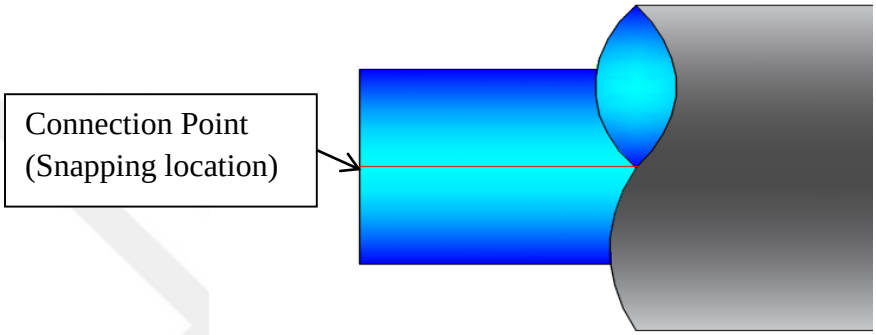

Figure B-1: Illustration of connection point between boundaries (Snapping)

Similar to above Figure B-1 all boundaries should be connected to each other from the right and left hand side edge of the boundary symbol.

a) There should be a pipe segment in between each and every interior boundary which means interior boundaries can not be connected to each other directly but a pipe segment of desired space increment should be located between each other. This rule applies to branching junctions aswell. Pipe segments on the upstream and downstream sides of interior boundaries should be identical which means diameter and pressure wave speed properties should be the identical. However, space increment can be arbitrary. Figure B-2 illustrates this restriction on one of the interior boundaries.

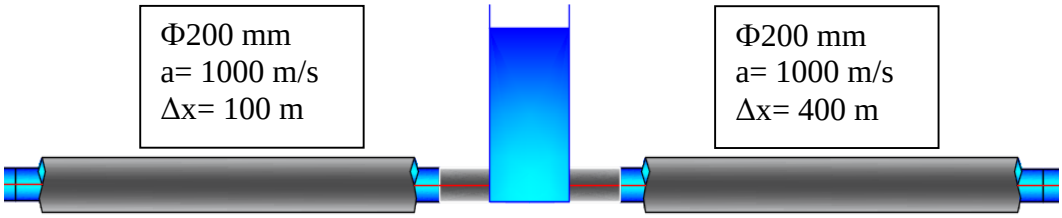

Figure B-2: Interior boundary restriction

b) Pipe divisions made by branching junctions should be identical. For example, if first row contains 2xΦ400 pipes with space increment of 100 and then 2xΦ300 pipes with space increment of 50 meters then second row below that should be exactly the same. Series junction can be used on pipe rows in branching junction divisions but the only restriction is that all pipe rows at the end should be identical. Figure B-3 illustrates this restriction.

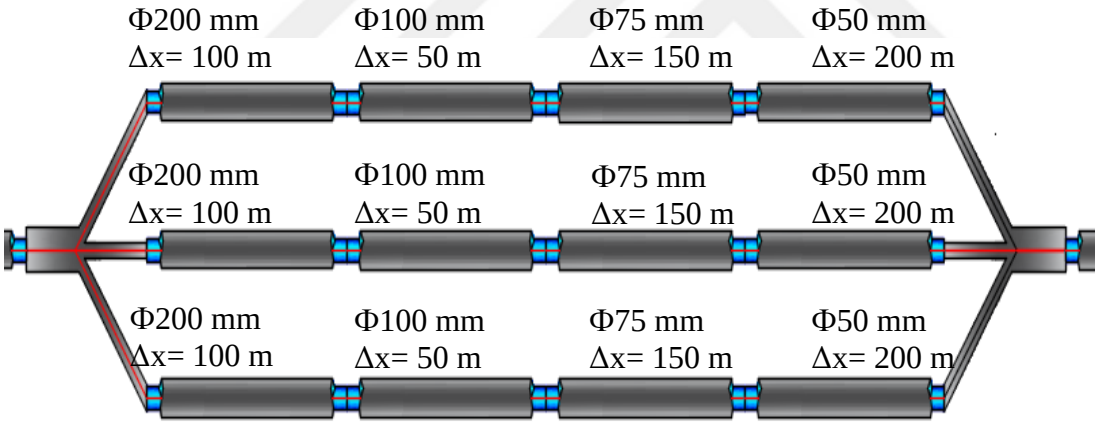

Figure B-3: Branching junction restriction

As it is seen from Figure B-3 all rows of branching junction is identical to each other. User can establish series junction in between divisions but the same series junction should also be established on all rows. In brief, number and properties of pipes in between branching junctions should be identical.

c) Branching junction dividers should be either finished by a connector or all end of the rows should be finished by a downstream boundary. Figure B-4 illustrates this

restriction. Downstream boundaries can be chosen arbitrarily the only restriction is that either all ends need to finish with downstream boundary or it shold be connected back to system by junction connector.

d) There should be minimum 2 pipe segments on each row after branching junction dividers.

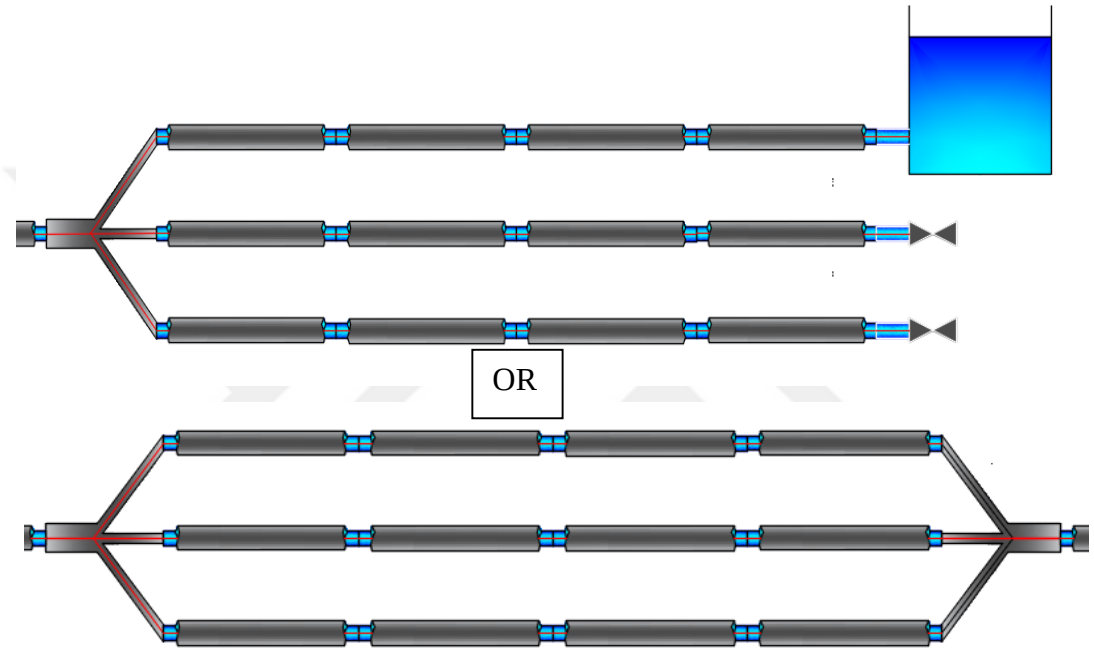

Figure B-4: Branching junction restriction-2

e) In case air chambers become fully depleted software will stop execution of simulation. Because during simulation it is assumed that air chambers never become fully depleted. In case it is depleted pipe system will vacuum the air inside chamber and software can not simulate air inside pipe system. In any case, it is highly undesirable situation to have air chambers fully depleted during transient events. Therefore, air chambers should be sized so that it will never become fully depleted during the simulation.

Other than these five there aren't any other restrictions and users can freely manipulate the system they are simulating.